MEASUREMENTS FOR LIQUID ROCKET ENGINE PERFORMANCE CODE VERIFICATION

October 1986

REMTECH INC.

RTR 157-01

MEASUREMENTS FOR LIQUID ROCKET ENGINE
PERFORMANCE CODE VERIFICATION

October 1986

Prepared By:

Sarat C. Praharaj

and

Richard L. Palko

REMTECH, Inc.
Huntsville, Alabama 35805

MEASUREMENTS FOR LIQUID ROCKET ENGINE
PERFORMANCE CODE VERIFICATION

October 1986

Prepared By:

Sarat C. Praharaj

and

Richard L. Palko

REMTECH, Inc.
Huntsville, Alabama 35805

FOREWORD

This final report presents work conducted for the Marshall Space Flight Center (MSFC) in response to the requirements of Contract NAS8-36548. The work presented here was performed by REMTECH, Inc., Huntsville, Alabama and is titled, "Measurements for Liquid Rocket Engine Performance Code Verification."

The project manager for this project was Dr. Sarat C. Praharaj. The project was very much aided by the technical support of the NASA contract monitor, Mr. Klaus Gross, EL 24 of the Systems Performance Branch of the Mission Analysis Division.

REMTECH INC.

TABLE OF CONTENTS

Section 1.0

INTRODUCTION

The various performance losses for liquid rocket thrust chambers are currently calculated by computer programs such as CICM, SDER, TDK, BLIMPJ and BLM. Systematic measurements to verify the calculated losses individually hardly exist, and the ones that exist are associated with high degree of uncertainty. Several years ago, the "JANNAF Rocket Engine Performance Test Data Acquisition and Interpretation Manual" (CPIA Publication 245) (Ref. 1) was prepared with reference to the recommended performance methodology. The procedures in this manual provided basic considerations for measuring various performance losses. The objective of the present work is to establish a procedure which complements the above CPIA publication. This work provides a general directory which would guide the test engineer to select the appropriate type of test, the parameters to measure, necessary test facility, required instrumentation with associated operation complexity and perform an uncertainty analysis to obtain the highest quality of test information.

The JANNAF thrust chamber evaluation procedures are based on a physical model that accounts for the major processes occurring in the thrust chamber, losses associated with these processes, and interactions among the processes. The basic processes are shown in Fig. 1.1. Propellants enter the combustion chamber through the injector, are mixed, vaporized and combusted. Deviations from complete homogeneous mixing and vaporization (or combustion) to
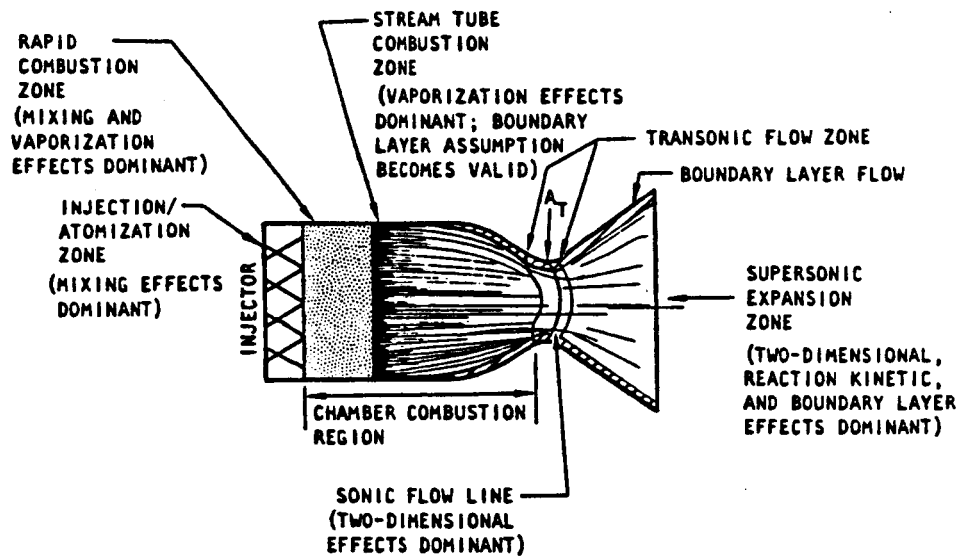
Fig. 1.1 Internal Process in the Real Rocket Thrust Chamber
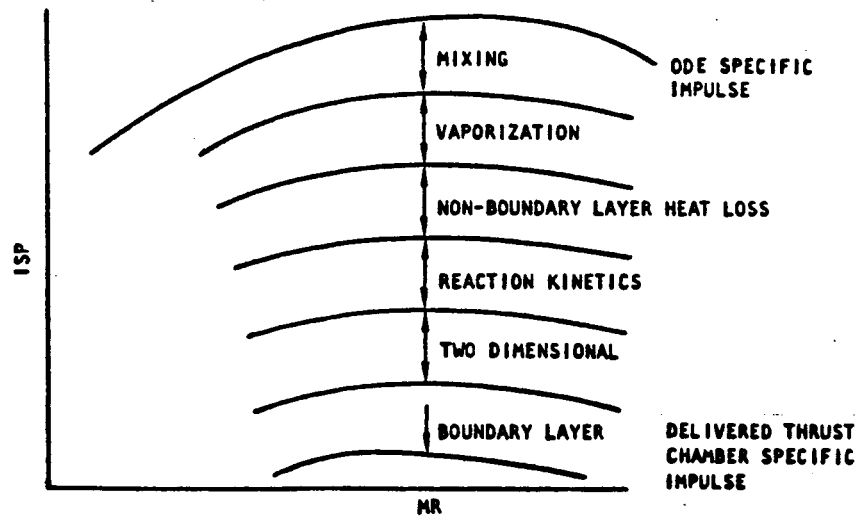
Fig. 1.2 Illustration of Thrust Chamber Losses from Ideal Performance

equilibrium are referred to as energy release losses or as <u>injector losses</u>. These losses have been theoretically modeled by previous investigators, and among the codes developed over the years, the currently-accepted ones by the propulsion community and recommended by JANNAF are the following injector characterization codes: Coaxial Injection Combustion Model (CICM) and Standard Distributed Energy Release Model (SDER).

The reaction products are expanded subsonically in the convergent part and supersonically in the divergent part of the nozzle, where the reactions continue. Deviations from local chemical equilibrium are referred to as <u>reaction kinetic losses</u>. These kinetic losses can be predicted by using the inviscid reacting flow code called the One-Dimensional Kinetics code (ODK) and comparing the results with the One-Dimensional Equilibrium code (ODE) solution.

In the physical expansion process, velocity components normal to the direction of thrust may develop. The losses due to the non-uniform expansion of the available momentum in the direction of thrust are referred to as <u>two-dimensional or divergence losses</u>. These losses can be calculated from the Two-Dimensional and One-Dimensional code solutions.

In the region close to the nozzle wall, viscous effects are significant. The losses due to the momentum decrement at the wall because of momentum and heat transfer in the wall region are referred to as <u>boundary layer losses</u>. These can be calculated by

using such codes as Boundary Layer Integral Matrix Procedure - Version J (BLIMPJ) and Boundary Layer Module (BLM).

Graphically, all the above-described losses are given in Fig. 1.2 which was reproduced from Ref. 1. All the losses are subtracted from the ideal I_{sp} calculated by the ODE program based on one-dimensional assumptions. The heat losses due to radiation and large-scale turbulence in the combustion gases and not included either in the boundary layer or injection analysis are lumped in the non-boundary layer heat losses.

This effort addresses the contract objectives in four sections. These topics yield answers to the following questions addressed in the contract Scope-of-Work:

How shall we conduct the testing for the best results?

What can we afford to be tested?

Are the final test data sufficient and accurate?

The first section focuses on identifying the potential measurements which directly relate to parameters in the input or output of the relevant computer code, the relationship between the measurement and associated parameter, direct measurement, if possible, for the specific performance losses, and measurement location in the thrust chamber. Measured parameters needed for data interpretation are vacuum thrust, flow rates, pressures, enthalpies, compositions, temperatures and velocities. These parameters are usually combined into meaningful performance parameters such as specific impulse (I_{sp}), various efficiencies (or losses), exhaust

properties and boundary layer properties. The above information has been summarized in charts and tables to make it easily accessible.

The second section specifies which type of test would produce the magnitude of individual losses without confounding the measurements with other effects. Many valuable suggestions were made in Ref. 1 as to how to measure individual losses. The recommendations given here extend these ideas and organize them in a systematic manner. Considerations were given to cold flow, hot flow, reactive flow, scaled model, full size configuration, small or large area ratio nozzles, hot wall, controlled heat transfer, etc. The results from these tests will provide the best data for verification of the analytical model.

The third section describes an uncertainty analysis procedure recommended for pre-test and post-test uncertainty evaluation of the measured data. Since it is imperative that these uncertainties be within certain specified bounds to represent useful data, such an analysis is essential particularly for individual loss quantification. Also, an error propagation analysis is provided with the objective to reach an overall performance (specific impulse) uncertainty of approximately one-quarter percent.

The last section identifies leading candidate instrumentation for making various measurements. It describes its manufacturer, presently quoted accuracy, complexity of calibration and operation, advantanges and limitations as well as current cost estimates. Some of the more modern and promising instrumentation are also

presented with their relative advantages or limitations over conventional instruments.

Section 2.0

IDENTIFICATION OF POTENTIAL MEASUREMENTS

The basic measure of rocket engine performance is the thrust per unit mass flow rate of expended propellants, commonly known as specific impulse (I_{sp}). The characteristic velocity (C^*) is also used as a measure of the basic impulse of the engine prior to expansion beyond choked conditions. Measured parameters needed for performance data interpretation are vacuum thrust, flow rates, pressures, enthalpies, compositions, temperatures and velocities. These parameters can be combined into such meaningful performance parameters representing various performance losses or efficiencies, exhaust properties and boundary layer properties in addition to I_{sp} and C^*. Both the data analyst and the test engineer must realize that the parameters of interest may not always be measured directly, but instead may be measured indirectly and related to the parameter through an analytical procedure. It should further be noted that the parameters of interest cannot always be measured directly at the location of interest.

Since the thrust of the present work is to quantify each individual loss present in a thrust chamber, one necessarily has to subtract the actual measured I_{sp} from the ideal or theoretical (ODE) calculation of I_{sp}. In some cases such as the boundary layer losses, they could be measured directly by probing the boundary layer thus providing an alternative to quantify the individual losses. In most rocket engine testing, all these losses may be

present in various proportions thus confounding the results with various effects. The procedure given in the next section separates the individual losses. Thus, if an experiment could be devised to measure only one loss then the loss may be calculated as follows:

$$I_{sp} \text{ Loss} = I_{sp} \text{ (ODE)} - I_{sp} \text{ (measured)} \qquad (2.1)$$

where I_{sp} (ODE) = Theoretical (ODE) I_{sp} calculation

and I_{sp} (measured) = Measured value of I_{sp} including only one loss quantity

In order to characterize the losses, it is necessary to gain insight into such aspects as the flowfield, heat transfer, mixture ratio, gas composition etc. in the thrust chamber. The various parameters used in the performance codes both in their input and output sections could be measured. If direct measurements of these parameters are not possible, then certain related measurements should be made and the parameters be determined from the measurements via appropriate analytical procedures. The rationale behind such painstaking measurements is to identify the current prediction quality and to conclude what could be done to improve the overall performance of the thrust chamber. Finally, the overall performance can be assessed by making direct measurement of thrust and the nozzle mass flow rate.

The measurements for various losses are summarized in the succeeding subsections. The procedures for converting the indirect measurements to the desired parameters are summarized in the attached tables. These tables specifically address the

identification of individual losses and the related input/output parameters in the performance codes.

2.1 INJECTOR LOSSES

As described earlier, the mixing and vaporization losses stemming from less than ideal mixing between the fuel and the oxidizer, improper atomization and vaporization in the case of liquid/liquid or liquid/gas propellant system, and finally, the combustion to equilibrium are lumped to yield the injector losses. The computer codes used in the rigorous procedure are the following:

LISP (DER) — Liquid Injector Spray Pattern Subprogram (of the distributed energy release model) — Calculates droplet spray pattern for liquid/liquid and gas/liquid injectors.

3DC — Three-Dimensional Combustion Program — Calculates simultaneous burning, dispersion, and collisions of sprays following initialization by LISP.

CICM — Coaxial Injection Combustion Model — Replaces LISP and 3DC for coaxial elements.

STC (DER) — Streamtube Combustion Subprogram of the DER Model — Calculates combustion after initiation of streamtube-type flow.

The most universally used parameter to characterize an injector is the characteristic velocity, C* defined by

$$C^* = \frac{P_C A_T}{\dot{m}_T} \qquad (2.2)$$

where P_C = Effective Combustion Chamber Stagnation Pressure
A_T = Throat Area
$\dot{m}_T$ = Mass Flow rate

This parameter is a measure of the maximum flow rate possible for a given system pressure and is also proportional to both the

specific impulse and sonic velocity. The C* parameter is often used as a measure of the injector excellence since fully mixed and reacted propellants generally have higher C* than poorly-mixed and partially-reacted propellants. Since the objectives of the measurements delineated in this section are to identify the discrepancies between the theoretical calculations and measurements, it will be necessary to check for the sources of error in the various processes occurring in the combustion chamber.

The indications of potential error or inefficiencies are:

- Injector losses and C* measurements are inconsistent with predictions.

- The various efficiencies are very low.

- Injector pressure drops are significantly different than predicted.

- Boundary layer start point is significantly different than predicted. (This basically refers to the assumption of ZOM).

- Exhaust compositions are significantly different than predicted.

The sources of discrepancies may lie in:

- Droplet size

- Mixture ratio distribution

- Mass distribution (size distribution)

- Effective chamber pressure

- Inlet enthalpies

- Droplet heating and vaporization rates

- Combustion chamber temperature

Table 2.1 summarizes the measurement parameters related to the

REMTECH INC.

Table 2.1 - INJECTOR LOSSES (MIXING AND VAPORIZATION)

Parameters in Performance Code	Potential Measurements Relating to the Parameters and Specific Performance Loss	Relationship between Measurements and Parameters	Location
INPUT PARAMETER			
Injector element, pattern, chamber length, throat diameter, contraction ratio and nozzle shape	Drawing	-	-
Propellant and operating conditions (T, p, H)	Measurements made at various locations	Same as parameter. Temperature related to enthalpy by temperature integration in the standard way.	-
OUTPUT PARAMETER			
Spray dorplet size distribution (input to predictions such as to STC section of the SDER code)	1. Cold flow tests - holographs with transparent chambers 2. Cold flow tests - photogrametric process with 2-D tranparent wall (unconventional) 3. Cold flow tests - streak photography	Same as parameter	Mixing region downstream of the injector
Spray mixture ratio and mass distribution (Input to predictions such as to STC section of SDER code)	Cold flow tests	Same as parameter	Same as above
Injector pressure loss (output of CICM)	Pressure measurements	Same as parameter	Ahead and aft of injector

REMTECH INC.

Table 2.1 - INJECTOR LOSES (MIXING AND VAPORIZAITON)* - (CONT.)

Parameters in Performance Code	Potential Measurements Relating to the Parameters and Specific Performance Loss	Relationship between Measurements and Parameters	Location
Combustion chamber temperature, T_o	CARS techniques are potential future measurements (unconventional)	—	Combustion chamber
Mass flow rate	Feed system measurement	Calculated from feed system measurement	Feed system
Exhaust gas composition	Radiometric studies, direct probe, etc.	Calulated from radiometric measurement	Nozzle exit plane
C* - Characteristic velocity	Combustion chamber wall pressure and mass flow rate	Simplified method for P_C, given in Ref. γ and $C^* = P_C A_T / \dot{m}_T$	Chamber wall and feed system
Thrust loss	Load cell (strain gage measurements)	Thrust loss = ideal thrust - measured thrust	—
ISP loss	Thrust loss and mass flow rate	$\Delta ISP = \Delta T / \dot{m}_T$	—

*CICM and SDER are two candidate codes.

input/output parameters in the relevant computer code, potential measurements relating to the parameter, relationship between the measurement and parameter, direct measurement, if possible, for specific performance loss, and measurement location in the thrust chamber.

2.2 DIVERGENCE LOSSES

The divergence losses are a result of axial momentum being lost to the radial component of the momentum as the flow contracts and expands through a thrust chamber and thus, are a strong function of the geometry of the thrust chamber. It is well known from the literature that for choked flow, the velocity (or Mach number) distribution in the sonic throat is non-uniform. As the flow expands supersonically in the expansion section of the nozzle, the velocity non-uniformity reduces because of the redistribution of flow velocities.

The appropriate computer codes applicable to the calculation of these two-dimensional losses are the following:

TDK – Two-Dimensional Kinetic Program – Calculates simultaneously expanding and reacting gas flow without viscous effects.

TDE – Two-Dimensional Equilibrium Subprogram contained in the TDK Code – Calculates non-uniform expansion effects using isentropic equilibrium relationships.

TDγ – Two-Dimensional Perfect Gas Subprogram contained in the TDK Code – Uses perfect gas relationships to obtain properties for analyzing non-uniform expansion.

All the above programs and subprograms are located in one code and may be called as required.

Theoretically, the divergence losses are calculated by either

$$\Delta I_{sp} \text{ (Div.)} = I_{sp} \text{ (ODE)} - I_{sp} \text{ (TDE)} \qquad (2.3)$$

or

$$\Delta I_{sp} \text{ (Div.)} = I_{sp} \text{ (ODK)} - I_{sp} \text{ (TDK)} \qquad (2.4)$$

Equation (2.3) is more accurate than Eq. (2.4) since the two codes in Eq. (2.3) calculate the performance based on equilibrium composition of the species, whereas the calculations in Eq. (2.4) contain the effects of kinetics in both codes and may not cancel exactly. However, the advantage of using Eq. (2.4) over Eq. (2.3) is that only one run needs to be made to output the ODE, ODK and TDK values. If an inert gas or air at low temperature is used as the flowing gas, both Eqs. (2.3) and (2.4) would yield the same results. A few calculations need to be made to compare the loss magnitudes from the above equations.

While making measurements on the thrust chamber to identify two-dimensional losses, it is of advantage to measure auxiliary parameters such as wall pressure, velocity distribution and mass flow rate, which would substantiate areas of uncertainty. Potential errors in measurement are indicated when:

- Wall pressures are significantly different than predicted.

- Throat flow rate is significantly different than predicted.

- Measured thrust loss is noticeably different from predictions.

- The exit plane velocity distribution is much different both in magnitude and direction from predictions.

When these discrepancies are indicated by comparing the

measurements with predictions, the sources of error lie in:

- Specification of potential wall contour

- Mixture ratio and mass distribution

- Inlet enthalpies (fuel and oxidizer)

- Effective chamber pressure

- Numerics in TDK in specifying characteristics mesh size

- Specification of the sonic line at the throat - This refers to the transonic solution at the throat region for choked flow situation.

- Non-boundary layer heat losses due to conduction, high scale fluctuations etc. in the combustion chamber.

The performance parameters to be measured, measurements necessary to relate to these parameters and measurements locations are summarized in Table 2.2.

2.3 REACTION KINETIC LOSSES

The reaction kinetic losses are a result of deviations of the reactions occurring in the thrust chamber from complete equilibrium conditions. Because of high temperature and pressure conditions in the combustion chamber, the reactions attain equilibrium. However, as the reaction products expand through the thrust chamber, pressure and temperature fall drastically in the nozzle expansion section, and the reaction kinetics play a significant part in determining reaction rates. The appropriate JANNAF computer codes applicable for the calculation of kinetic losses are the following:

TDK - Two-Dimensional Kinetic Program - Calculates simultaneously expanding and reacting gas flow without viscous effects.

- 15 -

Table 2.2 - DIVERGENCE LOSSES*

Parameters in Performance Code	Potential Measurements Relating to the Parameters and Specific Performance Loss	Relationship between Measurements and Parameters	Location
INPUT PARAMETER			
Mixture ratio - O/F	Cold flow tests (Conventional)	Same as parameter	Mixing region aft of injector
Combustion chamber pressure, P_C	Combustion chamber wall pressure	Simplified method for P_C, given in Ref. 1	Combustion chamber wall
**Inlet enthalpies, H	Temperature measurements. CARS techniques are potential future measurements (unconventional) for measuring temperature.	Temperature related to enthalpy	Propellant feed line
***Combustion chamber temperature, T_C	Thermocouple measurements	-	Combustion chamber
Geometry of the thrust chamber 1. Subsonic portion 2. Throat 3. Supersonic portion	Drawing	Same as parameter	-
Area ratio	Drawing	Same as parameter	-
OUTPUT PARAMETER			
Mass flow rate	Feed system measurement	Calculated from the feed system measurement	Feed system
Pressure distribution and profile	Wall pressure measurements at the nozzle wall and probe studies in the exit plane	Same as parameter	Nozzle wall and exit plane
Velocity profile	Probe studies or LDV	Same as parameter	Nozzle exit plane
Thrust loss	Load cell (strain gage measurements)	Thrust loss = ideal thrust - measured thrust	-
ISP	Thrust loss and mass flow rate	$\Delta ISP = \Delta T/\dot{m}_T$	-

* TDK is the standard JANNAF performance code
** Real propellants option
*** Perfect gas option

ODK - One-Dimensional Kinetic Subprogram contained in the TDK Code
  - Calculates kinetics effects for plane uniform flow.

Theoretically, the kinetic losses are given by

$$\Delta I_{sp} \text{ (Kin.)} = I_{sp} \text{ (ODE)} - I_{sp} \text{ (ODK)} \qquad (2.5)$$

The reason for subtracting the ODK value from the ODE value is to calculate only the kinetic losses, since the other losses would have already been taken out from the theoretical value to compare with the measurement.

While making measurements for determining kinetic losses, several auxiliary parameters relating to kinetic losses should be measured. Normally, the I_{sp} measurements would contain injector, boundary layer and divergence effects. Thus, it is important to identify and quantify these losses using the JANNAF codes before trying to quantify the kinetic losses. In turn, the uncertainties in the other measurements have a magnifying effect on the uncertainty with respect to the magnitude of the kinetic losses. In addition to determining the kinetic losses, other quantities, such as the mixture ratio, combustion chamber pressure, inlet enthalpies, chamber geometry and area ratio which represent the input parameters to TDK, and mass flow rate, pressure distribution, temperature distribution and species composition, which represent the output parameters to TDK, should be measured.

Potential errors in measurement are indicated when:

- Wall pressures are significantly different than predicted.
- Throat flow rate is significantly different than predicted.

- Measured thrust loss is noticeably different from predictions.

- Exhaust composition and temperatures are significantly different than predicted.

- The exit plane velocity distribution is much different both in magnitude and direction from predictions.

When these discrepancies are indicated in the measurements, the sources of error may lie in:

- Specification of potential contour (If non-equilibrium effects exist in the boundary layer which are not accounted for by the boundary layer code, BLIMPJ, there will be some error in specifying the potential contour.)

- Mixture ratio and mass distribution

- Inlet enthalpies (fuel and oxidizer)

- Effective chamber pressure

- Numerics in TDK in specifying the sonic line and mesh size

- Table look-up reaction rates

- Non-boundary layer heat losses

The performance code parameters to be measured, measurements necessary to relate to these parameters ad measurement location are summarized in Table 2.3.

2.4 BOUNDARY LAYER LOSSES

The boundary layer losses in the thrust chamber are a result of losses in the available thrust caused by transfer of momentum and heat to the wall. In most rocket engines, these losses are more significant than the other losses described earlier. Especially in engines, which utilize high area ratios to achieve a higher specific impulse, these losses might even be a higher

REMTECH INC.

Table 2.3 - REACTION KINETIC LOSSES[a]

Parameters in performance code	Potential measurements Relating to the parameters and specific Performance loss	Relationship between Measurements and Parameters	Location
INPUT PARAMETER			
Mixture ratio - O/F	Cold flow test (Conventional)	Same as parameter	Mixing region aft of injector
Combustion chamber pressure, P_C	Combustion chamber wall pressure	Simplified method for P_C, given in Ref. 1	Combustion chamber wall
Inlet enthalpies, H	Temperature measurements	Temperature related to enthalpy	Propellant feed lines
Combusiton chamber temperature, T_C	CARS techniques are potential future measurements (unconventional)	-	Combustion chamber
Geometry of the thrust chamber	Drawing	Same as parameter	-
Area ratio	Drawing	Same as parameter	-
OUTPUT PARAMETER			
Mass flow rate	Feed system measurements	Calculated from the feed system measurements	Feed system
Pressure distribution on the wall - expansion rate	Wall pressure measurements	Same as parameter	Nozzle wall
Pressure profiles	Probe studies	Same as parameter	Nozzle exit plane
Velocity profiles	Probe studies LDV	Same as parameter	Nozzle exit plane
Exhaust gas composition and temperature	Nonintrusive studies such as radiometric studies	Calculated from the radiometric measurements	Nozzle exit plane
Thrust loss	Load cell (strain gage measurement)	Thrust loss = ideal thrust - measured thrust	-
ISP loss	Thrust loss and mass flow rate	$\Delta ISP = \Delta T / \dot{m}_T$	-

[a]TDK is the standard JANNAF performance code

percentage of the total losses. The appropriate JANNAF computer code applicable for the calculation of boundary layer losses is the following:

BLIMPJ – Boundary Layer Integral Matrix Procedure: Version J – Calculates viscous effects at the wall assuming equilibrium composition in the boundary layer.

Theoretically, the boundary layer losses are given by

$$\Delta I_{SP} \text{ (Boundary Layer)} = \text{BLIMPJ calculation}$$
(Straight calculation from BLIMPJ using the computations of δ^* and θ)

In order to understand the flowfield and chemistry of the hot gas in the nozzle boundary layer, several auxiliary measurements are usually made. In addition to making direct thrust measurements, other quantities such as mixture ratio, combustion chamber pressure, total enthalpy, wall temperature, pressure distribution along the wall and geometry of the thrust chamber, which simulate the input parameters to BLIMPJ, and such quantities as heat transfer to the wall, velocity and temperature profiles in the boundary layer, turbulence in the boundary layer, and exhaust gas composition, which simulate the output of BLIMPJ, need to be measured.

Potential errors in measurement are indicated when:

● Wall temperature measurements are significantly different from predictions.

● Wall heat fluxes are significantly different from BLIMPJ predictions.

● Total heat load from the boundary layer is significantly different from BLIMPJ predictions.

- Boundary layer composition, and temperature, pressure and velocity profiles normal to the wall are significantly different from BLIMPJ predictions.

- The measured boundary layer thrust (or I_{sp}) loss is quite different from BLIMPJ math model predictions.

When these discrepancies are indicated in the measurements, the sources of error may lie in:

- Computation of wall temperature profile

- Starting point of the boundary layer

- Non boundary layer heat losses

- Mixture ratio and mass distribution

- Gas transport table look-up properties being incorrect

- Nonuniformity of pressure in the boundary layer, as evident in thick boundary layer situations.

- Presence of chemical kinetic effects in the boundary layer

- Friction and heat transfer correlations (turbulence model)

- Engineering assumptions made in computing boundary layer losses

The updated performance code (BLIMPJ) parameters to be measured, measurements necessary to relate to these parameters and measurement locations are summarized in Table 2.4.

Table 2.4 - BOUNDARY LAYER LOSSES[*]

Parameter in Performance Code	Potential Measurements Relating to the Parameters and Specific Specific Performance Loss	Relationship between Measurements and Parameters	Location
INPUT PARAMETER			
Mixture ratio - O/F	Cold flow test (conventional)	Same as parameter	Mixing region aft of the injector
Combustion chamber pressure, P_C	Combustion chamber wall pressure	Simplified method for P_C, given in Ref. 1	Combustion chamber wall
Edge gas total enthalpy, H_o	CARS techniques are potential future measurement (unconventional)	Combustion temperature equal to edge gas temperature and temperature related to enthalpy	Combustion chamber
Wall enthalpy, H_W	Wall temperature and C_p from thermocouple tables	$H_W = C_C T_W$	Nozzle
Gas transport properties	Not measured - JANNAF tables	Used in BLIMPJ	-
Pressure distribution on the wall	Wall pressure	Same as parameter	Nozzle wall
Geometry of the thrust chamber - combustion chamber, converging/ diverging nozzle	Drawing; measured area for either short or long duration testing	Same as parameter	-
Wall roughness, if present - may also develop in the whole of parts of the chamber wall while in operation; equivalent sand roughness	Roughness density, roughness profile data	Same as parameter; equivalent sand roughness is related to roughness parameters by expressions given in Ref. 4	Nozzle wall
Particle or condensation (two-phase) effects - particle size	Particle density and particle size	Same as parameter	Particle generator and nozzle exit plane
Mass flow rate through the nozzle throat	Feed system measurements	Calculated from the feed system measurements	Feed system

[*]BLIMPJ is standard JANNAF performance code.

REMTECH INC.

Table 2.4 - BOUNDARY LAYER LOSES - (CONT.)

Parameters in Performance Code	Potential Measurements Relating to the Parameters and Specific Performance Loss	Relationship between Measurements and Parameters	Location
OUTPUT PARAMETER			
Heat transfer rate at the wall	1. Thermocouple measurements 2. Heat transfer gage 3. Phase change 4. Calorimetric measurements	1. Thin-skin or thick-skin relationship 2. Same as parameter 3. Time-dependent 4. Temperatures related to heat transfer rate	Nozzle wall
Velocity and temperature profiles in the boundary layer	Probe studies for velocity and temperature. Integration of velocity profiles yields thrust loss.	Same as parameter	Nozzle boundary layer profiles
Turbulent length scale and turbulent shear stress variation in the boundary layer	Hot-wire anemometric measurements yield turbulent fluctuating quantities.	Turbulent fluctuation quantities related to Reynolds shear stress by standard methods. From this shear stress, by length scales can be derived and compared against BLIMPJ turbulence models.	Nozzle boundary layer profiles
Exit plane velocity	LDV or probe studies	Same as parameter	Nozzle exit plane
Exhaust gas temperature composition	Nonintrusive studies such as radiometric	Calculated from radiometric measurements	Nozzle exit plane
Thrust loss	Load cell (strain gas measurement)	Thust loss = ideal thrust - measured thrust	-
ISP loss	Thrust loss and mass flow rate	$\Delta ISP = \Delta T/\dot{m}_T$	-

Section 3.0

TESTS TO SEPARATE INDIVIDUAL LOSSES

The previous section dealt with the types of measurements necessary either to measure the individual performance loss directly or to measure important parameters which characterize a specific performance loss. For example, in determining the total boundary layer loss, it was advised to measure wall heat transfer rates in addition to the thrust loss measurement.

Many ideas have been tried in the past to design tests to measure individual losses without confounding the measurements with other effects. Many valuable suggestions were made in Ref. 1 how to measure individual losses. The recommendations given here extend these ideas and organize them in a systematic manner. Considerations were given to cold flow, hot flow, reactive flow, scaled model, full size configuration, small to large area ratio nozzles, hot wall, controlled heat transfer, etc. The results from these tests will provide the best data for verification of the analytical model.

There are at least two philosophies in trying to measure these losses. One is to design tests so that measured losses may be compared against results from the performance codes. In such a case, more than one nozzle design could exist and tests could be performed at various facilities to measure the appropriate losses. The other philosophy is to conduct various tests to improve the efficiencies of a particular nozzle in the design phase.

3.1 General

The overall philosophy and recommendations for separating individual losses with associated test designs are given in the following subsections.
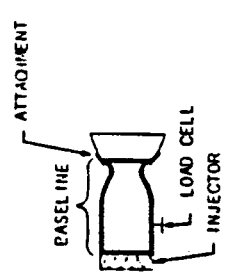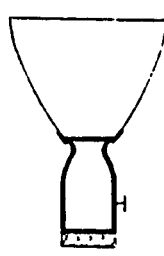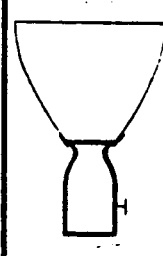
3.1.1 Injector Losses

Injector design can influence engine performance more significantly than any other component design. For many propellants and operating conditions, injector design and analysis procedures are still not clearly defined and testing is the only way to ultimately prove the superiority of a design concept. For high area ratio engines, it is necessary to test in an altitude facility. The expense of testing in such a facility is high and inexpensive ways must be employed in order to characterize the injectors.

Low area ratio nozzle tests are well suited substitutes which do not need elaborate altitude facilities. Information from these tests can be used to evaluate the relative performance of the injectors and to reduce the overall uncertainty in the high area ratio nozzle performance predictions. For these low area ratio tests, specific impulse is the primary parameter of interest in assessing injector performance. However, the characteristic velocity, C^* can also be used.

The low area ratio nozzle (See Table 3.1 Set-up 1) is particularly suited for characterizing the injector, because

● Reaction kinetics and boundary layer effects are small.

Table 3.1 – TESTS DESIGNED TO SEPARATE INDIVIDUAL LOSSES

Test Set-up	Nozzle Configuration	Flow type	Measured Loss Quantities*	Comments
1. (ATTACHMENT, BASELINE, LOAD CELL, INJECTOR)	• Baseline – Required measurement • Short expansion section – Additional measurement	• Reactive	$L_A = \boxed{A+B} + \boxed{C+D}$	• Injector and divergence losses are predominant. • Reaction kinetics are negligible. • Boundary layer effects are small. • Divergence effects are significant in low area nozzles. • Can determine the effects of varying nozzle lenths on L_A.
2.	• Base line – Required measurement • Short expansion – Additional measurement	• Cold or • Hot	$L_B = \boxed{B} + \boxed{D}$	• Divergence losses are predominant. • Boundary layer effects are small. • Can determine the effects of varying nozzle lengths on L_B.
3.	• Higher area ratio nozzles	• Reactive	$L_C = \boxed{A+C+D} + \boxed{B}$	• Reactive kinetics, injector, and boundary layer losses are predominant. • Divergence losses are small. • Can determine the effects of varying area ratios on L_C.
4.	• Higher area ratio nozzles	• Hot	$L_D = \boxed{D} + \boxed{B}$	• Boundary Layer losses are predominant. • Divergence losses are small. • Can determine the effects of varying area ratios on L_D.

* A. Injector (mixing and vaporization) losses
  B. Divergence losses
  C. Kinetic losses
  D. Boundary layer losses

L_A, L_B, L_C, L_D refer to measured quantities from the test set-ups and are defined as L_A, L_B, L_C, L_D = ODE – Measurement

□ (boxed) Predominant   □ Negligible
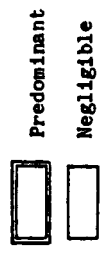
- The two-dimensional or divergence effects are more impor-
tant in low area ratio nozzles than high area ratio nozzles
for both hot flow and cold flow situations. The divergence
effects could, however, be separated from either computer
code results or other test results (described later).

Major concerns in setting up low area tests are:

- Avoiding separation - This was an important consideration
in the combustor design undertaken by REMTECH and reported
in Ref. 2. This testing was done on a short-duration basis
in the IBFF (Impulse Base Flow Facility) at Marshall Space
Flight Center.

- Accurate thrust measurement - This could be accomplished
using a load cell adjusted for vacuum thrust situation.
The accuracy is somewhat compromised when the thrust
chamber is calibrated with all the piping and attachements
for the injector. Inaccuracies also result if the thrust
is calculated from exit plane measurements with intrusive
probes.

- Minimizing aspiration - This can be accomplished with a
scaled model in a small altitude facility.

- Simulating actual propellant injection condition to accura-
tely model injector behavior.

Some key data that can be obtained from such tests are:

- Energy release efficiency or injector I_{sp} losses comprising
mixing and vaporization losses

- Heat transfer effects on the nozzle throat and other areas

- Wall pressure distribution in the chamber

- C* energy release efficiency

3.1.2 Divergence Losses

As previously described, the two-dimensional effects or the

divergence losses are usually much more pronounced in low than in

high area ratio nozzles, since the two-dimensional efficiency

decreases rapidly at low area ratios for the same percent length.

Cold-flow tests are particularly suitable for characterizing the divergence losses, because

- These losses are not functions of propellant combination, thrust, pressure, and mixture ratio.

- It is less expensive to test.

- Either full-scale or subscale nozzles can be used.

- By designing the right range of cold-flow temperatures, the heat transfer rates at the wall can be minimized. Depending on the size of the nozzle, the boundary layer effects can also be minimized.

The test Set-up could be similar to the one given in Set-up 1 of Table 3.1 except that no injector is required (Set-up 2). This would yield divergence losses only. In order to change the area ratio, an additional nozzle section could be attached to the existing section as shown in the above Set-up.

Some key data that can be obtained from such test are:

- Two-dimensional losses

- Variation of these losses as a function of area ratio, length, etc.

- Since testing was done on the same nozzle in Set-up 1 of Table 3.1, the two-dimensional losses necessary to correct those measurements can be evaluated from this set-up.

3.1.3 Kinetic Losses

These losses are a result of non-equilibrium effects of the reacting gases flowing through the thrust chamber and can only occur in reactive systems. Since reaction kinetic effects are virtually absent in the combustion chamber and in low area ratio nozzles, one should examine high area ratio nozzles with high

expansion rates. Low pressures in the divergent part of the nozzle are usually responsible for non-equilibrium effects.

Major steps in setting up this test are the following:

● The Set-up 3 given in Table 3.1 may be used for this measurement so that the injector element mixes the propellants well and the mixture is allowed to react in the combustion chamber.

● A medium to high area ratio nozzle must be used for the kinetics to be of significance in the nozzle expansion.

● Approximately two or more nozzle sections should be tested in order to differentiate the kinetic effects due to the size and the expansion ratio of the nozzle.

● Boundary layer effects will be present in the performance measurements. The measured thrust data must be corrected for boundary layer losses.

Some key data that can be obtained from such a test are:

● Kinetic losses

● Heat transfer rates to the wall

● Wall pressure distribution in the nozzle

● Exit plane product composition

3.1.4 Boundary Layer Losses

Boundary layer losses are a regular feature of all nozzles. An example of theoretical loss calulation relative to the 20K engine is given in Fig. 3.1. It is obvious that for such a moderately large area ratio nozzle, the boundary layer losses will be significant. It is expected that as the area ratio increases, these losses will also grow.

The moderate to large area ratio nozzles are suitable for making boundary layer loss measurements. Moreover, hot flow tests
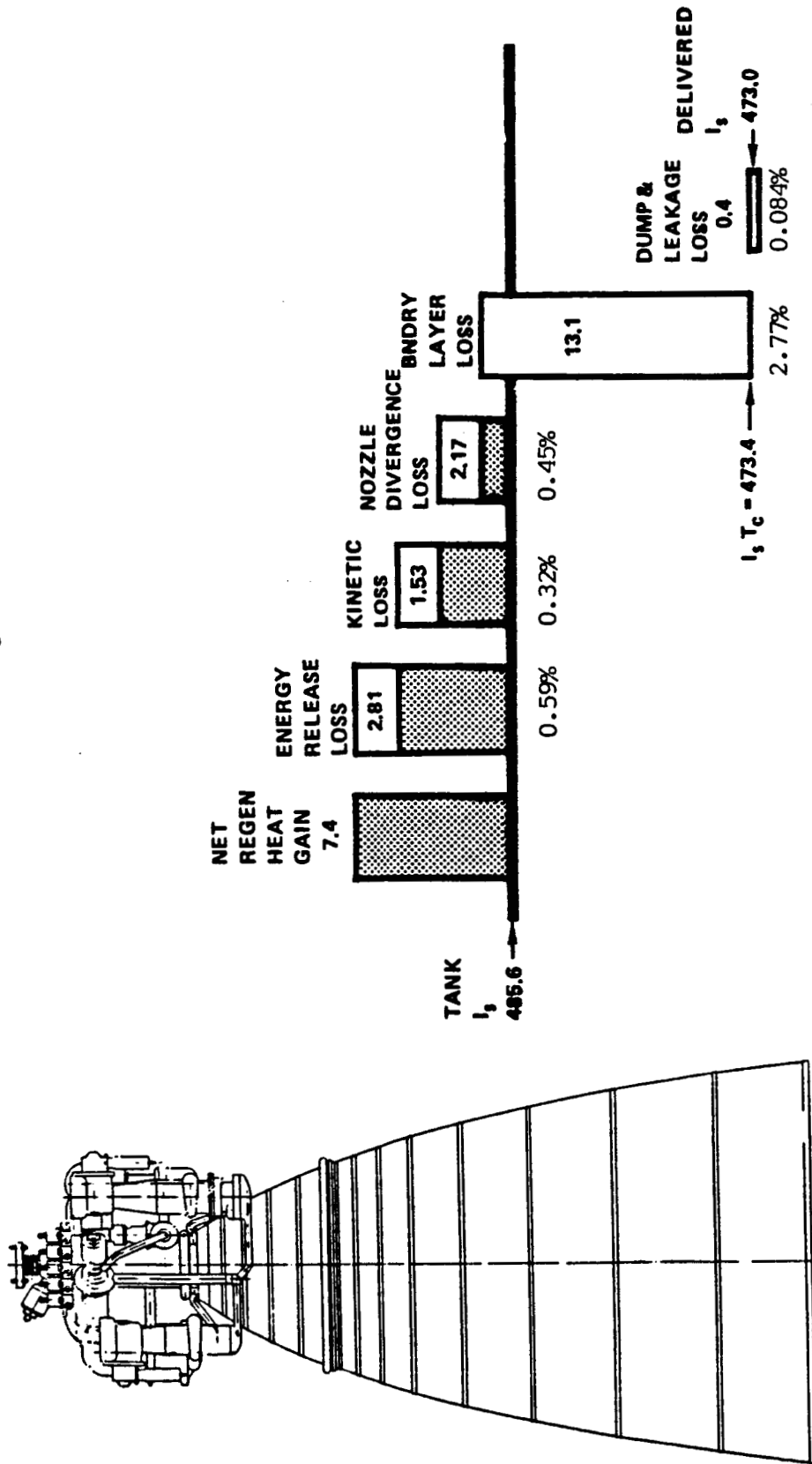
$\epsilon = 400$, $P_c = 2000$ psia

Fig. 3.1 -20K Engine Performance Breakdown (Courtesy of Rocketdyne Division of Rockwell International)

rather than reactive flow tests are more appropriate for measurements, because

- Injector losses and kinetic effects are absent.

- It is more cost effective to run a hot flow test than a reactive flow test.

- As the area ratio increases, the divergence losses are minimized. The measured data could be corrected for any divergence effects by using the data from the previous described testing.

The test Set-up is similar to the one described in Set-up 3 of Table 3.1, but the injector is not necessary. Major concerns in setting up this test (shown in Set-up 4 of Table 3.1) are:

- Using air only at moderately high temperatures $(T \simeq 300^{\circ}F)$ in the chamber to avoid reaction between N_2 and O_2.

- Using an inert gas such as argon, freon, etc. which do not react when heated to a high temperature.

- Avoiding nozzle flow separation

- Test duration – In short duration testing it is hard to measure thrust by a load cell. Also, it is more difficult to probe the boundary layer. In long-duration testing, however,

   1. Scaling problems are alleviated.
   2. More than one measurement per run can be made.
   3. High altitude simulation requires a very large facility.
   4. Depending on the nozzle size and test duration, cost can be a factor.

Some of the key data that can be obtained from such tests are:

- Boundary layer loss measurement

- Heat transfer effects on the nozzle wall

- Boundary layer probe measurements in the nozzle – An example is the tests by Back and Cuffel (Ref. 3).

3.2 PROCEDURE TO SEPARATE INDIVIDUAL LOSSES

Given the recommendations in Section 3.1, two procedures are suggested here to proceed with a test program and separate the individual losses from the test results.

- Rigorous Procedure
- Simplified Procedure

3.2.1 Rigorous Procedure

In this procedure, the test Set-ups required to measure the appropriate quantities are given in Table 3.1.

1. A base-line configuration needs to be designed first containing the combustion chamber section and a nozzle throat section.

2. The design should include ways to attach various area ratio nozzles to the base-line configuration.

3. Injector sections and the required lines should also be designed to be attached to the base-line configuration.

4. In this procedure, care must be taken to match p_C, T_C and throat mass flow rate in various Set-ups.

5. Assuming that A,B,C,D represent pure injector, divergence, kinetic and boundary layer losses, respectively, the corresponding measured quantities in the 4 Set-ups are L_A, L_B, L_C, and L_D, where L is defined by

$$L = I_{sp} \text{ (ODE)} - I_{sp} \text{ (measured)} \tag{3.1}$$

Each measured quantity contains the various losses in certain proportions as shown in Table 3.1 (column 4). Some comments are made in the next column as to the magnitudes of the confounding losses present in these measurements.

6. A procedure is given in Table 3.2 to separate individual losses from the above measurements. The separated individual losses (L_{Inj}, L_{Div}, L_{Kin}, and L_{BL}) still contain other losses in negligible quantities, which can be identified from the performance codes.

More details of the test set-up and instrumentation necessary to conduct these tests are given later in Section 5.0.

3.2.2 Simplified Procedure

Since it is extremely troublesome to match P_c, T_o and $\dot{m}_T$ in each of the Set-ups given in Table 3.1, it is suggested that a more simplified approach be adopted to separate the individual losses.

1. Test Set-ups 2 and 4 in Table 3.1 can be conducted with the nozzles at the the same facility or subscale nozzles at a different facility (test site) than Set-ups 1 and 3.

2. P_c, T_o and $\dot{m}_T$ need not be matched between set-ups (1,3) and (2,4), so long as they are the same within their groups.

3. Set-ups 2 and 4 could be designed with reasonable values of P_c, T_o and $\dot{m}_T$ using a hot or cold gas depending on the requirement.

4. Various gases and various chamber conditions could be used in set-ups 2 and 4 in order to check the validity of the measurements against the appropriate performance code and establish a math model for divergence and boundary layer losses.

5. A procedure is given in Table 3.3 to separate the individual losses from the measurements.

Table 3.2 - CALCULATION PROCEDURE TO SEPERATE INDIVIDUAL LOSSES IN RIGOROUS PRECEEDURE

Losses	Individual Losses Separated	Comments
Injector Losses	$L_{Inj} = L_A - L_B = \boxed{A} + \boxed{C}$	• A is predominant in L_{INJ} • L_{INJ} contains a small amount of C. • C may be taken out based either on measurements or on code. • Depending on which flow type is used in L_B, the boundary layer losses might not cancel exactly between L_A and L_B measurements. The boundary layer contributions may be minimized by adjusting the total temperature of the gas in L_B measurements.
Divergence Losses	$L_{Div} = L_B = \boxed{B} + \boxed{D}$	• B is predominant in L_{DIV} • L_{DIV} contains small amount of D. • D may be taken out based either on measurements in set-up or on code.
Kinetic Losses	$L_{Kin} = L_C - L_D = \boxed{A + C}$	• L_{KIN} contains both A and C. • A must be taken out based on previous model or code.
Boundary Layer Losses	$L_{BL} = L_D = \boxed{D} + \boxed{B}$	• D is predominant in L_{BL}. • L_{BL} contains a small amount of B. • B may be taken out based on measurements or code.

☐ Predominant   ☐ Negligible

ᵃA. Injector (mixing and vaporization losses)
B. Divergence Losses
C. Kinetic Losses
D. Boundary Layer Losses
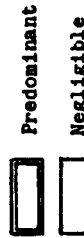
L_A, L_B, L_C, L_D refer to measured quantities and are defined as L_A, L_B, L_C, L_D = ODE - measurement

REMTECH INC.

Table 3.3 - Calculation Procedure to Separate Individual Losses in Simplified Procedure

| Losses	Individual Losses	Comments
Divergence Losses	$L_{Div} = L_B = \boxed{B} + \boxed{D}$	• B is predominant in L. • L_{Div} contains a small amount of D. • D may be taken out based on math model derived from measurements and/or code.
Boundary Layer Losses	$L_{BL} = L_D = \boxed{D} + \boxed{B}$	• D is dominant in L_{BL}. • L_{BL} contains a small amount of B. • B may be taken out based on math model derived from measurements and/or code.
Injector Losses	$L_{Inj} = \boxed{A} + \boxed{C+D}$	• A is predominant in L_{Inj}. • L_{Inj} contains small amounts of C and D. • D may be taken out based on math model in the second row. • C may be taken out based on math model derived from measurements and/or code.
Kinetic Losses	$L_{Kin} = L_C - D$ (Math Model) = $\boxed{A+C} + \boxed{B}$	• L_{Kin} contains both A and C, and negligible amount of B. • A must be taken out based on math model derived from measurements and/or code. • B may be taken out based on math model in the first row.
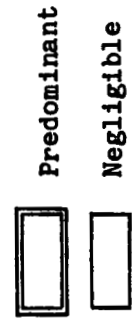
☐ Predominant   ☐ Negligible

* A. Injector (mixing and vaporization) losses
  B. Divergence Losses
  C. Kinetic Losses
  D. Boundary Layer Losses

L_A, L_B, L_C, L_D refer to measured quantities and defined as
L_A, L_B, L_C, L_D = ODE - Measurement

Section 4.0

MEASUREMENT ACCURACY

The accuracy of test results has always been a concern of the engineering community but the subject has been a source of controversy, argument and confusion. This has led some in the testing community to ignore the problem in hopes it would go away. However, all measurements have error and attempting to understand all the sources of error possible in the measurement one is making can indeed help eliminate or decrease this error. It will also lend confidence in using the measurement in analysis, design or for whatever purpose the measurement was made. Uncertainty is an estimate of the maximum measurement error. As has been stated earlier, the purpose of this document is to outline a sequence of tests that will permit an engineer to make measurements for Rocket Engine Performance Code Verification. The goal for the measurement uncertainty of the Specific Impulse (I_{sp}) for the code verification tests has been set at 0.25%. One of the tasks of this study was to provide guides in the selection of instrumentation and determine the uncertainty of the measurements for code verification testing. The absence of an uncertainty calculation standard has made comparisons of test results between facilities, companies, and laboratories difficult, if not impossible. However, a literature survey was conducted to select a Test Measurement Accuracy standard, which is presented in detail in Appendix A. This standard has relied heavily on the work of R.B. Abernathy and uncertainty standards

used at the Arnold Engineering Development Center (AEDC). The list of references is included with the appendix.

The specific impulse has been identified by JANNAF as the most significant performance parameter. Its value is either predicted analytically or obtained from measurements. In regard to the specified loss methodology the impulse is also used as a measure to determine the delta losses in the approach presented in this study. The effect of errors in the measurement of the variables used to determine the vacuum specific impulse ($I_{sp_{vac}}$) is analyzed. Actually $I_{sp_{vac}}$ is the parameter normally reported and is determined as

$$I_{sp_{vac}} = \frac{F_{vac}}{\dot{m}_T} = \frac{F_{SITE} + P_a \quad A_e}{\dot{m}_T},$$ (4.1)

where: F_{SITE} is the measured thrust,
P_a is the ambient or test cell static pressure,
A_e is the nozzle exit area,
and $\dot{m}_T$ is the mass flow rate to the thrust chamber.

Table 4.1a gives the method of determining the propagation of uncertainty in the calculation of $I_{sp_{vac}}$ using the measured variables and Table 4.1b gives a sample calculation. The effects of the measurement uncertainty for the variables in the propagation of error in I_{sp} is presented in Fig. 4.1. From Appendix A we see that

$$U_{ADD} = \pm \left(B + \frac{t_{95}S}{\sqrt{n}} \right)$$ (4.2)

For simplicity in the examples of this study we have assumed that the bias term (B) has been eliminated by calibration, the t_{95} term is equal to 2 (more than 30 samples), and the n term is equal to 1 (one test point), so that

TABLE 4.1 - PROPAGATION OF UNCERTAINTY IN MEASUREMENTS IN THE CALCULATION OF $I_{sp_{vac}}$

a. Equations

$$I_{sp_{vac}} = \frac{F_{vac}}{\dot{m}_T} = \frac{(F_{site} + p_a \cdot A_e)}{\dot{m}_T}$$

$$\Delta I_{sp_{vac}} = \left(\frac{\partial I_{sp_{vac}}}{\partial \dot{m}_T}\right) \cdot \Delta \dot{m}_T + \left(\frac{\partial I_{sp_{vac}}}{\partial F_{site}}\right) \cdot \Delta F_{site} + \left(\frac{\partial I_{sp_{vac}}}{\partial p_a}\right) \cdot \Delta P_a$$

$$+ \left(\frac{\partial I_{sp_{vac}}}{\partial A_e}\right) \cdot \Delta A_e$$

$$= \frac{-(F_{site} + p_a \cdot A_e)}{\dot{m}_T^2} \cdot \Delta \dot{m}_T + \frac{1}{\dot{m}_T} \cdot \Delta F_{site} + \frac{A_e}{\dot{m}_T} \cdot \Delta p_a + \frac{p_a}{\dot{m}_T} \cdot \Delta A_e$$

$$S_{I_{sp_{vac}}} = \sqrt{(F_{site} + p_a \cdot A_e)^2 \cdot \left(\frac{S_{\dot{m}_T}}{\dot{m}_T^2}\right)^2 + \left(\frac{S_{F_{site}}}{\dot{m}_T}\right)^2 + \left(\frac{A_e \cdot S_{p_a}}{\dot{m}_T}\right)^2 + \left(\frac{p_a \cdot S_{A_e}}{\dot{m}_T}\right)^2}$$

$$= \frac{1}{\dot{m}_T} \sqrt{\left(\frac{F_{site} + p_a \cdot A_e}{\dot{m}_T}\right)^2 \cdot S^2_{\dot{m}_T} + S^2_{F_{site}} + \left(A_e \cdot S_{p_a}\right)^2 + \left(p_a \cdot S_{A_e}\right)^2}$$

$$\%I_{sp_{vac_{S}}} = \frac{S_{I_{sp_{vac}}}}{I_{sp_{vac}}} \times 100$$

$$U_{add} = B + \frac{2S}{\sqrt{n}}$$

Assume B=0 and n=1, then U_{add} = 2S

$$\%I_{sp_{vac_{U_{add}}}} = 2 \left(\%I_{sp_{vac_{S}}} \right)$$

> b. Example using SSME and U= 0.25% for all parameters and Bias (B) = 0.

F_{site} = 405,300 lb_f, $S_{F_{site}}$ = ±507 lb_f, $U_{F_{site}}$ = ± 1014 lb_f

$\dot{m}_T$ = 1032 lbm/sec, $S_{\dot{m}_T}$ = ±1.29 lbm/sec, $U_{\dot{m}_T}$ = ± 2.58 lbm/sec

P_a = 10 psia, S_{P_a} = ±0.0125 psia, U_{P_a} = ± 0.025 psia

A_e=44.9 ft^2 (6465.6 in^2), S_{A_e} = ±8.082 in^2, U_{A_e} = ±16.164 in^2

$$I_{sp_{vac}} = \frac{F_{site} + p_a \cdot A_e}{\dot{m}_T} = \frac{405,300 + (10 \times 6465.6)}{1032}$$

$$= 455.4 \ lb_f \ sec/lbm$$

$$\left(\frac{F_{site} + p_a \cdot A_e}{\dot{m}_T}\right)^2 \cdot S_{\dot{m}_T}^2 = 345,116.3$$

$$\left(S_F\right)^2 = 257,049$$

$$\left(A_e \cdot S_{p_a}\right)^2 = 6531.9$$

$$\left(p_a \cdot S_{A_e}\right) = 6531.9$$

$$\sum(\quad) = 345116.3 + 257049 + 6531.9 + 6531.9$$

$$= 615,229.1$$

$$S_{I_{sp_{vac}}} = \sqrt{\frac{\sum(\quad)}{\dot{m}_T}} = 0.760$$

$$\%I_{sp_{vac_S}} = \frac{S_{I_{sp_{vac}}}}{I_{sp_{vac}}} \times 100 = 0.1669$$

$$U_{add} = 2 \cdot S_{I_{sp_{vac}}} = 1.520$$

$$\% I_{sp_{vac_{U_{add}}}} = \left(2 \ \%I_{sp_{vac_S}}\right) = 0.334$$

REMTECH INC.
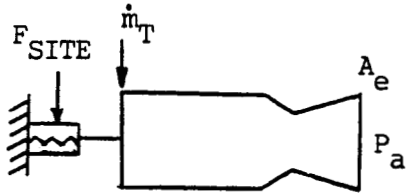
$$I_{SP_{VAC}} = \frac{F_{SITE} + P_a A_e}{\dot{m}_T}$$

○ U_F - Variable

($U_{\dot{m}_T}$, U_{P_a} & U_{A_e} = 0.25%)

△ $U_{\dot{m}_T}$ - Variable

(U_F, U_{P_a} & U_{A_e} = 0.25%)

+ U_{P_a} or U_{A_e} - Variable

(U_F, $U_{\dot{m}_T}$, U_{A_e} or U_{P_a} = 0.25%)
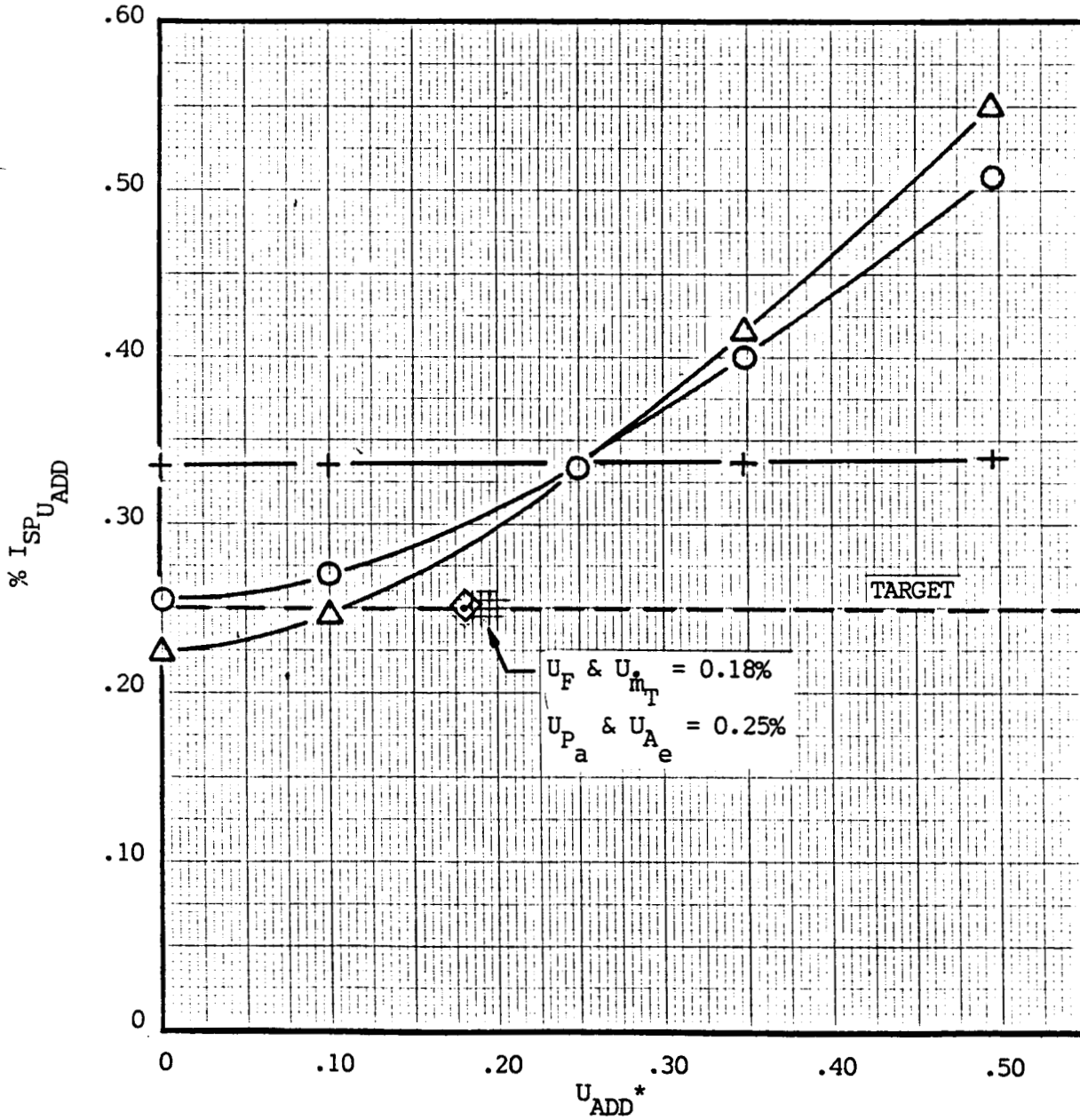
Fig. 4.1 – Effects of Parameter Measurement Uncertainty in the Propagation of Error in $I_{SP_{VAC}}$

$$U_{ADD} = \pm (2S) \tag{4.3}$$

From Fig. 4.1 we can see that the thrust and mass flow uncertainty terms are the primary drivers in the overall uncertainty calculation and that if all the variables are measured to an uncertainty of 0.25% the overall uncertainty in I_{sp} would be 0.33%. The figure also shows that if the measurement uncertainty for thrust and mass flow rate were both 0.19% and the measurement uncertainty of the pressure and nozzle area terms were both 0.25%, then the propagated uncertainty would approach the 0.25% uncertainty goal.

As has been described previously, the approach proposed for determining the losses in the I_{sp} for the code verification is to run a sequence of 4 tests that are designed to isolate the 4 sets of losses: (1) Injector Losses, (2) Divergence Losses, (3) Kinetic Losses, and (4) Boundary Layer Losses. Since the Boundary Layer Losses are the largest, at least for long nozzles, and require a combination of the measurements necessary to support the various loss verifications, the propagation of uncertainty for the measurements to determine the boundary layer losses are the only ones presented. Similar efforts need to be made to propagate uncertainties in other measurements. Table 4.2a gives the equations for propagating the uncertainty of measurements made to compute the input parameters of the boundary layer code and Table 4.2b gives the equations for propagating the uncertainty of measurements made to compute values representing the output parameters of the same code. The same assumptions for B, t_{95}, and n that were used

REMTECH INC.

Table 4.2 - PROPAGATION OF UNCERTAINTY IN MEASUREMENTS FOR BOUNDARY LAYER LOSSES CODE

a. Input

Parameter		Relationship to Measurement	Measurement	Uncertainty, U = ± 2S assuming B = 0 & n = 1
Combustion Chamber Stagnation Pressure	P_o	$P_c \sim$ Simplified Method from CPIA 245 $P_c = f(P_W, A_W, A_T)$	P_W = Comb. Chamber Wall Pressure A_W = Comb. Chamber Crossectional Area A_T = Throat Area	$S_{P_c}^2 \left(\frac{\partial P_c}{\partial P_W}\right)^2 \cdot S_{P_W}^2 \cdot S_{A_W}^2 \cdot \left[\left(\frac{\partial P_c}{\partial M}\right)\left(\frac{\partial A_W}{\partial M}\right)\right]^2 - \left[\left(\frac{\partial P_c}{\partial M}\right)\left(\frac{\partial A_W}{\partial A_T}\right)\right]^2 \cdot S_{A_T}$
Edge Gas Total Enthalpy	H_e	$H_e = C_p T_o$	T_o = Comb. Chamber Total Temperature ($C_p \sim$ Table lookup)	$S_{H_e} = (C_p S_{T_o})^2$
Wall Enthalpy	H_W	$H_W = C_p T_o$	T_W = Nozzle Wall Temperature ($C_p \sim$ Table lookup)	$S_{H_W} = C_p S_{T_W}^2$
Wall Pressure	P_W		P_W = Nozzle Wall Pressure	S_{P_W}
Feed System Mass flow	$\dot{m}$	$\dot{m} = \dot{m}_{ox} + \dot{m}_F$	$\dot{m}_{ox}$ = Oxidizer Mass Flow $\dot{m}_F$ = Fuel mass flow	$S_{\dot{m}} = S_{\dot{m}_{ox}} + S_{\dot{m}_F}$

*Where $\left(\frac{\partial P_c}{\partial P_W}\right) = \left(1 + \frac{\gamma-1}{2} M^2\right)^{\frac{\gamma}{\gamma-1}}$

$\left(\frac{\partial P_c}{\partial M}\right) = P_W \cdot \gamma \cdot M \left(1 + \frac{\gamma-1}{2} M^2\right)^{\frac{1}{\gamma-1}}$

$\left(\frac{\partial A_W}{\partial M}\right) = A_W \left[\frac{(\gamma+1)M}{2\left(1 + \frac{\gamma-1}{2} M^2\right)} - \frac{1}{M}\right]$

$\left(\frac{\partial A_W}{\partial A_T}\right) = \frac{1}{M}\left[\left(\frac{2}{\gamma+1}\right) \cdot \left(1 + \frac{\gamma-1}{2} M^2\right)\right]^{\frac{\gamma+1}{2(\gamma-1)}}$

Where M is determined from

$\frac{1}{M}\left[\left(\frac{2}{\gamma+1}\right) \cdot \left(1 + \frac{\gamma-1}{2} M^2\right)\right]^{\frac{\gamma+1}{2(\gamma-1)}} = \frac{A_W}{A_T}$

REMTECH INC.

Table 4.2 – (Concluded)

b. Output

Parameter		Relationship to Measurement	Measurement	Uncertainty, U = ± 2S assuming B = 0 & n = 1
Heat Transfer Rate	$\dot{q}$	(Calorimetric Measurement) $\dot{q} = C_p \, \dot{m}_c \, \Delta T_c$	$\dot{m}_c$ = Coolant mass flow rate ΔT_c = Coolant differential temp. C_p Table lookup	$S_q = (C_p \, \Delta T_c \, S_{\dot{m}_c})^2 + (C_{p\dot{m}_c} \, S_{\Delta T_c})^2$
Boundary Layer Pressure Distribution (total)	$P_{T_{BL}}$		$P_{T_{BL}} \sim$ Probe or rake	$S_{P_{T_{BL}}}$
Boundary Layer Temperature Distribution (total)	$T_{T_{BL}}$		$T_{T_{BL}} \sim$ Probe or rake	$S_{T_{T_{BL}}}$
Vacuum Thrust	T_{VAC}	$T_{VAC} = T_{site} + P_a A_e$	T_{site} = Measured Thrust (load cell) P_a = Ambient Pressure (test Cell) A_e = Nozzle Exit Area	$S_{T_{VAC}}^2 = S_{T_{SITE}}^2 + (A_e S_{P_a})^2 + (P_a S_{A_e})^2$

previously have been made. However, if such data is available, the bias (B) term is calculated with the same equation as the precision (S) term and the t_{95} term can be determined as shown in the Appendix A.

A letter was sent to members of the rocket testing community to acquire information as to the present measurment uncertainties. The results of the survey confirmed thatthere is no universally accepted standard of reporting measurement uncertainty. Interestingly enough, the two major sources of information for the uncertainty standard have reported measurement uncertainties very nearly the same. Information was requested for measurement of thrust (Axial and Side Force), mass flow rate, pressure, and temperature. Table 4.3 gives the summary of the information received with some information excluded due to the difficulty of interpretation. Since part of the proposed testing will be conducted in a controlled, non-reactive environment, data from some facilities other than rocket engine test facilities have been included. Overall, it appears that in a hot fire test, the goal of 0.25% uncertainty in I_{sp} measurement is not being achieved at present.

ORIGINAL PAGE IS
OF POOR QUALITY

TABLE 4.3
MEASUREMENT AND SPECIFICATION
(A) FORCE

MEASUREMENT	ENVIRONMENT		INSTRUMENT			UNCERTAINTY			REMARKS	INFORMATION SOURCE
	REACTIVE FLOW	COLD/HOT FLOW	TYPE	INSTRUMENT	RANGE CALIBRATION	±B	±S	±U		
Axial Force	X		Load Cell	380K,1bf	20K to 380K*	1236 lbf (0.32%FS)	264 lbf (0.07%FS)	1760 lbf (0.46%FS)	• MV/V Calibrated	AEDC/ETF J-4
Axial Force	X		Load Cell	24K,1bf	4K to 24K*	0.06%Rdg	0.079%Rdg	0.22%Rdg	• Dead Wt. Calibrated	AEDC/ETF T-3
Axial Force	X		Load Cell	120K,1bf	20K to 50K*	0.16%Rdg	0.08%Rgd	0.32%Rdg	• Dead Wt. Calibrated	AEDC/ETF J-5
Axial Force	X		Load Cell	120K,1bf	50K to 80K*	0.11%Rdg	0.05%Rdg	0.21%Rdg	• Dead Wt. Calibrated	AEDC/ETF J-5
Axial Force	X		Load Cell	120K,1bf	80K to 120K*	0.07%Rdg	0.03%Rdg	0.14%Rdg	• Dead Wt. Calibrated	AEDC/ETF J-5
Side Force	X		Load Cell	±40K,1bf	± 40K*	232 lbf (0.58%FS)	220 lbf (0.55%FS)	670 lbf (1.67%FS)	• MV/V Calibrated	AEDC/ETF J-4
Force		X	4-inch diameter 6-component Balance	FA±1000lbf	FS*	0.1501bf	1.2531bf	2.6561bf	• Dead Wt. Calibrated Single Component Loading	AEDC/PWT 16T/S
Force		X	8-inch diameter 6-component Balance	FA±15001bf	FS*	0.1961bf	1.3941bf	2.9041bf	• Dead Wt. Calibrated Single Component Loading	AEDC/PWT 16T/S
Force		X	5-component Hollow Sidewall Balance	FN ± 9000 lbf FY ± 1000 lbf	FN ± 2000 lbf* FY ± 1000 lbf**			FN 3.26 lbf FY 0.41 lbf	• Dead Wt. Calibrated ** Used to Measure Axial Force	AEDC-TR-80-42
Force	X		Load Cell	50K,1bf	0 to 50K	0.1%	0.2%	0.5%		United Technologies, Pratt & Whitney West Palm Beach, FL
Force	X		Calibration Load Cell	2000 1bf				-1.075%FS[1]		NASA/Lewis Research Center High Area Ratio Project
Force	X		Load Cell	1000 1bf				-0.08%FS[1]		NASA/Lewis Research Center High Area Ratio Project
Force	X		Load Cell	1000 1bf				-0.286%FS[1]		NASA/Lewis Research Center High Area Ratio Project
Force	X		Load Cell	1000 1bf				-0.286%FS[1]		NASA/Lewis Research Center High Area Ratio Project
Axial Force	X		Load Cell	300K 1bf	19K to 210K			0.08 to 0.25%[2]	Inplace Calibration	Rocketdyne Division, Rockwell International Sytems Performance and Decision Analysis
Axial Force	X		Load Cell	300K 1bf	10K to 210K			0.23%[2]	Inplace Calibration	Rocketdyne Division, Rockwell International Systems Performance and Decision Analysis
Horiz Force	X		Load Cell	100K 1bf				0.19 to 0.40%[2]	Inplace Calibration	Rocketdyne Division, Rockwell International Systems Performance and Decision Analysis

NOTES:

1 These are values of residual zero and are not values of uncertainty per se.

2 These are standard deviation (sigma) values based on results of instrument calibration for the SSME, NSTL Test Stand A2. It should also be noted that this is a unique test stand for a particular engine and does not represent the accuracy that can normally be obtained during a standard engine test.

TABLE 4.3 (CON'T)
(B) FLOWRATE

| MEASUREMENT | ENVIRONMENT | | INSTRUMENT | | | UNCERTAINTY | | | REMARKS | INFORMATION SOURCE |
| | REACTIVE FLOW | COLD/HOT FLOW | TYPE | RANGE | | | | | | |
				INSTRUMENT	CALIBRATION	±B	±S	±U		
Massflow (Air/Gas)		X	Venturi (1.2502 in.)					0.43 to 0.38 % measured Flow Rate	*Based on theoretically determined flow coefficient (extensive calibration in progress)	AEDC/PWT 16T/S
Massflow (Storable Fuels)	X		Turbine Flowmeter	10 lbs/sec to 1000 lbs/sec		0.2% Rdg	0.15% Rdg	0.5% Rdg	Liquid Rocket Testing	AEDC/ETF
Massflow (cryogenics)	X		Turbine Flowmeter	10 lbs/sec to 1000 lbs/sec		0.4% Rdg	0.3% Rdg	1.0% Rdg	Liquid Rocket Testing	AEDC/ETF
Massflow (Hydro-Carbons)	X		Turbine Flowmeter	50 lbs/hr to 100,000 lbs/hr	5% of meter range full-scale	0.4% Rdg / 0.2% Rdg	0.3% Rdg / 0.15% Rdg	1.0% Rdg / 0.5% Rdg	Turbojet Testing	AEDC/ETF
Volume Flow (Lox)	X		Turbine Flowmeter	70 GPM to 700 GPM	100 GPM to 250 GPM	0.12%	0.165%	0.45%	From test data	United Technologies, Pratt & Whitney West Palm Beach, FL
Volume Flow (LH$_2$)	X		Turbine Flowmeter	70 GPM to 700 GPM	450 GPM to 700 GPM	0.10%	0.20%	0.50%	From test data	United Technologies, Pratt & Whitney West Palm Beach, FL
Mass Flow (oxygen)	X		Venturi Flowmeter	100 PSID Transducer				0.58% FS [1]	Pressure Measurement	NASA/Lewis Research Center High Area Ratio Project
Mass Flow (fuel)	X		Venturi Flowmeter	100 PSID Transducer				-0.38% FS [1]	Pressure Measurement	NASA/Lewis Research Center High Area Ratio Project
Volume Flow	X		Turbine Flowmeter	8500 GPM	5500 to 6200 GPM			0.14% [2]	Hot Fire Calibration	Rocketdyne Division, Rockwell International Systems Performance and Decision Analysis
Volume Flow	X		Turbine Flowmeter	22K GPM	15K to 16.4K GPM			0.04% [2]	Hot Fire Calibration	Rocketdyne Division, Rockwell International Systems Performance and Decision Analysis
Volume Flow	X		Turbine Flowmeter	18K GPM	16.8K GPM			0.45% [2]	Hot Fire Calibration	Rocketdyne Division, Rockwell International Systems Performance and Decision Analysis

TABLE 4.3 (CON'T)
(C) PRESSURE

| MEASUREMENT | ENVIRONMENT | | INSTRUMENT | | | UNCERTAINTY | | | REMARKS | INFORMATION SOURCE |
	REACTIVE FLOW	COLD/HOT FLOW	TYPE	RANGE INSTRUMENT	CALIBRATION	±B	±S	±U		
Pressure	X		Strain gage Transducer	1.0 psia	0.1 to 1.0 psia	0.0036 psia	0.0017 psia	0.007 psia		AEDC/ETF
Pressure	X		Strain gage Transducer	5.0 psia	1.0 to 5.0 psia	0.0175 psia	0.00875 psia	0.035 psia		AEDC/ETF
Pressure	X		Strain gage Transducer	2000 psia	15 to 2000 psia	0.45% Rdg	0.16% Rdg	0.77% Rdg		AEDC/ETF
Pressure		X	Strain gage Transducer	500 psia	0 to 150 psia 150 to 500 psia			~0.5 psia * ~2.0 psia	*End to end measurement calibrated in place.	AEDC/VKF
Pressure		X	Strain gage Transducer	2500 psia	500 to 2500 psia			1.2% + 0.16% Rdg *	*End to end measurement calibrated in place.	AEDC/VKF
Pressure		X	Electronically scanned, silicon press transducer	15 psid	F.S.			0.1% FS		AEDC/PWT
Pressure		X	Electronically scanned, silicon press transducer	100 psia	F.S.			0.1% FS		AEDC/PWT
Pressure		X	Pressure Transducer	5,15,100,250 500,1000,3000 psia	F.S.	0.08% F.S. + 0.07% Rdg	0.023% F.S.	0.12% F.S. + 0.07% Rdg		AEDC/PWT
Pressure		X	Pressure Transducer	4000 psfa		1.2 + 0.012%* Rdg psf	0.3 + 0.005%* Rdg psf	2.0 + 0.028%* Rdg psf	Values for nominal tunnel operating conditions	AEDC/PWT
Pressure	X		Pressure Transducer	15 psia	0 to 15 psia	0.25%	0.125%	0.5%		United Technology, Pratt & Whitney West Palm Beach, FL
Pressure	X		Pressure Transducer	1000 psia	0 to 1000 psia	0.25%	0.125%	0.5%		United Technology, Pratt & Whitney West Palm Beach, FL
Pressure	X		Pressure Transducer	1000 psig				-0.77% FS[1]	Chamber Pressure	NASA/Lewis Research Center High Area Ratio Project
Pressure	X		Pressure Transducer	1500 psig				0.2 to 47% FS[1]	Chamber Pressure	NASA/Lewis Research Center High Area Ratio Project
Pressure	X		Pressure Transducer	10 psid				-0.08% FS[1]	Nozzle Wall Pressure	NASA/Lewis Research Center High Area Ratio Project
Pressure	X		Pressure Transducer	5 psid				0.24% FS[1]	Nozzle Wall Pressure	NASA/Lewis Research Center High Area Ratio Project
Pressure	X		Pressure Transducer	1 psid				1.7 to 5.14% FS[1]	Nozzle Wall Pressure	NASA/Lewis Research Center High Area Ratio Project
Pressure	X		Pressure Transducer	0.6 psid				0.395% FS[1]	Nozzle Wall Pressure	NASA/Lewis Research Center High Area Ratio Project

KEMTECH INC.

ORIGINAL PAGE IS
OF POOR QUALITY

TABLE 4.3 (CON'T)
(C) CON'T

| MEASUREMENT | ENVIRONMENT | | INSTRUMENT | | | UNCERTAINTY | | | REMARKS | INFORMATION SOURCE |
	REACTIVE FLOW	COLD/HOT FLOW	TYPE	RANGE INSTRUMENT	CALIBRATION	±B	±S	±U		
Pressure	X		Pressure Transducer	1 psid				1.6% FS [1]	Capsule Pressure	NASA Lewis Research Center High Area Ratio Project
Pressure	X		Pressure Transducer	15 psid				-0.97 to 2.3% FS [1]	B.L. Total Pressure	NASA Lewis Research Center High Area Ratio Project
Pressure	X		Pressure Transducer	15 psia				0.5% [2]		Rocketdyne Division, Rockwell International Systems Performance and Decision Analysis
Pressure	X		Pressure Transducer	500 psig	0 to 400 psi			0.04% [2]		Rocketdyne Division, Rockwell International Systems Performance and Decision Analysis
Pressure	X		Pressure Transducer	350 psi				0.2% [2]		Rocketdyne Division, Rockwell International Systems Performance and Decision Analysis
Pressure	X		Pressure Transducer	100 psi	0 to 80 psi			0.22% [2]		Rocketdyne Division, Rockwell International Systems Performance and Decision Analysis
Pressure	X		Pressure Transducer	250 psi	0 to 200 psi			0.12% [2]		Rocketdyne Division, Rockwell International Systems Performance and Decision Analysis
Pressure	X		Pressure Transducer	250 psid	0 to 200 psi			0.06% [2]		Rocketdyne Division, Rockwell International Systems Performance and Decision Analysis
Pressure	X		Pressure Transducer	500 psi	0 to 400 psi			0.11% [2]		Rocketdyne Division, Rockwell International Systems Performance and Decision Analysis
Pressure	X		Pressure Transducer	3500 psia	0 to 3500 psia			0.03% [2]		Rocketdyne Division, Rockwell International Systems Performance and Decision Analysis
Pressure	X		Pressure Transducer	600 psia	0 to 600 psi			0.06% [2]		Rocketdyne Division, Rockwell International Systems Performance and Decision Analysis
Pressure	X		Pressure Transducer	4500 psia	0 to 4500 psi			0.15% [2]		Rocketdyne Division, Rockwell International Systems Performance and Decision Analysis
Pressure	X		Pressure Transducer	300 psia	0 to 300 psi			0.02% [2]		Rocketdyne Division, Rockwell International Systems Performance and Decision Analysis

REMTECH INC.

TABLE 4.3 (CONCL)
(D) TEMPERATURE

MEASUREMENT	ENVIRONMENT		INSTRUMENT			UNCERTAINTY			REMARKS	INFORMATION SOURCE
	REACTIVE FLOW	COLD/HOT FLOW	TYPE	RANGE		±B	±S	±U		
				INSTRUMENT	CALIBRATION					
Temperature		X	Thermocouple					3 to 5 °F *	*Curve fits of NBS data for all thermocouples	AEDC/PWT 16 T/S
Temperature		X	Digital Temperature Instrument	32°F to 530°F / 530°F to 2300°F				4°F / 2°F + 0.375% RDG	Ref - Internal compensation Readout in °F	AEDC/VKF
Temperature		X	Low Level Multiplexer	32°F to 530°F / 530°F to 2300°F				4°F / 2°F + 0.375% RDG	Ref - Isothermal region measured with RTD readout in counts	AEDC/VKF
Temperature	X		Thermocouple (Cu/Con)	0°F to 530°F		2.0°F	0.3°F	2.6°F	Ref - fixed	AEDC/ETF J-3, 4, & 5
Temperature	X		Thermocouple (C/A)	32°F to 2300°F		0.4% Rd	1.1°F	0.4% Rdg + 2.2°F	Ref - fixed	AEDC/ETF J-3, 4, & 5
Temperature	X		Thermocouple (C/A)	0°F to 300°F		0.9°F	0.6°F	2.1°F	Ref - Ambient	AEDC/ETF T-3
Temperature	X		Thermocouple (C/A)	250°F to 1500°F		0.36% Rd	0.6°F	0.36% Rdg + 1.2°F	Ref - Ambient	AEDC/ETF T-3
Temperature	X		Thermocouple (Cu/Con)	-300°F to 100°F				1°F *	*Vendor Calibration	United Technology, Pratt & Whitney West Palm Beach, FL
Temperature	X		Thermocouple (C/A)	32°F to 2000°F				5°F or 3/8% Rdg		United Technology, Pratt & Whitney West Palm Beach, FL
Temperature	X		Thermocouple [Pt/Rh(s)]	2000°F to 3000°F				2.5°F or 1/4% Rdg (whichever is less)		United Technology, Pratt & Whitney West Palm Beach, FL
Temperature	X		Thermocouple (C/A)	80°F to 1200°F				± 1°F *	*Special Calibration	United Technology, Pratt & Whitney West Palm Beach, FL
Temperature	X		Resistance Temperature Device (RTD)	160 to 210°R				0.03% ²		Rocketdyne Division, Rockwell International Systems Performance and Decision Analysis
Temperature	X		Resistance Temperature Device (RTD)	160 to 180°R				0.07% ²		Rocketdyne Division, Rockwell International Systems Performance and Decision Analysis
Temperature	X		Resistance Temperature Device (RTD)	460 to 2460°R	-321 to 1221°F			0.05% ²	*Spec. Tol. Requirement	Rocketdyne Division, Rockwell International Systems Performance and Decision Analysis
Temperature	X		Resistance Temperature Device (RTD)	160 to 210°R	-294 to -244°F			0.22% ²	*Spec. Tol. Requirement	Rocketdyne Division, Rockwell International Systems Performance and Decision Analysis
Temperature	X		Resistance Temperature Device (RTD)	405 to 1165°R	-55 to 705°F			0.10% ²	*Spec. Tol. Requirement	Rocketdyne Division, Rockwell International Systems Performance and Decision Analysis

TABLE 4.3 (CONC'L)

(D) CON'T

MEASURMENT	ENVIRONMENT		INSTRUMENT			UNCERTAINTY			REMARKS	INFORMATION SOURCE
	REACTIVE FLOW	COLD/HOT FLOW	TYPE	RANGE INSTRUMENT	CALIBRATION	±B	±S	±U		
Temperature	X		Resistance Temperature Device (RTD)	110 to 610°R	-350 to 150°F			$0.22°^2$	"Spec. Tol. Requirement	Rocketdyne Division, Rockwell International Systems Performance and Decision Analysis
Temperature	X		Thermocouple	300 to 800°R				$0.4°^2$	MFR Tol. Band	Rocketdyne Division, Rockwell International Systems Performance and Decision Analysis
Temperature	X		Thermocouple	160 to 1900°R				$0.4°^2$	MFR Tol. Band	Rocketdyne Division, Rockwell International Systems Performance and Decision Analysis
Temperature	X		Thermocouple	160 to 1100°R				$0.4°^2$	MFR Tol. Band	Rocketdyne Division, Rockwell International Systems Performance and Decision Analysis

Section 5.0

INSTRUMENTATION

If only the vacuum specific impulse was required for verification of the rocket engine performance codes, then only 5 measurements would be required, one geometry measurement prior to the test (nozzle exit area) and four instrumentation measurements during the test (Thrust or Axial Force, Test Cell or Ambient Pressure, and Fuel and Oxidizer Mass Flows). These measurements are combined to give the vacuum specific impulse. For verification of routines involved in the analysis, additional measurements are necessary with locations shown in Table 5.1. This table divides the measurements into 5 components: (1) injector system; (2) fuel and oxidizer system; (3) combustion chamber; (4) nozzle; and (5) complete system. Each component will be considered as it applies to the code verification tests, both reactive and non-reactive, whichever is applicable.

In addition to describing the measurements required and/or desired, manufacturer specification for specific instruments and their quoted accuracies are also included. The mentioned specific instruments and manufacturers do not constitute endorsement of either, but are given as examples to show what accuracies and costs can be expected.

Before beginning the discussion of the individual components, a general discussion of the possible testing techniques is in order.
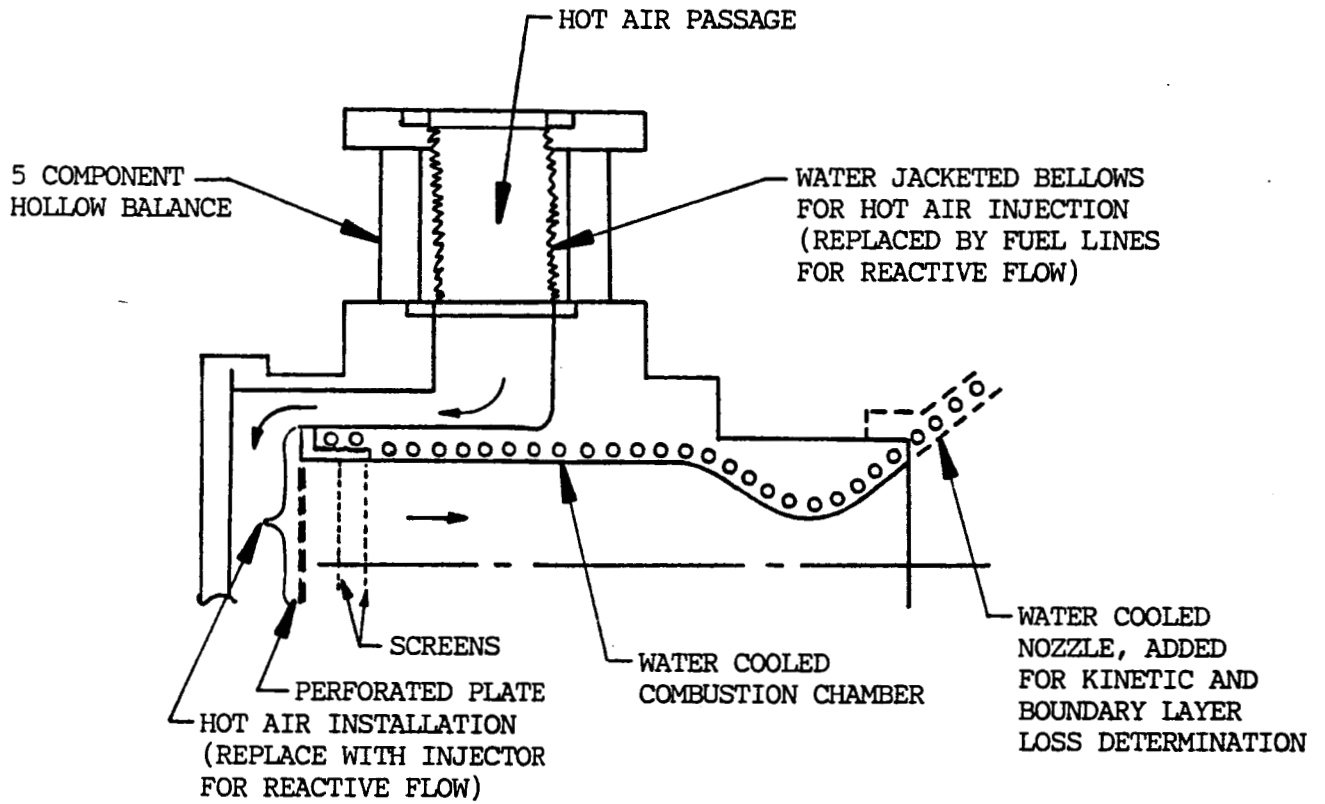
Table 5.1

LOCATION AND MEASUREMENT REQUIREMENTS
FOR CODE VERIFICATION TESTING

1. Pre-test, Injector Sub-system

    a. Injector Mixing Characteristics
    b. Injector Spray Droplet Size

2. Fuel and Oxidizer System

    a. Mass Flow (Fuel and Oxidizer)
    b. Pressure Upstream and Downstream of Measurement Device
    c. Temperature Upstream or Downstream of Measurement Device

3. Combustion Chamber

    a. Wall Pressure
    b. Wall Temperature
    c. Wall Heat Transfer Rate
    d. Total Temperature (Hot Gas Simulation)

4. Nozzle

    a. Wall

        (1) Pressure Distribution
        (2) Temperature Distribution
        (3) Heat Transfer Rate

    b. Boundary Layer (Hot Gas Simulation)

        (1) Pressure Profile
        (2) Temperature Profile
        (3) Turbulence

    c. Exit

        (1) Pressure Profile
        (2) Temperature Profile
        (3) Turbulence (Hot Gas Simulation)
        (4) Exhaust Gas Temperature
        (5) Exhaust Gas Composition (Reactive)

5. Complete System

    a. Thrust (Force)
    b. Side Load (Side Force)

5.1 TESTING TECHNIQUES

The method of separating the various losses for the performance codes verifications that has been proposed in this study calls for 4 basic test Set-ups (2 reactive and 2 hot gas simulation, see Table 3.1). If at all possible, it is desirable to have an exact simulation in pressure, temperature, and mass flow of the actual conditions that exist during the reactive tests or during the hot gas simulation tests. This would be virtually impossible with an operational rocket engine; however, if a test article were designed specifically for codes verification testing, then near simulation should be possible with both operations. Of course the fuel used during the reactive tests would need to burn at a low enough temperature so that close simulation could be accomplished during the hot gas tests as well. An example of a possible model design is shown in Fig. 5.1. Care would need to be taken in sizing the components for flow simulation. At least two hollow balances of the type proposed have been built and operated with high pressure gases and fluids passing through the center, one is at NASA Ames Research Center (Ref. 5) and the other is at AEDC (Ref. 6).

In the event that an operational (or experimental) rocket engine is used for the reactive tests and a separate simulation model is used for the hot gas tests, then separation of the losses is still possible through use of the performance codes as described in Section 3.0, but with some compromising of the data accuracy. In the event that the two test-article approach is taken, the

HOT AIR PASSAGE

5 COMPONENT HOLLOW BALANCE

WATER JACKETED BELLOWS FOR HOT AIR INJECTION (REPLACED BY FUEL LINES FOR REACTIVE FLOW)

SCREENS

PERFORATED PLATE

HOT AIR INSTALLATION (REPLACE WITH INJECTOR FOR REACTIVE FLOW)

WATER COOLED COMBUSTION CHAMBER

WATER COOLED NOZZLE, ADDED FOR KINETIC AND BOUNDARY LAYER LOSS DETERMINATION

1. Nozzle Diameter = 2.5 IN
   Nozzle Area = 4.91 IN^2

2. Chamber Diameter = 4.3 IN.
   Chamber C.S. Area = 14.55 IN^2

3. Hot Air Duct Through Balance Diameter = 4.3 IN.
   H.A. Duct C.S. Area = 14.55 IN^2

4. Hot Air Feeder Line Diameter = 6 IN.
   H.A. Feeder Line C.S. Area = 28.27 IN^2

Fig. 5.1 - Sketch of Rocket Model Concept for Both Reactive and Hot Gas Testing

instrumentation on the rocket engine may be somewhat limited, with the majority of the distribution and profile measurements being made on the hot gas model. If the special one model approach is used, then the instrumentation would be basically the same.

5.2 INJECTOR

The injector mixing characteristics and spray droplet sizes, along with the other combustion chamber flow characteristics, have until now remained problems hard to solve. Because of the hostile environment in the combustion chamber during operation, it has been difficult to make any meaningful measurements. Most of the injector characteristics and droplet size measurements have been made on the injector sub-system, sometimes as a single element and sometimes as multiple elements, using compartmental techniques for mixing characteristics and hot wax for droplet sizing as examples. However, in recent years, due to the advances in instrumentation and measuring techniques, much progress is being made in the areas for nonintrusive measurement of injector performance. Most of these studies are being supported by individual rocket engine manufacturers and are proprietary in nature. However, advances in fiber optics have made it possible to look directly into the combustion chamber to measure the mixing characteristics in the actual operational environment. One such probe is shown in Fig. 5.2. This probe uses a single cable and through the use of back-scatter the focusing and receiving optics can be contained in one probe. Another technique that is being studied (basically for mixing

Fig. 5.2 – Example Specifications for Fiber Optic Probes
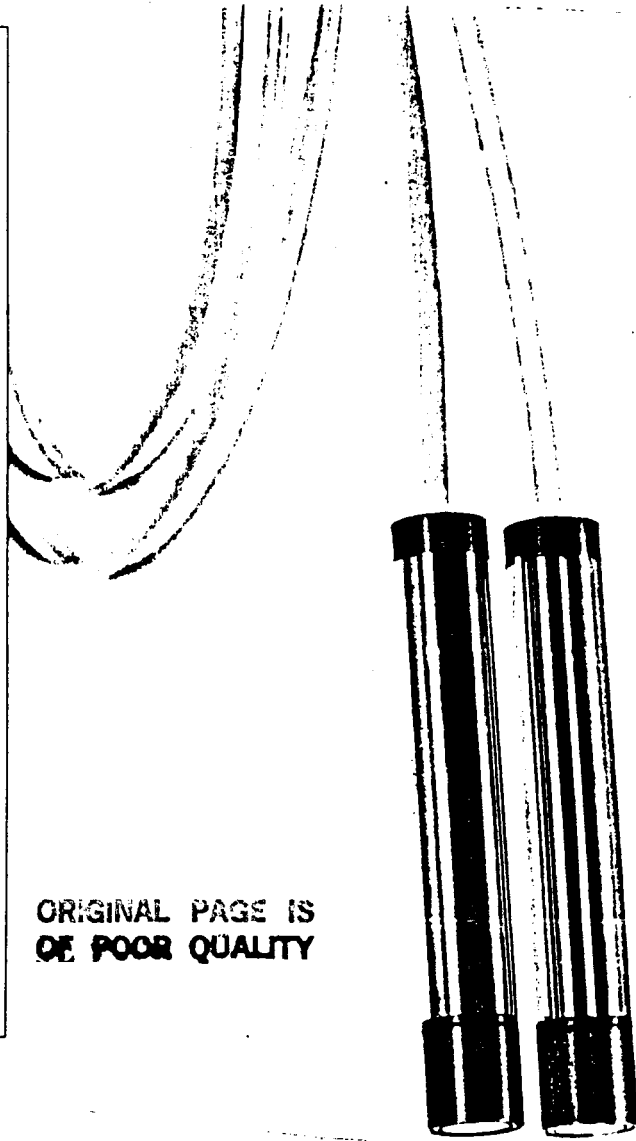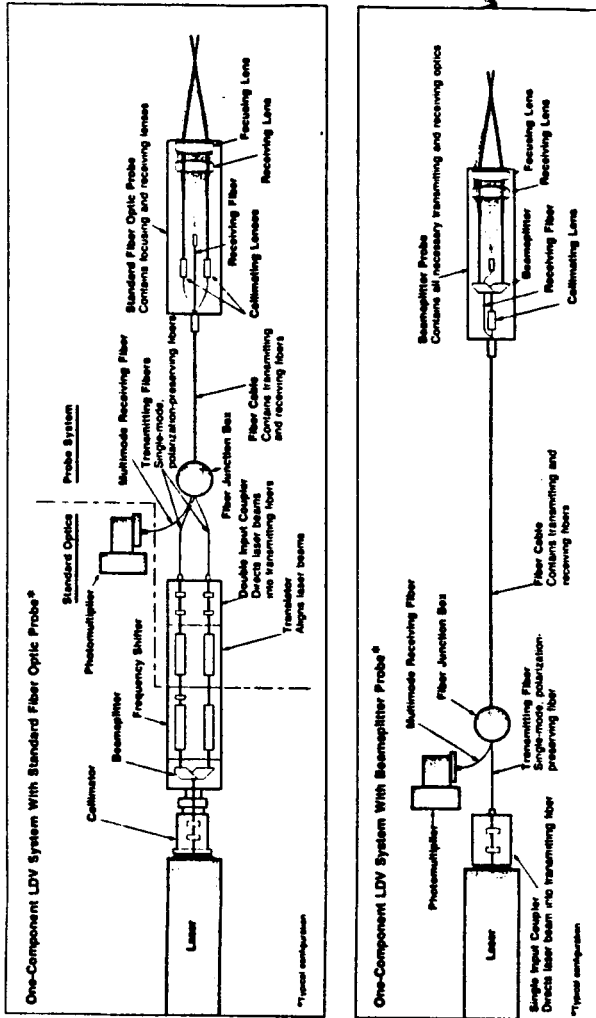
ORIGINAL PAGE IS
OF POOR QUALITY

TSI Fiber Optic Probes

TSI offers a complete series of fiber optic probes. They are available in a variety of sizes, focal lengths, and wavelengths, and most probes are also available in one- or two-component versions.

Standard probes. TSI's standard probes can be used with most laser systems. Even systems with a frequency shifting capability are easily accommodated because each laser beam is transmitted individually through a single fiber. This is beneficial for applications involving flow reversals or low velocities, or those where high turbulence may be encountered.

The small probes (14 mm and 25 mm diameters) create very little disturbance in the flow. Because they are watertight, they can even be immersed in liquids. They can also be placed inside test models to eliminate flow disturbances.

The large probes (83 mm and 190 mm diameters) are available for making measurements at greater distances from the probe's end. Their larger focal lengths and lens apertures provide good spatial resolution and maintain signal quality. Standard large probes are dust tight and can be made watertight on special request.

Beamsplitter probe. TSI also offers a unique beamsplitter probe. Available only in the 14mm diameter size, this probe is fitted with a single transmitting fiber for a single laser beam. A miniature beamsplitter, focusing lens, receiving lens, and a receiving fiber are all contained inside the probe. It is, therefore, a complete one-component optics system in itself, making it ideally suited for applications where the flow is unidirectional. Frequency shifting is not possible with the beamsplitter probe.

System Number	Beamsplitter Probe 9700	Small Diameter Probes				Large Diameter Probes			
		9710	9712	9722	9732	9720	9730	9760	9762
Fiber Outside Dia (mm)	14	14	14	25	25	83	83	190	190
Length (mm)	125	100	100	156	156	300	300	660	660
Velocity Components	One	One	Two	One	Two	One	Two	One	Two
Lens Aperture (mm)	10	10	10	20	20	60	60	150	150
Working Dist. (mm) Air	60	60	60	102,135*	102,135*	120,250 350**	120,250 350**	450,750 1200**	450,750 1200**
Water	80	80	80	135,180†	135,180†	350†	350†	600†	600†

*These probes can be ordered with one of two available lenses.
**These probes can be ordered with one of three lenses available for use in air.
†Available on special request
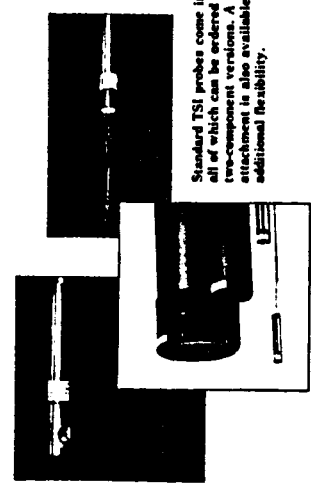
Standard TSI probes come in four sizes, all of which can be ordered in one- and two-component versions. A side-looking attachment is also available to provide additional flexibility.

characteristics) is LDV measurements in a water facility (Ref. 7). The use of photogrametric techniques (Ref. 7) using laser lighting has good potential for application to both mixing characteristics and droplet sizing.

In summary, the measurement of the injector mixing characteristics and droplet sizes is a very important parameter in the verification of the rocket engine performance codes. Great strides are being made in the field of instrumentation and measuring techniques. However, to recommend a standard measuring technique at the present time would be senseless. It is nearly impossible to quote an uncertainty value to the injector mixing characteristics and droplet size measurements. Laser velocimeter type measurements can be made to high degrees of accuracy (0.1%) in carefully controlled experiments, however, to suggest that measurements of 1.0% uncertainty can be made for injector performance would be extremely optimistic (Ref. 8). The engineer involved in a test sequence, or designing a test, for verification of rocket engine performance codes, should select the best technique available at the time, that will give the required input information for the performance codes in question.

5.3 FUEL AND OXIDIZER SYSTEM

The measurement of the mass flow of the engine during a reactive test is usually obtained by measuring the mass flow of the fuel and oxidizer separately and then combining the two measurements to get the total quantity. Precise measurement of

these quantities is critical for accurate determination of the engine I_{sp} (see Fig. 4.1 in previous section). The mass flow measurement uncertainty goal set by Ref. 9 was 0.25% of the operating point. Uncertainty of this magnitude, however, will not yield an overall uncertainty in I_{sp} of 0.25%. Therefore, the measurement uncertainty should be considerably less than 0.25%. Traditionally, the fuel/oxidizer mass flow has been measured with a turbine flowmeter. The nominal uncertainty reported in Table 4.3 appears to be $\pm$ 0.5%, although one rocket company reports a much better accuracy, possibly due to the method of determining uncertainty or to the numerous times the exact same system has been calibrated in place.

The manufacturer's specification sheet for one turbine flowmeter is given in Fig. 5.3. The accuracy for this meter is quoted to be $\pm$ 0.05% for liquid measurement. It should be noted that the linearity is quoted to be $\pm$ 0.5%. Through calibration this meter should give an overall operational accuracy somewhere between these two quoted values.

The specification for a non-intrustive (sonic) flowmeter are given in Fig. 5.4. This meter utilizes the comparison of sound waves transmitted upstream and downstream through the liquid to determine the mass flow rate. Since the meter uses the sound speed difference rather than absolute speed, the effects of such factors as process temperature, pressure, density, or viscosity cancel out. This meter, however, still quotes only an accuracy of $\pm$ 0.5% F.S. (Full Scale). This meter is non-intrusive and it may be possible
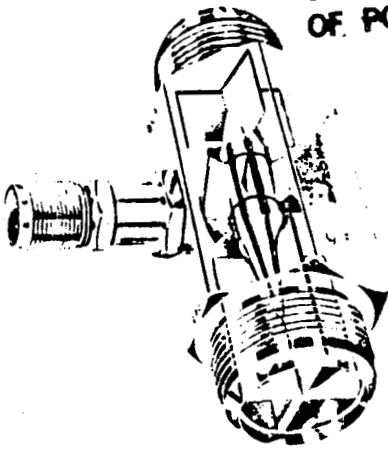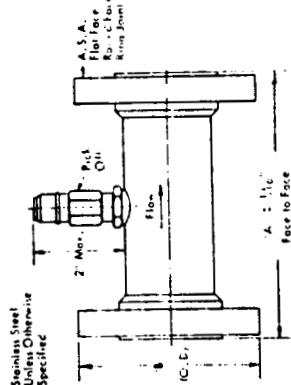
AN (MS 33656) (through 2")
NPT (through 8")
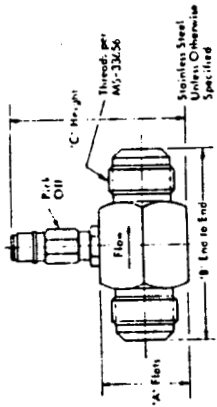
END FLANGED (ASA B16.5):

Stainless Steel Unless Otherwise Specified

SIZES (1 1/2" - 14")

ORIGINAL PAGE IS OF POOR QUALITY

Size & Model	A	B	C
1/4" - 3/8" - 1/2" FT-8M	1" sq	2.45	3
5/8" FT-10M	1 5/16	2.72	3 3/16
3/4" FT-12M	1 3/8	3.25	3 1/4
1" FT-16M	1 5/8	3.56	3 1/2
1 1/2" FT-24M	2 1/8	4.59	4 3/8
2" FT-32M	2 3/4	6.06	4 3/4

Size & Model	A		Size & Model	A
1/2" FT-8C	5		4" FT-64C	12
3/4" FT-12C	*5 or 7		5" FT-80C	14
1" FT-16C	*5, or 8		6" FT-96C	14
1 1/2" FT-24C	*6 or 9		8" FT-128C	16
2" FT-32C	*6 or 9		10" FT-160C	20
2 1/2" FT-40C	9		12" FT-192C	24
3" FT-48C	10		14" FT-224C	28

*Specify at time of order.

Mark No	Nominal End Fitting Size (in)	Normal Flow Range (US GPM or ACFM) Minimum	Maximum	Extended Flow Range (US GPM) Minimum	Maximum	Approximate Frequency Output (CPS)	Approximate K Factor Pulse US Gal or ACFM
FT-4B	1/2	0.25	2.5	0.03	3.0	2300	55000
FT-6B	1/2	0.5	5.0	0.05	5.0	2160	25000
FT-8B	1/2	0.75	7.5	0.1	10.0	2000	16000
FT-8	1/2	1.0	10.0	0.1	10.0	2000	12000
FT-10	5/8	1.25	12.5	0.15	15.0	2000	9600
FT-12	3/4	2.0	20.0	0.25	25.0	2000	6000
FT-16	1	5.0	50	0.6	60.0	2000	2400
FT-20	1 1/4	9.0	90	0.9	90.0	1950	1200
FT-24	1 1/2	15	150	1.5	150.0	1300	800
FT-32	2	20	225	2.5	250.0	900	350
FT-40	2 1/2	30	400	4.5	450.0	650	100
FT-48	3	40	650	7.5	750.0	812	75
FT-64	4	75	1250	15	1500.0	625	30
FT-80	5	90	2000	25	2500.0	390	9
FT-96	6	130	3000	35	3500.0	...	...
FT-128	8	250	5500	60	6000.0	...	...
FT-160	10	400	8500	100	10000.0	...	...
FT-192	12	550	12000	150	15000.0	...	...
FT-224	14	750	16000	200	23000.0	...	...

Other sizes available, check with factory.
The above data is based upon a liquid at 60°F, 1.00 sp. gr. and 1.0 centistoke viscosity. Flow, fluids and frequencies other than shown available upon request.
The extended range requires an actual FTI pick-off and a Range Extending Amplifier, Model FA-300.
* The calibrated range at normal flow range.
** At maximum of normal flow range.
*** Consult Factory

STANDARD LINE TURBINE FLOWMETERS

- FLOW RATES FROM 0.03 TO 20,000 GALLONS PER MINUTE
- LIQUID OR GAS MEASUREMENT
- TEMPERATURES FROM −430°F. TO +750°F.
- HIGH ACCURACY — ±0.05%
- DYNAMIC FLUID THRUST BEARING
- HIGH OVERSPEED CAPABILITY
- LOW MASS ROTOR FOR HIGH DYNAMIC RESPONSE, LONG BEARING LIFE
- WIDE CHOICE OF MATERIALS
- ADDED SAFETY OF BOTH UPSTREAM AND DOWNSTREAM ROTOR SUPPORTS
- LOW PRESSURE DROP

FLOW TECHNOLOGY, INC.

GENERAL SPECIFICATIONS
(* Terminology per ANSI C85.1 and ISA S37.1)

DYNAMIC RESPONSE:
3 milliseconds or better response to step input change of flow rate for meters smaller than 1½ inches, increasingly longer response times as the size of the meter and the mass of the rotor increases.

END CONNECTIONS:
Flowmeters FT-8 through FT-32 available with either AN Series 37° flared tube (MS-33656) or NPT end connections. Sizes FT-8 through FT-224 available with ASA B16.5 flanges, 150 lb. through 2500 lb. ratings. Other end connections available on request.

ELECTRICAL CONNECTIONS:
AN3102A-10SL-4P with mating connector supplied. Flowmeters with explosion-proof pickoffs terminate in ½" conduit union.

MATERIALS:
All portions of FTI Standard Line turbine flowmeters that come into contact with the fluid are fabricated of 300-series and 400-series stainless steels. An extremely wide choice of materials is available to satisfy even the most severe specifications. See Options.

OPERATING TEMPERATURE RANGE:
FTI Standard Line turbine flowmeters can be fabricated to measure fluids without a temperature range of −430°F to +750°F. Nominal temperature range unless otherwise specified is −100°F. to +450°F.

ACCURACY:
±0.05% at all points in the linear flow range.

LINEARITY:
±0.5% over the nominal range.
±0.1% special premium linearity for special pre-selected ranges.

ELECTRICAL OUTPUT:
The output level conforms with ISA RP 31.1 and is a minimum of 30 mV peak-to-peak for frequencies at the bottom of the nominal flow range.

PRESSURE DROP:
Ask for Technical Data Report TD-019.

CALIBRATION:
Each turbine flowmeter is furnished with a calibration with the standard reference fluid, MIL-C-7024B. Special calibrations available for applications where viscosity varies considerably.

OPERATING PRESSURE:
In general, the limiting factor governing the operating pressure of an FTI Standard Line turbine flowmeter is the rating of the end connectors. Because there is no porting of the flowmeter body, the flowmeter can be constructed to handle exceptionally high pressures if desired.

Fig. 5.3 — Example Specifications of a Turbine Flowmeter

Design Specifications

PERFORMANCE

Accuracy .... ± 0.5% of full
scale flow*
Repeatability .... ± 0.03 ft sec
Resolution .... ± 0.01 ft sec
Rangeability................... 30.1*
Minimum Full Scale Flow .... 3 f s

ELECTRONICS OPERATING PARAMETERS

Temperature 32 to 122° F (Standard)
-20 to 130° F (Optional)
Humidity .... 0 to 100%
Enclosure .. NEMA 4x Weatherproof
(Standard)
NEMA 7 9 Explosion Proof
(Optional)
Outputs.... 4-20, 0-20 ma Grounded
(Standard)
(1000 ohms max)
4-20 ma Isolated
(Optional)
(1000 ohms max)
0 to 10 VDC (Optional)
5 amp 28 VDC. 120 VAC
Form C dry contact relays
(4 each)
(Optional)
Power .... 115 230 VAC (± 10%)
50 Watts

PROCESS PARAMETERS

Temperature 0 to 250 ° F (Standard)
-364 to +500° F (Optional)
Pressure ... Up to 500 psi (Standard)
Up to 3,000 psi (Optional)
Flow Range .. 0.03 to 200,000 GPM*
(Depending on line size)
Standard Materials... ¼ to 1½"
316 S.S. flow section
and tranducers.

2 to 48":
Carbon Steel flow section
and Ryton transducers

OPTIONS

|	
Special Materials	Oxygen Cleaning
Isolated Current Output	Mirror Finish
Triple Limit Alarms	Tranducer Wells
Fail Safe Output	Anti-corrosion Coatings
Bi-directional Flow	Purge Ports
Totalizer	
Isolated Pulse Output	
Analog Meter	## ACCESSORIES
Sampler Contact Output	Pipe Mounting Kit
Steam Jacketing	Extender Board
Vacuum Jacketing	External Counter

*Assuming a consistant flow profile. Flow profiles often vary, however,
in which case accuracy and rangability will depend on specific flow
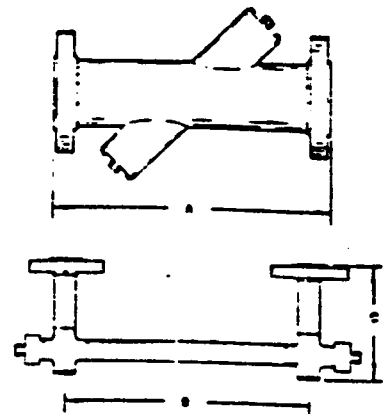parameters.
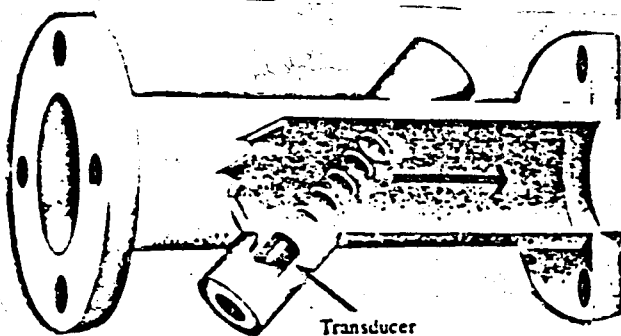
Transducer
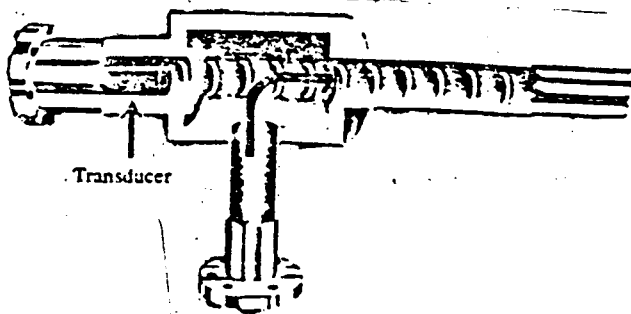
Transducer

DIMENSIONS

PIPE SIZE	A	B	C
½		10 00	5 7
¾		12 00	6 0
1		15 00	6 9
1½		24 00	8 5
2	21 0		
2½	21 0		
3	21 0		
4	18 0		
6	23 0		
8	26 0		
10	28 0		
12	30 0		
14	32 0		
16	35 0		
18	38 0		
20	40 0		
24	46 0		
30	54 0		
36	62 0		
42	70 0		
48	76 0		

Transmitter Housing:
15 "H x 13 ; W x 6 ; D

Flow section:

manning
TECHNOLOGIES. INC

Fig. 5.4 - Example Specifications of a Nonintrusive (Sonic) Flowmeter

to better the overall uncertainty with multiple in-place calibrations and continuous use.

The temperature of the cryogenic fuels is normally measured with resistance temperature devices (RTD). The specification sheet for a series of ceramic RTD elements capable of measuring the cryogenic fuel temperatures is given in Fig. 5.5.

Although the turbine flowmeter described in Fig. 5.3 can be used with either liquid or gas, the usual and most reliable way to measure the mass flow of gaseous propellants (both fuel and oxidizer) during reactive testing and the mass flow during a hot gas simulation is with a venturi flowmeter. For the hot gas testing condition, the temperature limits on the turbine flowmeter would restrict its use, therefore a venturi flowmeter will be required for the mass flow measurements for this type of test. A sketch of the standard venturi design used in the Propulsion Wind Tunnel Facility (PWT) at the U.S.A.F. Arnold Engineering and Development Center (AEDC) is shown in Fig. 5.6. The present quoted uncertainty (see Table 4.3) for this type venturi flowmeter is approximately $\pm$ 0.4% of the measured value, however, a special calibration is being conducted on several of the AEDC/PWT venturi flowmeters that is expected to decrease the uncertainty. The table also shows the NASA Lewis Research Center venturi flowmeter to give similar uncertainty. It should be noted here that the uncertainty in the measurement of the mass flow with the venturi flowmeter is a function of the uncertainties in measurement of throat area, differential pressure, gas temperature, and composition of the gas. The in-

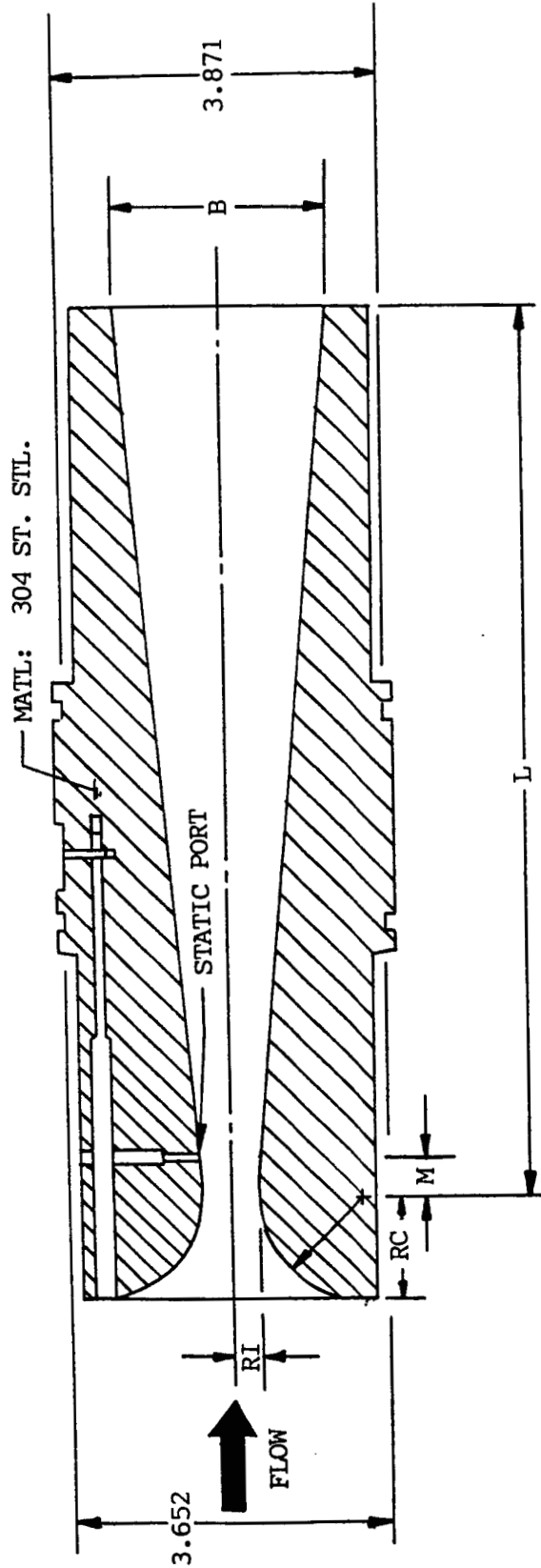# CERAMIC RTD ELEMENTS — Platinum Resistance Thermometer

Series	Dimensions (millimeters) 25.4 millimeters = 1.0 inch / All Styles In Stock For Immediate Delivery	Nominal Resistance Ohms	Temperature Range °C	Catalog Number	Price	Self Heating Error in °C/mW — flowing air v = 1 m/s	still air	Response Time — flowing water v = 0.4 m/s, 50% Response	90% Response	moving air v = 1 m/s, 50% Response	90% Response
K Ko 1 Pt 100	Most Popular Style	1 × 100	−200 to +750 intermittently up to 850	1 Pt 100 K 45 15	$17	0.06	0.24	0.2	0.6	6.0	20.0
		1 × 100	−200 to +750 intermittently up to 850	1 Pt 100 Ko 25 28	$40	0.07	0.20	0.4	1.2	18.0	60.0
	Most Popular Style	1 × 100	−200 to +750 intermittently up to 850	1 Pt 100 K 20 28	$27	0.12	0.33	0.25	0.7	14.0	50.0
	Most Popular Style	1 × 100	−200 to +750 intermittently up to 850	1 Pt 100 K 20 15	$19	0.08	0.34	0.2	0.8	5.0	18.0
		1 × 100	−200 to +750 intermittently up to 850	1 Pt 100 K 20 10	$28	0.02	0.70	0.2	0.6	2.5	9.0
2 Pt 100		2 × 100	−220 to +750 intermittently up to 850	2 Pt 100 Ko 25 28	$40	0.07	0.20	0.4	1.2	15.0	60.0
	Most Popular Style	2 × 100	−200 to +750 intermittently up to 850	2 Pt 100 K 20 17	$50	0.08	0.34	0.3	1.0	5.0	18.0
1 Pt 50		1 × 50	−200 to +750 intermittently up to 850	1 Pt 50 K 25 18	$18	0.05	0.11	0.2	0.6	6.0	18.0
Kn 1 Pt 100		1 × 100	−200 to +600	1 Pt 100 Kn 25 28	$17	0.06	0.22	0.25	0.7	15.0	60.0
		1 × 100	−200 to +600	1 Pt 100 Kn 25 38	$17	0.06	0.23	0.30	1.1	3.0	130.0
		1 × 100	−200 to +600	1 Pt 100 Kn 25 48	$17	0.06	0.24	0.35	1.4	95.0	135.0
2 Pt 100		2 × 100	−200 to +600	2 Pt 100 Kn 25 28	$38	0.06	0.22	0.25	0.7	15.0	60.0
		2 × 100	−200 to +600	2 Pt 100 Kn 25 38	$38	0.06	0.23	0.3	1.1	30.0	130.0
		2 × 100	−200 to +600	2 Pt 100 Kn 25 48	$34	0.06	0.24	0.35	1.4	40.0	140.0
3 Pt 100		3 × 100	−200 to +600	3 Pt 100 Kn 25 48	$73	0.06	0.13	0.35	1.4	40.0	140.0

Discount Schedule   1 to 10 units = NET   25 to 100 units = 12%   501 up = 17%
11 to 24 units = 10%   101 to 500 units = 15%

Fig. 5.5 — Example Specifications for Resistance Temperature Detectors

OMEGA ENGINEERING, INC.

MATL: 304 ST. STL.

STATIC PORT

ALL DIMINSIONS IN INCHES

3.871

B

L

M

RC

RI

FLOW

3.652

RT   As Required

RC = 3.635 RT

M = 0.828 RT

L = 14(RT) or (3.16 - RC) Whichever is Greater

B = 1.9724(RT) + 0.1743(L)

Fig. 5.6 - AEDC/PWT Standard Venturi Design

strumentation for measurement of the pressure and temperature will be dealt with later.

5.4 COMBUSTION CHAMBER

There are normally three basic measurements made in the combustion chamber during a reactive test: (1) combustion chamber wall pressure, (2) combustion chamber wall temperature, and (3) combustion chamber wall heat flux. The wall pressure is used to determine the combustion chamber pressure (P_c) (see Table 4.2 in the previous section). An additional measurement for combustion chamber total temperature is desired for using it in the performance code verification. However, because of the high temperature and hostile environment during reactive testing, this temperature is usually calculated with the combustion code and not actually measured in the combustion chamber.

The combustion chamber pressure can vary from 120 psia to 3500 psia dependent on the type of rocket engine and fuel used, and the location of the pressure orifice can vary from behind the injector face to near the nozzle throat. For a hot gas simulation test the pressure should be measured at several locations along the chamber wall starting just aft of the injector face and ending just forward of the throat contraction. This will provide better information for determination of P_c for input into the performance code. The specifications for a series of high accuracy pressure transducers that cover the range of normal combustion chamber pressures are given in Fig. 5.7.

High Output/High Accuracy Pressure and Vacuum Transducers and Transmitters
Summary of Specifications

Most Transducers and Transmitters available on GSA

Models 204, 204D, 239, 261, 280 and 280E are available as 4-20 ma output Pressure Transmitters for two wire current loop systems

Quality assurance: Setra's quality control system conforms to MIL-I-45 208 A and Mil-Std 45 662 A

Detailed Product Bulletins with complete performance and engineering specifications are available for all products described below

APPLICATION	204 series (204B 204D) DIFFERENTIAL PRESSURE (204D) ABSOLUTE PRESSURE (204D) GAGE PRESSURE VACUUM (204)	205-2 ABSOLUTE PRESSURE GAGE PRESSURE	280 series (280 & 280E) ABSOLUTE PRESSURE GAGE PRESSURE	239 LOW GAGE PRESSURE DIFFERENTIAL PRESSURE AND DIFFERENTIAL PRESSURE	261-1 LOW STATIC DIFFERENTIAL PRESSURE (HVAC)	270 SETRACERAM Sensor ABSOLUTE PRESSURE GAGE PRESSURE	271 SETRACERAM Sensor DIFFERENTIAL PRESSURE GAGE PRESSURE
Media Compatibility[2] — Pressure and Vacuum	Gas or liquid compatible with Stainless Steel	Gas or liquid compatible with stainless steel	Gas or liquid compatible with stainless steel	Gas compatible with stainless steel, aluminum	Clean, dry, non-corrosive gas, such as air	Gas or liquid compatible with aluminum, alumina ceramics, gold and fluorosilicon elastomer sealant	Clean, dry, non-corrosive gas, such as air
Media Compatibility[2] — Reference Pressure (for Differential Pressure)	Clean, dry, non-corrosive gas			Clean, dry, non-corrosive gas, such as air	Clean, dry, non-corrosive gas, such as air		
Absolute Pressure Ranges[8] — Lowest Pressure		0 to 25 psia FS	0 to 25 psia FS			Barometric, 800 to 1100 mB 0 to 5 psia FS	
Absolute Pressure Ranges[8] — Highest Pressure		0 to 5,000 psia FS	0 to 5,000 psia FS			0 to 100 psia FS	
Gage Pressure Ranges[8] — Lowest Pressure	0 to 25 psig FS	0 to 25 psig FS	0 to 15 psig FS 3 to 15 PA	0 to 0.5 inch WC FS	0 to 0.1 inch WC FS	0 to 5 psig FS	0 to 5 psig FS
Gage Pressure Ranges[8] — Highest Pressure	0 to 10,000 psig FS	0 to 5,000 psig FS	0 to 10,000 psig FS	0 to 10 psig FS	0 to 25 inch WC FS	0 to 100 psig FS	0 to 100 psig FS
Differential Pressure Ranges[8] — Lowest Pressure	0 to 25 (or ±10) psid FS			0 to 0.5 (or ±0.25) inch WC FS	0 to 0.1 (or ±0.1) inch WC FS		0 to 5 (or ± 2.5) psid FS
Differential Pressure Ranges[8] — Highest Pressure	0 to 10,000 (or ±5,000) psid FS			0 to 10 (or ±5) psid FS	0 to 25 (or ±5) inch WC FS		0 to 100 (or ± 20) psid FS
Vacuum Range[8] — Highest Vacuum	0 to 14.7 psiv			0 to 10 psiv			
Maximum Line Pressure (for Differential Pressure)	1000 psig Max on reference port			250 psig[7]	14 inch WC on reference port		200 psig
Pressure Port	¼" 18 NPT, internal	¼" 18 NPT, internal	¼" 18 NPT, internal	¼" 27 NPT, internal	¾₁₆" OD tube	¼" 27 NPT, internal	¼" 27 NPT, internal
Response to Pressure Changes[3] (milliseconds)	1 to 5 ms	1 to 5 ms	1 to 5 ms	2 to 5 ms	50 ms	50 ms	50 ms
Accuracy % FS[4]	0.11%	0.11%	0.11%	0.14%	1%	0.05%	0.04%u
Temperature Effects[6] Zero Shift ± % FS/100° F / Sensitivity Shift ± % FS/100° F 30° F to 150° F	0.4 Max[5] / 0.3 Max	2 Max / 1.5 Max	280: 0.6 Max / 0.5 Max	280E: 1 Max / 1.5 Max	1 Max / 1 Max	2 Max[7] / 2 Max	0.1 Max (0.2% Barom) / 0.1 Max	0.2 Max / 0.2 Max
Transducer Output[9]	0 to 5 VDC (0 to ± 2.5 VDC)	0 to 5 VDC 0 to ±2.5 VDC	0 to 5 VDC	0 to 5 VDC 0 to ±2.5 VDC	0 to 5 VDC	0 to 5 VDC	0 to 5 VDC 0 to ± 2.5 VDC
Transducer Excitation	22 to 30 VDC	18 to 30 VDC	15 to 32 VDC	22 to 30 VDC	12 to 24 VDC	22 to 30 VDC	22 to 30 VDC
Transducer Circuit[10]	4 wire	4 wire	3 wire	4 wire	3 wire	4 wire	4 wire

Notes:
1. Stainless Steel housing (optional)
2. See catalog sheet for detail
3. For typical application, incompressible fluid (except models 239, 261, 270, 271) Exact response time depends on pressure range and system characteristics
4. Accuracy as RSS of non-linearity, hysteresis repeatability (at constant temperature)
5. Thermal zero shift 50% higher for vacuum range units
6. Thermal effects listed for 24 V circuit (Slightly higher for some options)
7. Over 40° F to 100° F ranges Calibrated at 70° F
8. Special ranges are available at extra cost
9. Transmitters have 4 to 20 ma
10. Transmitters have a 2 wire circuit

Notations:
Gage Pressure: Pressure measured relative to ambient atmospheric pressure Referred to as pounds per square inch (gage) or psig
Absolute Pressure: Pressure measured relative to high vacuum Referred to as pounds per square inch (absolute) or psia
Vacuum: Vacuum measured relative to ambient atmospheric pressure Referred to as pounds per square inch (absolute) or psia

FS: Full Scale
WC: Water Column

Specifications subject to change without notice

Price Range: $250 to $700 (Basic Transducer)

Fig. 5.7 – Example Specifications for High Accuracy Pressure and Vacuum Transducers

The combustion chamber wall temperature and heat flux which are also used in the performance code verification are normally measured. The heat flux can be obtained from calormetric measurements by measuring the chamber coolant temperature (cryogenic fuel when used as the coolant or water in the case of hot gas simulation) at various stations along the coolant passages and then using the $\Delta T_{coolant}$, mass flow of coolant, and C_p for coolant from a thermodynamic Table (see Table 4.2 previous section) to calculate the heat flux. The same RTD specifications shown in Fig. 5.5 could be used for these measurements.

The combustion chamber total temperature during reactive testing is usually not measured but rather calculated based on the enthalpy of the propellant. However, advances in instrumentation technology, specifically in the field of fiber optics, are making it possible to measure this temperature. The use of Coherent Anti-Stokes Raman Spectroscopy (CARS) has been demonstrated by UTRC (United Technology Rocket Center) in measurement of temperature in reactive hydro-carbon combustors. The work reported in Ref. 7 is primarily for open flames but with the advances made in the use of fiber optics it should be possible to apply this technique to the measurement of the combustion chamber total temperature. The uncertainty of these measurements may be in the order of 5.0% based on a comparison given in Ref. 7. Another option that is now available is a sapphire black body optical fiber thermometry system that has been tested by the National Bureau of Standards and certified

to be accurate to 0.2% at approximately 4000°R. The specifications for this probe are given in Fig. 5.8. It should be noted, however, that the cost of measuring the combustion chamber total temperature during normal reactive testing will not be low.

The measurement of the combustion chamber total temperature during the hot gas simulation testing can be made with a standard high temperature probe of similar design as those used in the stilling chamber of a hypersonic wind tunnel where total temperature measurements of 1500°F may be required.

The specification sheet for high temperature insulations and thermocouple wire of the order required for use with the temperature probe is given in Fig. 5.9. The measurement of the combustion chamber total temperature is required during the hot gas simulation testing since there are no combustion characteristics to permit calculation of this temperature and this temperature is required to determine one of the inputs into one of the performance codes.

5.5 NOZZLE

The nozzle measurement will be considered in three groups: (1) Wall, (2) Boundary Layer, and (3) Exit.

5.5.1 Wall

There are three sets of measurements desired along the nozzle wall to aid in the verification of the performance codes: (1) Pressure distribution (2) Temperature distribution, and (3) Heat transfer rate. During normal reactive testing of a liquid rocket

ORIGINAL PAGE IS
OF POOR QUALITY

Optical fiber sensors broaden temperature measurement limits

Sapphire blackbody designs make possible readings to 2000 C with 0.2% accuracy.

Hugh Amick
Accufiber Inc.
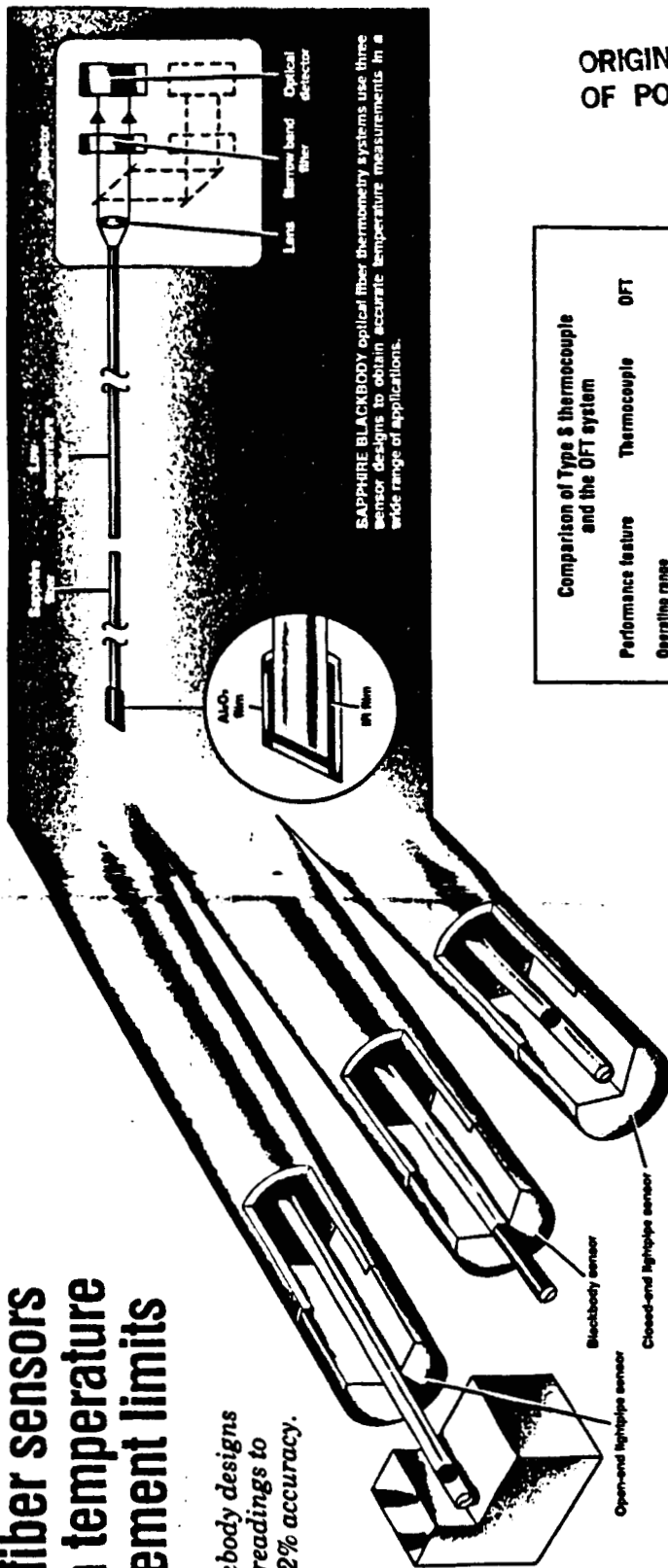
SAPPHIRE BLACKBODY optical fiber thermometry systems use three sensor designs to obtain accurate temperature measurements in a wide range of applications.

Comparison of Type S thermocouple and the OFT system

Performance feature	Thermocouple	OFT
Operating range		
Maximum temperature	1500 C	2000 C
Minimum velocity		
1 atm	45 ft/sec	5 ft/sec
20 atm	4.5 ft/sec	0.5 ft/sec
Accuracy (1000 C)		
NBS Type S thermocouple	0.1%	0.1%
NBS radiometric standard	0.05%	0.01%
OFT certifiable		
practical		
best experimental		0.0025%
Resolution (1800 C)		
Sensitivity	10 µV/C	200 mV/C
Minimum detection signal	0.15 µV	1.5 µV (shot noise)
Temperature resolution	0.015 C	0.0000075 C
Relative bandwidth (Hz) (1993 C, 1 atm)		
10 ft.sec gas velocity		
0.050-in. TC dia	1	
0.003-in. TC dia	500	
0.050-in. standard fiber		50,000
1,000 ft/sec gas velocity		
0.050-in. TC dia	1	
0.003-in. TC dia	30	
0.050-in. standard fiber		50,000

Sapphire blackbody OFT systems have the following general characteristics:
- a 2000 C high-temperature measurement limit.
- immunity to EM and RF interference.
- certifiable accuracy to 0.2% at 1000 C.
- resolution to 2×10^{-5} C at 1200 C.
- a 10-kHz bandwidth.
- signal-to-noise ratio of 1×10^6 at 1000 C.
- minimal sensor degradation in many harsh environments.

Fig. 5.8 – Example Specifications of a High Temperature Optical Fiber Sensor

Consult Sales Department for Prices

Calibration	Recommended Atmosphere O.I.R.V.***	Maximum Service Temp.	Sheath	Calibration	Diameter–Gage–Insulation–Termination	Base Price 6" Sheath	Per addl'l 1"	Recommended Junction Style****
W5% Re vs W26% Re	I.V.	4200°F	XTA	W5R26	.062-30-B	$170	21	U,G
			XTA	W5R26	.125-30-B	290	36	U,G
			XTA	W5R26	.125-24-B	345	43	U,G
Pt vs Pt 13% Rh**	I.V.	2700°F	XTA	P13R	.062-30-M	110	11	U
			XTA	P13R	.125-24-M	295	37	U
			XTA	P13R	.062-30-B	220	22	U
			XTA	P13R	.125-24-B	350	44	U
Pt vs Pt 13% Rh	O.I.V	2700°F	XPA	P13R	.062-30-M	SPEC. QUOTE	SPEC. QUOTE	U,G
			XPA	P13R	.125-25-M	SPEC. QUOTE	SPEC. QUOTE	U,G
W5% Re vs W26% Re	I.V.R. 3000°F		XMO	W5R26	.125-30-B	170	21	U
	I.V.R. 4000°F		XMO	W5R26	.250-30-B	SPEC. QUOTE		G
			XMO	W5R26	.250-30-M	SPEC. QUOTE		U,G
	O.V.R. 2800°F		XPA	W5R26	.062-30-A	SPEC. QUOTE		U
			XPA	W5R26	.125-30-A	SPEC. QUOTE		E,U,G
Pt vs Pt 13% Rh**	O.V.R. 2700°F		XPA	P13R	.125-24-A	SPEC. QUOTE		E,U
W5% Re vs W26% Re	I.R.V. 2700°F		XMO	P13R	.125-30-A	220	22	U
	I.R.V. 2800°F		XMO	W5R26	.250-24-A	SPEC. QUOTE		E,U
			XMO	W5R26	.062-30-A	110	12	U
			XMO	W5R26	.125-30-A	100	8	U
W5% Re vs W26% Re	I.R.V. 2100°F		XIN	W5R26	.020-39-M	SPEC. QUOTE		E,U
			XIN	W5R26	.040-36-M	48	4	U
			XIN	W5R26	.062-30-M	48	4	U
Pt vs Pt 13% Rh	O.I.R.V. 1600°F		XIN	P13R	.125-30-M	60	7	E,U
			XIN	P13R	.125-24-M	60	7	E,U
			XIN	P13R	.187-26-M	220	20	E,U
			XIN	P13R	.250-24-M	235	30	E,U
			XIN	P13R	.250-20-M	385	50	E,U

NOTES: All P13R Probes also available with Pt6R elements.

*Molybdenum sheathed probes cannot be bent.

*All styles and calibrations may not be in stock at all times.

***O—oxidizing, I—inert, V—vacuum, R—reducing atmospheres only

****Recommended atmospheres listed are valid for U and G junction styles only

Consult Sales Department when using exposed junctions

Prices subject to change without notices.

Ungrounded junctions on Tungsten/Rhenium thermocouples with compacted insulation have a history of low reliability with premature junction area open circuits. These will be supplied if mandatory, but warranty repairs will not be performed.

Tantalum sheathed probes can be bent, but this must be done at the factory. If the customer chooses to bend a tantalum sheathed probe himself, all warranties are voided. Consult Sales Department for pricing.

Table 1 High Temperature Sheath Materials

Sheath Material	Maximum Operating Temperature	Workability	Working Environment	Approx. Melting Point	Remarks
††Molybdenum (XMO)	4000°F	Brittle	Inert, Vacuum, Reducing	4730°F	Relatively good hot strength. Sensitive to oxidation above 930°F. Resists many liquid metals, most molten glasses.
†Tantalum (XTA)	4200°F	Malleable	Inert, Vacuum	5425°F	Resists most acids and weak alkalies. Very sensitive to oxidation above 570°F.
Platinum/Rhodium Alloy (XPA)	3000°F	Malleable	Oxidizing, Inert, Vacuum	3400°F	No attack by SO_2 at 2000°F. Silica is detrimental. Halogens attack at high temperature.
Inconel 600 (XIN)	2100°F	Malleable	Oxidizing, Inert, Vacuum	2570°F	Excellent resistance to oxidation at high temperature. Do not use in presence of sulphur above 1000°F. Hydrogen tends to embrittle.

††Refractory metals are extremely sensitive to any trace of oxygen above approximately 500°F (260°C). Must be used in vacuum or very pure inert gases such as Helium or Argon.

†Suitable for exposure to certain reducing atmospheres as well as inert gases and vacuum.

The Maximum Operating Temperature for the cold end of the probe is 425° for termination styles O, T, J and S.

Table 2 High Temperature Insulations and Wires

Insulation	Approx. Upper Useful Temperature	Approx. Melting Point	Remarks
Magnesia (MgO) **M**	*3000°F	5070°F	Hygroscopic, compacts well.
Alumina (Al₂O₃) **A**	*2800°F	3660°F	Requires considerable volume reduction to compact satisfactorily.
Beryllia (BeO) **B	*4200°F	4620°F	Compacts well. High thermal conductivity.
Sensing Wires Pt-10% Rh vs. Pt / Pt-13% Rh vs. Pt	2700°F	3150°F	Some decalibration at continued high temperature use due to Rhodium volatilization.
W vs. W-26% Re / W-5% Re vs. W-26% Re / W-3% Re vs. W-25% Re	4200°F	5600°F	Brittle; avoid flexing.

*At temperatures above 1800°F all insulating materials experience a substantial decrease in resistivity with increasing temperatures.

**Beryllium Oxide and Thorium Oxide are toxic. Do not handle. For any needed repairs or alterations return to the factory.

*Values given are for compacted insulation. For uncompacted hard fired insulators, useful temperature range can be 100 to 200°F higher.

OMEGA ENGINEERING, INC.

Fig. 5.9 – Example Specifications for High Temperature Thermocouple Wire and Sheath Material

engine, measurements of this type are usually limited to temperature measurements and these are concentrated on measuring the temperature of the nozzle coolant. However, if the measurements are made in the fashion described earlier, the heat-transfer rate can be determined by the calorimetric method. Since most engine manufacturers do not like to drill holes through the nozzle wall, the measurement of pressure distribution is usually very limited. Therefore, the basic nozzle wall data required for code verification should be obtained with hot gas simulation.

The nozzle design for the hot gas simulation model should be such that static pressure orifices and thermocouples can be located along the nozzle wall starting as near the throat as possible and continuing at moderate intervals to the exit. Normally Chromel-Alumel thermocouples are used for the temperature measurements, although most of the basic thermocouple types could be used. A specification sheet for basic thermocouples is given in Fig. 5.10. The temperature measurements could also be measured using RTD's as described earlier (specification shown in Fig. 5.5). The accuracy of the temperature measurements is usually the accuracy of the curve fit used to convert the thermocouple millivolt output to degrees. The measurement of the static pressures is made with pressure transducers. The specification for a pressure scanner that could be used to measure the static pressures is given in Fig. 5.11. This particular pressure transducer system quotes an accuracy of $\pm$ 0.10% Full Scale.

Thermocouple Technical Data

SYMBOL	RECOMMENDED THERMOCOUPLES			
	CALIBRATION & USE	POSITIVE (+)	NEGATIVE (−)	COLOR CODE
T	Copper-Constantan (very low temperature) Suitable for subzero temperatures. Can be used in oxidizing, reducing, inert or vacuum atmospheres up to 700°F (370°C)	Copper (yellow metal)	Constantan (silver metal)	Blue
K	Chromel-Alumel (Oxidizing Atmosphere) Recommended temperature range is −330 to 2300°F (−200 to 1260°C). Should not be used in reducing or sulfurous atmospheres. Can only be used in vacuum for short time until calibration shifts.	Chromel (Non-magnetic)	Alumel (Magnetic)	Yellow
J	Iron-Constantan (reducing atmosphere) Recommended temperature range is 32 to 1400°F (0 to 760°C). Can be used in oxidizing, reducing, inert or vacuum atmospheres.	Iron (Magnetic)	Constantan (Non-magnetic)	Black
E	Chromel-Constantan (high output) Recommended temperature range is −330 to 1600°F (−200 to 900°C). Can be used in oxidizing or inert atmospheres. Should not be used in reducing or vacuum atmospheres.	Chromel (Non-magnetic)	Constantan (Non-magnetic)	Purple

SPECIFICATIONS

DIAMETERS Standard diameters 1/16", 1/8" and 1/4", with two wires.

LENGTH Standard OMEGA thermocouples have 12 inch immersion lengths. Other lengths available.

SHEATHS Type 304 stainless steel and Inconel are standard. Other sheath materials available; write for price and availability.

INSULATION Magnesium Oxide is standard. Minimum insulation resistance wire to wire or wire to sheath is 1.5 megohms at 500 volts dc in all diameters.

CALIBRATION Iron-Constantan (J), Chromel-Alumel (K), Copper-Constantan (T), and Chromel-Constantan (E) are standard calibrations.

ACCURACY The wires used in OMEGA thermocouples are selected and matched to meet ANSI Limits of Error.

BENDING Easily bent and formed. Bend radius should be not less than twice the diameter of the sheath.

DELIVERY Off-the-Shelf, other sheaths available; write for price and delivery.

Fig. 5.10 – Thermocouple Specifications for Standard Temperature Ranges
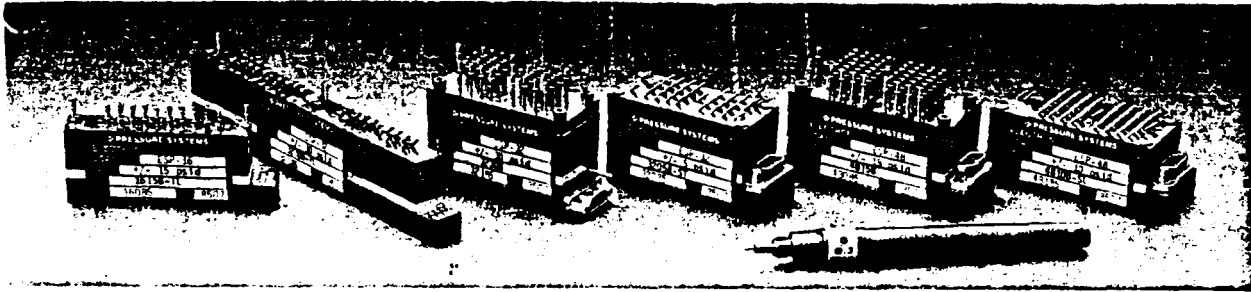
Miniature ESP Scanners

PRESSURE SCANNERS

Pressure System's line of pressure scanners are transducer per port electronically scanned instruments designed for multiple pressure measurement applications where high data rates and accuracy are paramount. These pressure scanners incorporate silicon pressure transducers, internal multiplexing and amplification with an integral calibration valve. They are designed to accurately measure pressures of dry, non-corrosive gaseous media. Several configurations are available, all fully compatible with the 780B Pressure Measurement System.

MINIATURE

The ESP Pressure Scanner line is designed to offer miniature high transducer density modules which satisfy applications where space is critical as in wind tunnel model testing. All ESP scanners interface to the 780B Data Acquisition and Control Unit using the Scanner Interface Modules.

RACKMOUNT

The S1600, S1600D and S3200 Pressure Scanners are rack mounted instruments for use in test stand applications where pneumatics can be brought to a

central location. These scanners feature complete field repairability down to the transducer level and include front panel quick disconnects of all input pressures. Electrical interface to the DACU is provided by the Scanner Interface Racks where all pneumatic and electrical connections to the pressure scanners are automatically made once secured in the rack.
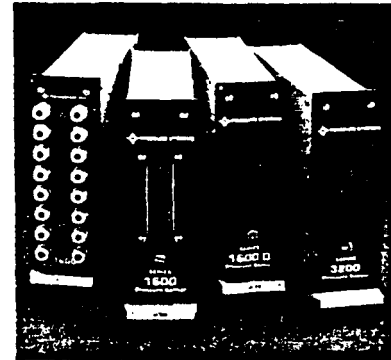
Rackmount Scanners

ESP Scanners	ESP-16TL	ESP-32TL	ESP-32	ESP-32SL	ESP-48	ESP-48SL	
INPUTS	16	32	32	32	48	48	CHANNELS
RANGE	±1-100	±1-100	±1-100	±1-100	±1-100	±1-100	PSID
STATIC ERROR	±0.10	±0.10	±0.10	±0.10	±0.10	±0.10	%F.S.
SCAN RATE	20,000	20,000	20,000	20,000	20,000	20,000	READINGS/SEC
TRANSDUCER DENSITY	7.6	7.6	7.1	8.9	10.7	13.4	TRANSDUCER/IN³

Rack Scanners	S1600	S1600-D	S3200	
INPUTS	16	16*	32	CHANNELS
RANGE	±10"	±10"	±10"	WC
	500	100	250	PSID
STATIC ERROR	±0.10	±0.10	±0.10	%F.S.
SCAN RATE	20,000	20,000	20,000	READING/SEC
FIELD REPAIRABLE	YES	YES	YES	
DENSITY PER 19" RACK	96	96	192	CHANNELS

*S1600-D are True Differential

Price Range: $150 to $200 per channel (Basic Transducer)

Fig. 5.11 - Example Specifications for High Accuracy Miniature Pressure Scanners

Since the heat-transfer rate along the wall is one of the output parameters in the boundary layer losses code, it is very desirable to have an accurate measurement of this parameter. It would be difficult to measure the heat transfer rate using the thin skin technique and it is difficult to determine the accuracy of the calorimetric method, therefore, it would be better to design the hot gas simulation model so that heat flux transducers could be used to measure the heat-transfer rate. Some calorimetric measurements could be made in the coolant passages as a back-up if desired. The specification of a heat flux transducer is given in Fig. 5.12. The accuracy quoted for this specific transducer is $\pm$ 3%.

5.5.2 Boundary Layer

The boundary layer measurement being considered here are in the nozzle (as opposed to the exit plane) and are normal to the nozzle surface. It will be very difficult to make boundary layer measurements during a normal reactive test, therefore, they are only recommended for the hot gas simulation tests or controlled reactive testing such as described in Section 5.1. Measurement of three profiles are desired: (1) Pressure profile, (2) Temperature profile, and (3) Turbulence profile.

There are two things that must be considered in obtaining profile measurements: first, the measuring device and second, the support or survey device. For pressure or temperature profile surveys there are actually three methods that have been used

64 Series HEAT FLUX TRANSDUCERS

DESCRIPTION

MEDTHERM 64 Series Heat Flux Transducers offer dependable direct measurement of heat transfer rates in a variety of applications due to careful design, rugged quality construction and versatile mounting configuration. Each transducer will provide a self-generated 10 millivolt output at the design heat flux level. Continuous readings from zero to 150% design heat flux are made with infinite resolution. The transducer output is directly proportional to the net heat transfer rate absorbed by the sensor. Each transducer is provided with a certified calibration traceable through temperature standards to the National Bureau of Standards. These transducers have been proven in thousands of applications in aerospace applications, heat transfer research, and boiler design.

FEATURES

* LINEAR OUTPUT
* OUTPUT PROPORTIONAL TO HEAT TRANSFER RATE
* ACCURATE, RUGGED, RELIABLE
* CONVENIENT MOUNTING
* UNCOOLED, WATER COOLED, GAS PURGED MODELS
* RADIOMETER AND LIMITED VIEW ACCESSORIES
* MEASURE TOTAL HEAT FLUX
* MEASURE RADIANT HEAT FLUX
* REMOTE MEASUREMENT OF SURFACE TEMPERATURE

CONSTRUCTION FEATURES

ACCURACY, RUGGEDNESS AND RELIABILITY are provided by the thoroughly proven Gardon and Schmidt-Boelter sensors.

LONG TRANSDUCER LIFE AND SIGNAL STABILITY are enhanced by the massive body of pure copper, gold plated to protect against corrosion, contamination, and excess radiant heat absorption by the heat sink.

PROTECTION AGAINST ROUGH HANDLING in mounting is provided by a stainless steel flange when specified.

SIGNAL INTEGRITY is protected by the use of welded connections, stranded lead wire with braided copper shielding and teflon insulation firmly secured in the transducer body with strain relief to ensure resistance to rough handling and stray signals.

ACCESSORIES

REMOVABLE SAPPHIRE WINDOW ATTACHMENTS are available to limit the basic transducer to measurement of radiation heat flux only.

VIEW RESTRICTOR ATTACHMENTS are available to limit the angle of view for the basic transducer to 60°, 30°, 15 °, or 7° for narrow view angle measurements.

DIRECT READING HEAT FLUX METER Model H-200 is available for direct meter readout in any heat flux units from any linear heat flux transducer input. A 0-1 volt recorder output is also provided. Ask for Bulletin 700.

BODY TEMPERATURE THERMOCOUPLE measurement is provided by an optional copper constantan 30 AWG solid conductor thermocouple, TIG welded junction, with fiberglass insulation and metallic overbraid.

OPERATING PRINCIPLES

The 64 Series transducers are of two basic sensor types, the Gardon type (5 to 4000 BTU/ft^2-sec) and the Schmidt-Boelter thermopile type (0.2 to 5 BTU/ft^{2}sec). In both type sensors heat flux is absorbed at the sensor surface and is transferred to an integral heat sink which remains at a temperature below that of the sensor surface. The difference in temperature between two points along the path of the heat flow from the sensor to the sink is proportional to the heat being transferred, and, therefore proportional to the heat flux being absorbed. At two such points, MEDTHERM transducers have thermocouple junctions which form a differential thermoelectric circuit providing a self-generated emf between the two output leads directly proportional to the heat transfer rate. No reference junction is needed.

Gardon Gauges absorb heat in a thin metallic circular foil and transfer the heat radially (parallel to the absorbing surface) to the heat sink attached at the periphery of the foil; the difference in temperature is taken between the center and edge of the foil.

Schmidt-Boelter gauges absorb the heat at one surface and transfer the heat in a direction normal to the absorbing surface; the difference in temperature is taken between the surface and a plane beneath the surface.

OPTIONAL FEATURES include four mounting configurations, water cooling provisions, gas purge provisions, or thermocouples for body temperature measurement. Water cooling should be specified if the uncooled transducer is expected to reach above 400°F.

The gas purging provision should be included on radiation transducers to be used in a sooty environment. The MEDTHERM purge is designed to pass rigid NASA performance tests with fuel-rich oxy-acetylene flames directed toward the window at close range.

STANDARD CONFIGURATIONS

The basic transducer may be selected with either of four mounting configurations and with or without provisions for water cooling of transducer body. It may also be provided with gaseous purging to keep the radiation-transmitting window clean, but when the purging provision is included, the window is installed and is not an accessory.
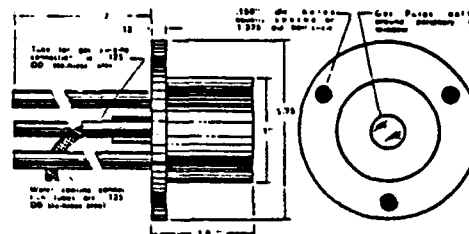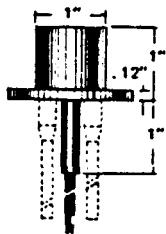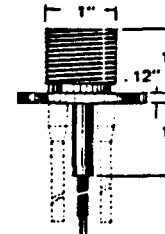
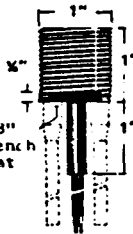### RADIOMETER WITH GAS PURGING PROVISIONS

Fig. 5.12a – Example Specifications for Rapid Response Heat Flux Transducers

REMTECH INC.

The four available mounting configurations are illustrated below. There is the smooth body with flange, the threaded body with flange, the smooth body without flange, and the threaded body without flange. All mounting flanges are 1.75" dia. with .150" dia. mounting holes equally spaced on a 1.38" dia. bolt circle. Water cooling tubes (when specified) are .1/8" dia. stainless steel and gas purge tubes are 1/8" dia. stainless steel. All tubes are 2" long. The threaded transducer bodies are 1-12 UNF-2A threads.
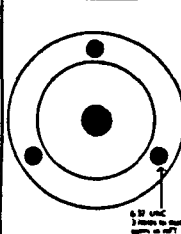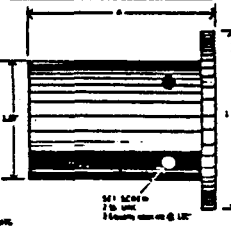
SMOOTH BODY WITH FLANGE		THREADED BODY WITH FLANGE		SMOOTH BODY, NO FLANGE		THREADED BODY, NO FLANGE	
VERSION	MODEL NO.	VERSION	MODEL NO.	VERSION	MODEL NO.	VERSION	MODEL NO.
BASIC, NO COOLING	64-xx-16	BASIC, NO COOLING	64-xx-17	BASIC, NO COOLING	64-xx-14	BASIC, NO COOLING	64-xx-15
WATER COOLED	64-xx-20	WATER COOLED	64-xx-21	WATER COOLED	64-xx-18	WATER COOLED	64-xx-19
RADIATION, PURGED COOLED	64P-xx-24	RADIATION, PURGED COOLED	64TP-xx-25	RADIATION, PURGED COOLED	64P-xx-22	RADIATION, PURGED COOLED	64TP-xx-23

SAPPHIRE WINDOW ATTACHMENT may be added for elimination of convective heat transfer, thus making the transducer a radiometer or radiation heat flux transducer. Three view angles are available: 90°, 120°, and 150°. Windows are removable and replaceable by user. When the window is used the sensitivity of the basic transducer is reduced to a nominal fraction of the original as follows: 90°, 43%; 120°, 64%; 150°, 79%. Thickness of the attachment varies with view angle and sensor type from 1/16" to 3/8".

BODY STYLE "D"	CALIB?	MODEL	
SMOOTH	1.0	NO	SW-1-YY
THREADED	.84	NO	SW-2-YY
SMOOTH	1.0	YES	SW-1C-YY
THREADED	.84	YES	SW-2C-YY

VIEW RESTRICTOR ATTACHMENTS for limiting the area view or seen by the sensor are sometimes desired for making radiation or remote temperature measurements.

VIEW ANGLE	"A"	NOMINAL % BASIC SENSITIVITY	MODEL NO.
7°	3.9"	.4%	VR-7
15	2.3	1.7	VR-15
30	1.6	6.6	VR-30
60	1.2	25.0	VR-60

SPECIFICATIONS

RANGES AVAILABLE: 4000, 3000, 2000, 1000, 500, 200, 100, 50, 20, 10, 5, 2, 1, 0.2 BTU/ft^2-sec. design heat flux level.

OUTPUT SIGNAL: 10 millivolts $\pm$ 1.5 millivolts at full range.

MAXIMUM ALLOWABLE OPERATING BODY TEMPERATURE: 400°F.

OVERRANGE CAPABILITY: 150% for 5-2000 BTU/ft^2-sec. ranges; 500% for 0.2-2 BTU/ft^2 sec ranges.

MAXIMUM NON-LINEARITY: $\pm$2% of full range

REPEATABILITY: $\pm$1/2%

ACCURACY: $\pm$3% for most ranges

CALIBRATION: Certified calibration provided with each transducer.

SENSOR ABSORPTANCE: 92%, nominal, from 0.6 to 15.0 microns.

SPECTRUM TRANSMITTED BY SAPPHIRE WINDOW (When used): 85% nominal from 0.15 to 5.0 microns.

LEAD WIRE: 24 AWG stranded copper, two conductor, teflon insulation over each, metallic overbraid, teflon overall, 36" long, stripped ends.

RESPONSE TIME (63.2%):
500 to 4000 BTU/ft^{2}sec: less than 50 msec.
50 to 200 BTU/ft^{2}sec: less than 100 msec.
5 to 20 BTU/ft^{2}sec: less than 290 msec.
0.2 to 2 BTU/ft^{2}sec: less than 1500 msec.

SENSOR TYPE
5 to 4000 BTU/ft^{2}sec: Gardon Gauge
0.2 to 4 BTU/ft^{2}sec: Schmidt-Boelter

NOMINAL IMPEDANCE:
Less than 10 ohms on Gardon Gauges
Less than 100 ohms on Schmidt-Boelter Gauges.

Amount of heat which can be absorbed by transducer in an adiabatic (perfectly insulated thermally) installation before exceeding the 400°F limitation:
Models without water cooling provisions: 6.2 BTU
Models with water cooling provision but without water in passages: 4.2 BTU.
Maximum gas pressure for gas purged models: 150 psig.

Fig. 5.12b – Example Specifications for Rapid Response Heat Flux Transducers

successfully: (1) survey rake, that is multiple pressure or tem-
perature probes that record the profile from one fixed position;
(2) single survey probe that is inserted through a hole in the noz-
zle wall and moved from position to position, normal to the wall,
by means of an external drive mechanism; and (3) single survey
probe that is mounted to a support mechanism that is inserted
through the exit of the nozzle with a provision to remotely move
the probe normal to the nozzle wall and also be remotely moved from
one nozzle station to another. The latter will be the most expen-
sive to build, but will also be the most versatile. Regardless of
which method used, all are subject to causing interference in the
boundary layer and should be designed to minimize this interfer-
ence. All of these supports can be water-cooled if required by
test conditions.

The probes used for measurement of the pressure profiles are
usually small diameter tubes that are flattened slightly on the end
to allow surveying nearer to the nozzle wall. The type of material
used for the tubes will depend on the combustion chamber total tem-
perature. It is not recommended that measurement of nozzle boun-
dary layer profiles be attempted if the temperature is such that
the actual probe must be cooled because the size of the probe and
the accompanying interference would yield data that would be very
questionable. The pressure transducers used to make the measure-
ment should be rated to measure the pressure behind the normal
shock based on the lowest supersonic Mach number occurring at a

measurement location nearest the throat. Transducers of the type given in either Fig. 5.7 or 5.11 could be used.

There are two types of temperature probes that are used: (1) exposed thermocouple, where the thermocouple wires extend out of the end of a support tube and the thermocouple junction is external to the support; and (2) shielded junction, where a shield covers the thermocouple to prevent radiation and bleed holes are located in the shield aft of the thermocouple junction to permit flow to pass the junction. A sketch of both types is shown in Fig. 5.13. There are pros and cons for both types. With the exposed junction, measurements can be made nearer to the wall but there are radiation losses, whereas, with the shielded junction, measurements start further from the wall but the shield prevents the radiation losses. In either case, if the total temperature (T_O) has been accurately measured in the combustion chamber and the freestream temperature (T_m) has been determined with the probe, then the T_m/T_O factor can be applied to the measurements taken through the boundary layer with a reasonable degree of confidence.

To measure the turbulence in the boundary layer requires the use of a hot-wire probe (thermal anemometer). Hot-wire probes have been used to measure flow turbulence in wind tunnels for many years with varying degrees of success. Basically the same type of single probe support system used for the pressure or temperature profile measurements could be used with the hot wire probe. However, since not only the possibility, but the probability, exists that the

TC Junction

FLOW
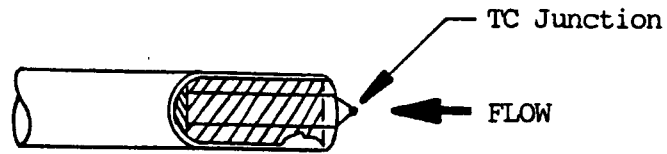
Exposed Thermocouple Junction

TC Junction

FLOW
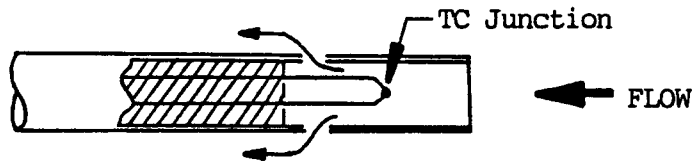
Shielded Thermocouple Junction

Recovery = Tm/T_o

where Tm is temperature measured with probe in the
freestream (℄ of nozzle)

and T_o is total temperature measured in the
combustion chamber

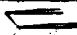Fig. 5.13 – Sketch of Two Types of Temperature Probes
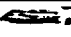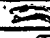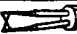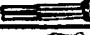
probes will have to be replaced several times during a test, because of the fragile nature of the sensing element, the system should be designed for easy access. Hot-wire results are usually very repeatable, so accuracy is really a function of how closely the calibration conditions are reproduced in the flow to be measured. In practice, contamination, temperature changes, and other factors generally limit the accuracy to 2 to 3%. The hot-wire can be used to resolve one, two, or all three components of a flow field, depending on the type of probe used. The specifications for a variety of probes are given in Fig. 5.14.

5.5.3 Exit

The majority of the measurements made on the nozzle during a reactive test are in the region of the exit. The reason for this is accessibilty. There is space to put water-cooled equipment without causing interferance in the flowfield, space for setting up non-intrusive type measurement equipment, and for CARS or infared type measurements there is no requirement for windows to provide an optical path. There are four different types of measurements that are desired during the reactive testing, all of which have been accomplished in the past with some degree of success. These four measurements are: (1) Pressure profile, (2) Temperature profile, (3) Flowfield characteristics, (4) Exhaust gas composition. The same measurements should be made with the hot gas simulation test except that the exhaust gas composition requirement is eliminated and a turbulence measurement requirement should be added.

CYLINDRICAL PROBES

Description	Model No.
Gen. Purpose	1210
High Temp. Straight	1220
Extreme High Temp. Straight	1226
Mini. Straight	1260A
Submini. Straight	1276
Standard	1211
High Temp.	1221
Extreme High Temp.	1228
Submini.	1277
1 Sensor (Sensor Upstream)	1212
High Temp. 1 Sensor	1222
Mini. Probe	1262A
Submini. Probe	1279
1 Sensor 45° to Probe	1213
1 Sensor 45° to Probe	1263A
Mini. 1 Sensor—Boundary Layer	1261A
1 Sensor—Streamlined	1214
1 Sensor—Boundary Layer	1218
Standard "X"	1240
High Temp. "X"	1250
Mini. "X"	1247A
Std. "X" Wire	1241
High Temp. "X" Wire	1251
Mini. "X" Wire	1248A
Boundary Layer "X"	1243
Standard 90° "X"	1246
Mini. 90° "X"	1249A
Parallel Sensor	1244
Split Film Boundary Layer	1287
Split Film	1288
3 Component High Turb.	1294
3 Component Std.	1295

NON-CYLINDRICAL PROBES

Description	Model No.
Straight Conical	1230
Standard 90° Conical	1231
Miniature Conical Probe	1264A
Standard Straight Wedge	1232
High Temp. Straight Wedge	1232H
90° Wedge	1233
Standard Flush Surface	1237
Mini. Flush Mnt. Sens. Element	1268
Mini. Flush Mnt. Surf. Sens.	1471
Submini. Flush Mnt. Surf. Sens.	1472
45° Sensor Edge—Wedge	1238
Ruggedized Hemisphere	1239W
Ruggedized Side-Flow	1269W
Ruggedized Metal Clad	1266
Side Flow Wedge	1229
High Temp.—Side Flow Wedge	1234H

TEMPERATURE COMPENSATED PROBES

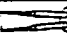| Description	Model No.
Std. Temp. Comp. (1200 Series)	1310
High Temp.—Temp. Comp. (for 1200 Series)	1311
Std. Temp. Comp.	1330
High Temp.—Temp. Comp.	1332
Ruggedized Temp. Comp.	1366

Fig. 5.14a – Example Specifications for Hot Wire and Hot Film Sensors

REMTECH INC.

Specifications
Hot Wire and Hot Film Sensors

Type	Dash No Designation Suffix in Probe No (See page 6)	Diameter (D) of Sensing Area or Width μm (in.)	Length (L) of Sensing Area μm (in.)	Distance Between Supports μm (in.)	Minimum Recommended Velocity m/s (ft/s)	Maximum Recommended Velocity m/s (ft/s)	Maximum Ambient Temp (°C)	Maximum Sensor Operating Temperature in Air (°C)	Typical Upper Freq Response in Air at 100 m/s (300 ft/s) (TSI 1050 Anemometer)	Freq Response as Temperature Sensor — Constant Current — at 30 m/s (100 ft/s) (-3db Point)	Typical Resistance Ambient (Re) OHMS	Typical Operating Resistance (Ro) OHMS	Temp Coefficient of Resistance (/°C)
Hot Wire													
Tungsten Platinum Coated	T1.5	4 (0.00015)	1.25 (0.050)	1.5 (0.06)	15 (5)	200 (600)	150	300	600 kHz	750	6	10.8	0.0042
Platinum	P2	5 (0.0002)	1.25 (0.050)	1.5 (0.06)	15 (5)	100 (300)	750	800	500 kHz	450	6	11.2	0.003
Platinum Iridium (Alloy)	PI2.5	6.3 (0.00025)	1.25 (0.050)	1.5 (0.06)	15 (5)	350 (1000)	750	800	200 kHz	500	11.5	14	0.0009
Platinum Iridium (Alloy)	PI5	12.7 (0.0005)	2.5 (0.10)	3.5 (0.15)	15 (5)	350 (1000)	750	800	10 kHz	120	3.8	4.5	0.00094
Hot Film													

Cylindrical

Gas Hot Film

Type	Dash No	Diameter	Length	Distance	Min Vel	Max Vel	Max Amb Temp	Max Sensor Op Temp	Upper Freq	Freq Temp Sensor	Re OHMS	Ro OHMS	Temp Coeff
10A	25 (0.001)	.25 (0.010)	75 (0.03)	15 (5)	350 (1000)	150	425	200 kHz	70	6.5	9	0.0024	
10	25 (0.001)	51 (0.020)	1.25 (0.05)	15 (5)	350 (1000)	150	425	300 kHz	75	6.5	9	0.0024	
20	51 (0.002)	1.0 (0.040)	1.67 (0.065)	15 (5)	350 (1000)	150	425	250 kHz	20	6.5	9	0.0024	
60	152 (0.006)	2.0 (0.080)	3.0 (0.12)	15 (5)	350 (1000)	150	425	200 kHz	3	6	8.5	0.0024	
Split Film	152 (0.006)	2.0 (0.080)	3.5 (0.15)	15 (5)	350 (1000)	150	350	20 kHz	3	10 (ea sensor)	14	0.0024	

Liquid Hot Film

Type	Dash No	Diameter	Length	Distance	Min Vel	Max Vel	Max Amb Temp	Max Sensor Op Temp	Upper Freq	Freq Temp Sensor	Re OHMS	Ro OHMS	Temp Coeff
10AW	25 (0.001)	.25 (0.010)	75 (0.03)	.03 (.01)	10 (30)	100	80 (H$_2$O)	Note 1	850	5.5	5.8	0.0024	
10W	25 (0.001)	51 (0.020)	1.25 (0.05)	.03 (.01)	10 (30)	100	80 (H$_2$O)	Note 1	850	6	6.4	0.0024	
20W	51 (0.002)	1.0 (0.040)	1.67 (0.065)	.03 (.01)	10 (30)	100	80 (H$_2$O)	Note 1	320	6	6.4	0.0024	
60W	152 (0.006)	2.0 (0.080)	3.0 (0.12)	.03 (.03)	15 (5)	100	80 (H$_2$O)	Note 1	60	4	4.3	0.0024	
Split Film	152 (0.006)	1.0 (0.040)	3.5 (0.15)	.03 (.01)	15 (5)	100	80 (H$_2$O)	Note 1	60	6 (ea sensor)	6.4	0.0024	

Non-Cylindrical

Gas Hot Film

Type	Dash No	Diameter	Length	Distance	Min Vel	Max Vel	Max Amb Temp	Max Sensor Op Temp	Upper Freq	Freq Temp Sensor	Re OHMS	Ro OHMS	Temp Coeff
Wedge	127 (0.005)	1.0 (0.040)	–	.15 (5)	350 (1000)	150	425	300 kHz	–	5	7	0.0024	
Conical	127 (0.005)	1.0 (0.040)	–	15 (5)	350 (1000)	150	425	150 kHz		4.5	6.4	0.0024	
Flush Mount	127 (0.005)	1.0 (0.040)	–	15 (5)	–	150	425	–	–	4.5	6.4	0.0024	
Metal Clad	40 (0.016)	2.54 (0.100)	–	15 (5)	66 (200)	100	125	10 Hz	-	9	13	0.0024	

Liquid Hot Film

Type	Dash No	Diameter	Length	Distance	Min Vel	Max Vel	Max Amb Temp	Max Sensor Op Temp	Upper Freq	Freq Temp Sensor	Re OHMS	Ro OHMS	Temp Coeff
Wedge	127 (0.005)	1.0 (0.040)	–	.03 (.01)	30 (100)	100	80 (H$_2$O)	Note 1	–	4.5	4.8	0.0024	
Conical	127 (0.005)	1.0 (0.040)	–	03 (01)	30 (100)	100	80 (H$_2$O)	Note 1	-	5	5.3	0.0024	
Flush Mount	127 (0.005)	1.0 (0.040)	–	.03 (.01)	–	100	80 (H$_2$O)	–	–	4.5	4.8	0.0024	
Hemi	127 (0.005)	1.0 (0.040)	–	03 (01)	15 (50)	100	80 (H$_2$O)	10 kHz	-	4.5	4.8	0.0024	
Patch	25 (0.010)	1.0 (0.040)	–	03 (01)	15 (50)	100	80 (H$_2$O)	10 kHz	-	4.5	4.8	0.0024	
Metal Clad	40 (0.016)	2.54 (0.100)	–	015 (005)	15 (5)	100	80 (H$_2$O)	Note 1		9	10.5	0.003	

Fig. 5.14b – Example Specifications for Hot Wire and Hot Film Sensors

The pressure profile, temperature profile, and turbulence (Hot-wire) measurements made at the exit during the hot gas simulation testing should use the same basic approach as was used to obtain this information in the nozzle. If survey rakes are used in the nozzle, then rakes can be used at the exit; if a single probe is used in the nozzle, then a single probe can be used at the exit. However, for the pressure profile measurements it may be desirable to use a smaller range transducer for better accuracy. Again, selection of the transducer range should be based on the pressure behind a normal shock for the Mach number at the exit. All the other measurements will use the same basic approach for either reactive or hot gas simulation and will be addressed together.

To obtain the pressure profile at the exit during reactive testing, a survey rake has traditionally been used and, as stated earlier, with varying degrees of success dependent on the exhaust temperature. Two reasons for using a rake, as opposed to a single probe, are: (1) first, a complete profile is obtained at one time, thus if burnout occurs, all is not lost, and (2) it is just as easy to cool a whole rake as it is for a single probe. Of course, some survey rakes are designed to permit traversing during the run so that the profile can be described more accurately. Some pressure survey probes are designed to not only measure the total pressure, but also the flow angularity. The sketch of a pressure survey rake with five water cooled flow angularity probes that has been designed and fabricated at the Engine Test Facility (ETF) at AEDC

is shown in Fig. 5.15. Since the pressure transducers are usually located some distance away from the hostile environment, any transducer with good accuracy and repeatability, of the types given in Figs. 5.7 and 5.11, Section 5.4 or 5.5.1 can be used.

The temperature profiles at the exit during a reactive test are also normally obtained using a water-cooled survey rake. The design of a water-cooled boundary layer temperature rake used at the NASA Lewis Research Center is shown in Fig. 5.16. This rake consists of an airfoil-shaped copper water jacket with tungsten rhenium thermocouples located in six aspiration channels. The pressure rake installation sketch in Fig. 5.15 also shows the installation of a temperature probe. Although it is our understanding that this is a rather simple probe, a probe of the same design as the NASA probe could be attached to the drive system shown and the temperature profile could be obtained.

The exhaust gas temperature can be obtained with the probe or rake used to obtain the temperature profiles whenever the gas temperature is such that this method is effective. However, in cases where the exhaust gas temperatures are above the technology to measure with a probe or rake, such as SSME exhaust temperature, then the use of infared technique or CARS can be used. Both of these methods utilize nonintrusive techniques and both have been used effectively to measure the exhaust gas temperature at the nozzle exit. However, neither are what can be called routine measurements, in that, both require expertise both in setup and

WATER FLOW

4 STATIC

COPPER

0.135

0.1306

0.35R

30°

0.10

0.50

0.70

END VIEW

a. Probe Tip
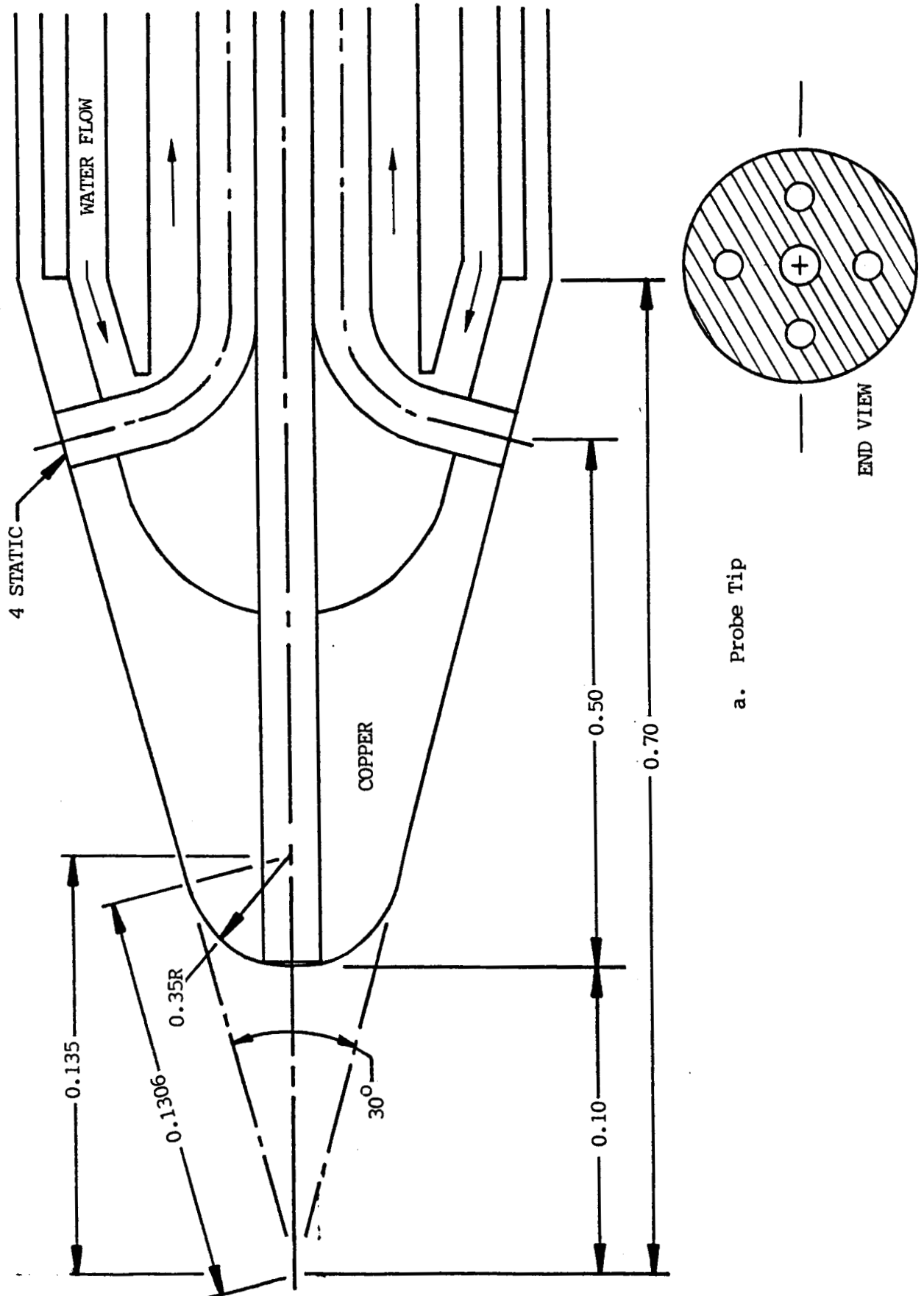
Fig. 5.15a- Sketch of AEDC/ETF Water-Cooled Pressure Survey Rake

.12

FLOW

4.0 TRAVERSE
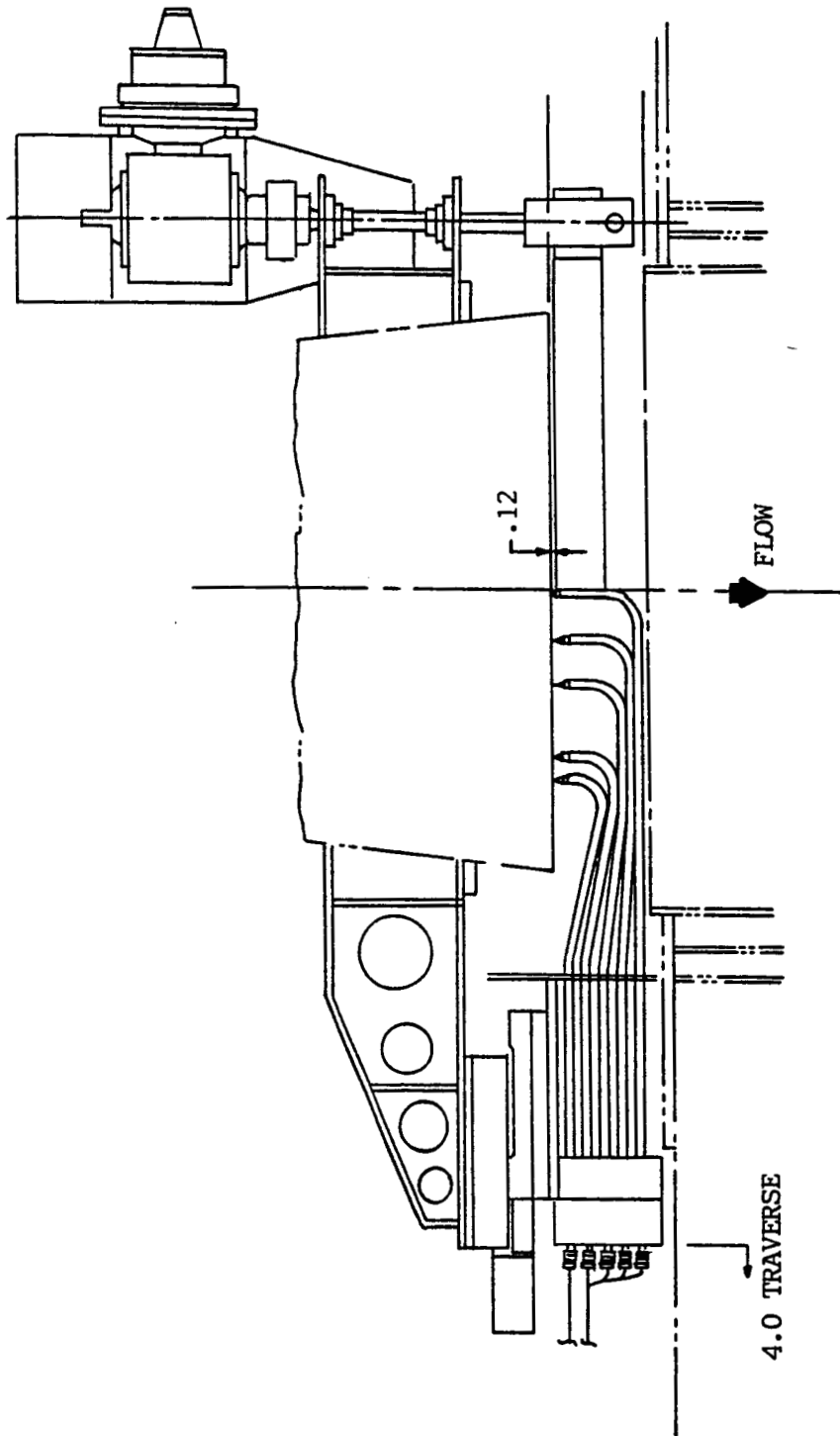
b. Rake Installation

Fig. 5.15b– Sketch of AEDC/ETF Water-Cooled Pressure Survey Rake

ASPIRATION
CHANNELS

5"

3"

COPPER

H20

H20

H20

H20

FLOW
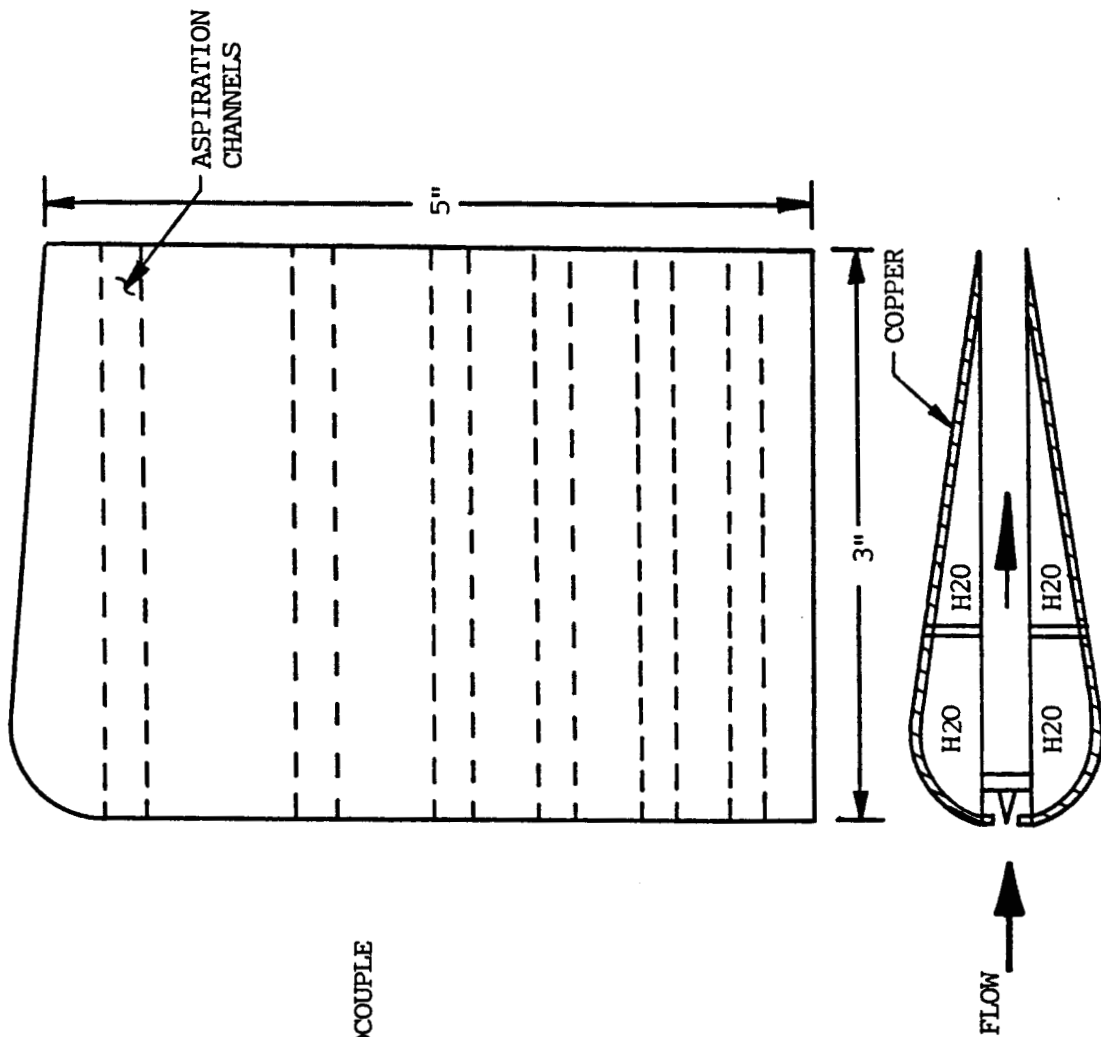
BOUNDARY LAYER TEMPERATURE PROBE

● COPPER

● TUNGSTEN RHENIUM THERMOCOUPLE

● WATER COOLED

Fig. 5.16 – Sketch of NASA Lewis Research Center Boundary Layer Temperature Rake

interpretation. Because of the nature of the measurements, both can also give partial gas composition. Research and development is being carried out in both fields to increase the use of both techniques as measurement tools.

As stated in the previous paragraph, both infared and CARS have been used to obtain partial gas composition. However, the conventional way is the use of a sampling probe, wherein difficulties in freezing the reactions are well recognized. The probe will need to be water-cooled and the probe support system should be designed so that samples of the exhaust gas can be obtained at various locations across the exit plane. If this is done, means of purging the system and separating the sample must be provided. After the gas samples are obtained they can be analyzed at the chemical laboratory that is usually located at most engine test facilities.

5.6 COMPLETE SYSTEM

The final measurements required are the thrust and side load. In determining the I_{sp}, the thrust and the mass flow (described in Section 5.3) are the dominant measurements. Traditionally a primary load cell, aligned with the thrust axis of the engine, is used to measure the engine thrust and a secondary load cell, with a tension and compression capability, is aligned perpendicular to the thrust axis to measure the side load (or load due to misalignment). The specifications for a load cell that are available at accuracies in the range required for performance code verification testing are

shown in Fig. 5.17. An uncertainty of 0.10% is quoted for a Class No. 1 load cell.

To measure the thrust and side loads during the performance codes verification test such as described in Section 5.1 and shown in Fig. 5.1 a special hollow balance is required. The AEDC hollow balance used in Ref. 6 is shown in Fig. 5.18 along with the load calibration range used and the uncertainty. The gauge that would be used to measure the thrust in the proposed installation has an uncertainty of 0.16%.

5.7 SUMMARY

As stated earlier, the goal of the rocket engine performance code verification tests is to obtain the I_{sp} with an accuracy of 0.25% or less. This needs to be done during the sequence of 4 related tests (two reactive and two hot gas simulation) to best utilize the loss separation technique recommended in this study. In addition to I_{sp}, the measurements of the input and output parameters for the codes are needed.

This study has shown two things in regard to obtaining the I_{sp} uncertainty within the 0.25% target. First, this target is generally not being realized at the present time, and second, the instrumentation and testing technology does exist to obtain this 0.25% uncertainty goal. However, to achieve this goal will require carefully planned, designed, and conducted testing. In addition, the test-stand (or system) dynamics must be evaluated in the pre-test and post-test phases of the design of the experiment and

TOROID SERIES 35 LOAD CELL SPECIFICATIONS

ORIGINAL PAGE IS
OF POOR QUALITY

SPECIFICATIONS

	CLASS NO. 1	CLASS NO. 2	CLASS NO. 3
FULL SCALE OUTPUT	± .10% F.S.	± .25% F.S.	± .25% F.S.
NON-LINEARITY	± .05% F.S.	± .10% F.S.	± .17% F.S.
HYSTERESIS	± .02% F.S.	± .02% F.S.	± .07% F.S.
REPEATABILITY	± .02% F.S.	± .02% F.S.	± .05% F.S.
ZERO LOAD OUTPUT SHIFT WITH TEMPERATURE PER °F	± .0015% F.S.	± .0025% F.S.	± .0025% F.S.
FULL SCALE OUTPUT SHIFT WITH TEMPERATURE PER °F	± .0008% F.S.	± .005% F.S.	± .005% F.S.

GENERAL SPECIFICATIONS
(COMMON TO ALL LOAD CELLS IN THIS SERIES)

RECOMMENDED INPUT VOLTAGE	10 VOLTS AC OR DC
INPUT RESISTANCE AT 77°F (OHMS)	350 ± 1.5 OHMS
OUTPUT RESISTANCE AT 77°F (OHMS)	350 ± 3.5 OHMS
MAXIMUM INPUT VOLTAGE	20 VOLTS AC OR DC
COMPENSATED TEMPERATURE RANGE	+ 30° TO 130°F
MAXIMUM SAFE EXPOSURE TEMPERATURE	275°F
SAFE OVERLOAD	150%
MAXIMUM OVERLOAD	300%
INSULATION RESISTANCE AT 77°F	5000 MEGOHMS
ZERO LOAD OUTPUT @ 77°F	1%

S.G. = MODULUS / FACTOR / TERMINAL / BALANCE

RED
ORANGE
WHITE
YELLOW
OUTPUT
GREEN
BLUE
BLACK
BROWN
INPUT
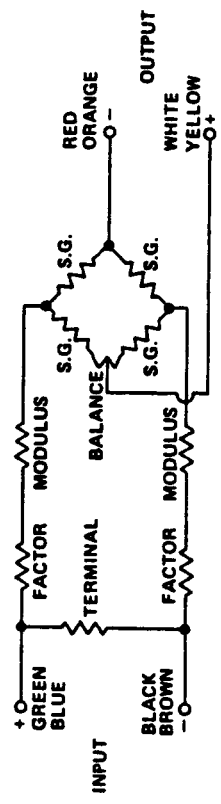
ORDERING INFORMATION

CLASS
1 – .05%
2 – .10%
3 – .25%

FACTORY USE ONLY
SPECIFICATION OR SYSTEM

CONNECTIONS
A – CONNECTOR (SPEC)
B – CABLE –10' 0"

MODEL NO. — 3 5 U – 1 3 3 – 1 A

BRIDGE RESISTANCE
1 = 120 Ohm
2 = 350 Ohm
3 = Other

MV/VOLT RATING
1 = 1 mv/VOLT
2 = 2 mv/VOLT
3 = 3 mv/VOLT
4 = OTHER

NUMBER OF BRIDGES
1 = SINGLE
2 = DOUBLE
3 = TRIPLE
4 = N (4 OR MORE)

CLASS OF SERVICE
T = TENSION
C = COMPRESSION
U = UNIVERSAL

TOROID SERIES 35 LOAD CELL....

T TYPICAL BOTH ENDS

HOLES CAN BE DRILLED WITHIN THIS AREA TO RECEIVE LOCKING SCREWS
MAXIMUM DEPTH OF HOLES IS—M—
DIMENSION –P– IS THREAD SIZE

CONNECTOR OR TEN FOOT CABLE OPTIONAL
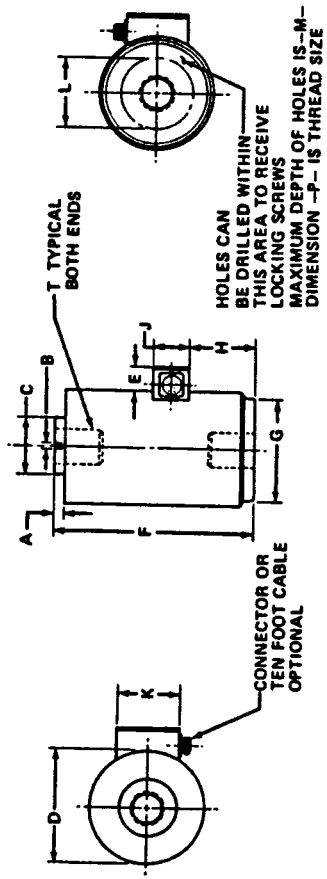
RANGE	A	B	C	D	E	F	G	H	J	K	L	M	T THREAD	P THREAD SIZE
100-3,000	.24	.06	.70	3.00	.78	4.44	2.63	1.13	1.50	2.63			1/2-20 UNF-2B x .66 DP	3/8-24 UNF 2B
5,000-10,000	.28	.13	1.42	3.50	.78	5.94	2.95	1.85	1.50	2.63	2.50	.50	1-14 UNS-2B x .13 DP	3/8-24 UNF 2B
25,000	.44	.19	2.50	5.00	1.00	8.50	4.45	2.81	1.50	2.63	2.38	.38	1 1/2-12 UN-2B x 2.0 DP	1/2-20 UNF 2B
50,000	.56	.25	3.25	6.50	1.06	11.44	5.88	3.70	1.50	2.63	2.38	.38	2-12 UN-2B x 2.63 DP	5/8-16 UNF 2B
100,000	1.06	.38	5.00	9.00	1.19	17.75	8.10	6.25	1.50	2.63	4.00	.75	3-8 UN-2B x 3.13 DP	5/8-16 UNF 2B
200,000	1.25	.50	6.00	12.00	1.22	22.00	10.13	10.75	1.50	2.63	5.00	1.00	4-8 UN-2B x 5.63 DP	3/4-16 UNF 2B
250,000	1.25	.50	6.00	12.00	1.22	22.00	10.13	10.75	1.50	2.63	5.00	1.00	4-8 UN-2B x 5.63 DP	3/4-16 UNF 2B
300,000	1.25	.50	6.00	12.00	1.22	24.00	8.20	8.00	1.50	2.63	5.50	1.13	4-8 UN-2B x 5.63 DP	3/4-16 UNF 2B
500,000	1.40	.50	7.00	12.00	1.22	25.00	10.75	11.75	1.50	2.63	5.50	1.13	4-1/2-8 NS-2B x 5.63 DP	3/4-16 UNF 2B
500,000	1.45	.50	9.50	14.00	1.25	30.00	11.50	12.00	1.50	2.63	5.50	1.13	5 1/2-8 NS-2B x 6.4 DP	3/4-16 UNF 2B
750,000	1.65	.63	10.00	16.00	1.25	34.00	14.00	14.00	1.50	2.63	5.50	1.13	7-4 NS-2B x 7.5 DP	3/4-16 UNF 2B
1,000,000	1.65	.75	11.50	18.00	1.25	38.00	15.00	15.00	1.50	2.63	8.00	1.13	7-4 NS-2B x 7.5 DP	3/4-16 UNF 2B
1,000,000	1.65	.75	14.00	30.00	1.25	50.00	20.00	20.00	1.50	2.63	8.00	1.13	8-4 NS-2B x 11.0 DP	3/4-16 UNF 2B

SINGLE BRIDGE WITH CONNECTOR

SINGLE OR DOUBLE BRIDGE WITH CABLE

DOUBLE BRIDGE WITH CONNECTOR

SINGLE BRIDGE OR DOUBLE BRIDGE WITH LOAD BUTTON
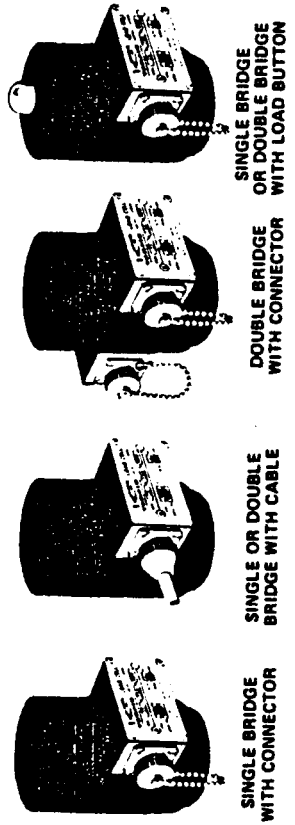
Fig. 5.17 – Example Specifications for High Accuracy Load Cells

REMTECH INC.
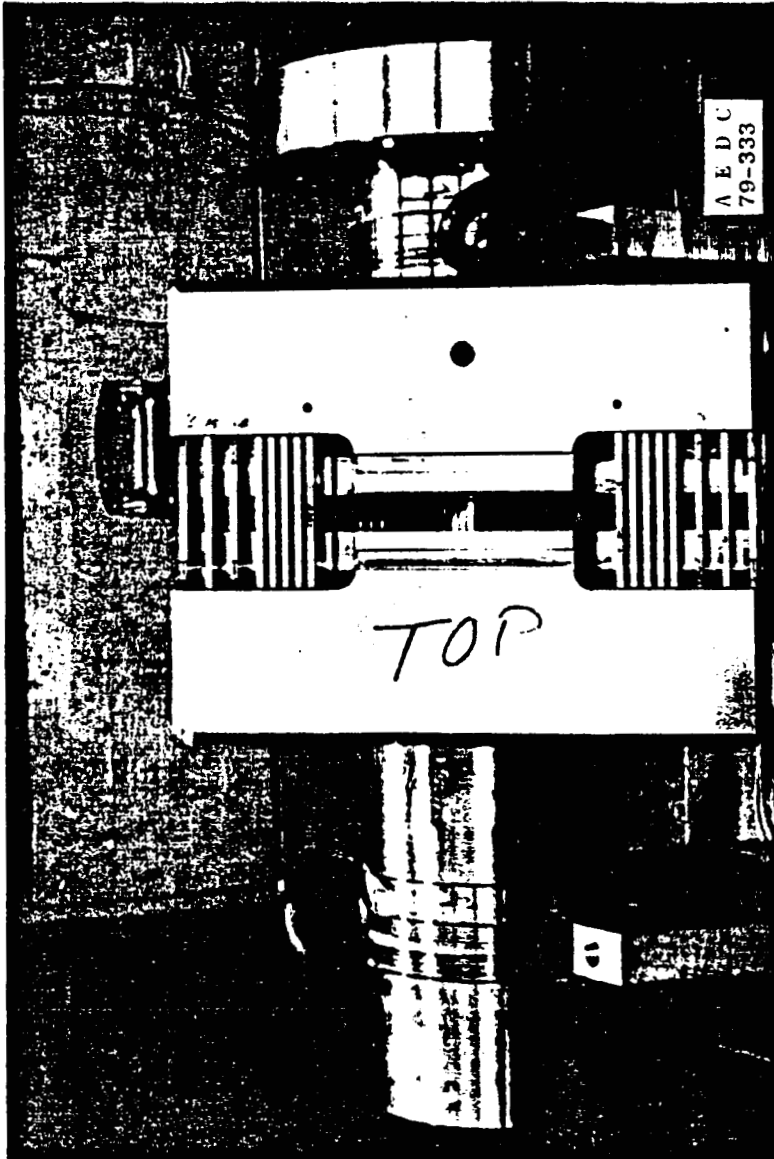
Dead Weight
Calibration Range

$F_N = \pm 2{,}000 \, lb,$

$F_Y = \pm 1{,}000 \, lb,$

$M_l = \pm 60{,}000 \, in.\text{-}lb,$

$M_m = \pm 63{,}638 \, in.\text{-}lb,$

$M_n = \pm 32{,}122 \, in.\text{-}lb$

Probable
2-D Error

$F_N = 3.26 \, lb$

$F_Y = 0.41 \, lb,$

$M_l = 34.6 \, in.\text{-}lb,$

$M_m = 128.7 \, in.\text{-}lb,$ and

$M_n = 81.1 \, in.\text{-}lb.$

Fig. 5.18 - AEDC/PWT Hollow Sidewall Balance (Ref. 6)

REMTECH INC.

data analysis, respectively always keeping in mind that a .25% overall uncertainty in I_{sp} is targetted. Table 5.2 gives the maximum allowable uncertainty required for obtaining I_{sp} with 0.25% uncertainty, the currently-quoted instrument specification, and present test uncertainty for the parameters. In general, it appears that measurement of the mass flow parameter within the required uncertainty, may be the most difficult.

Table 5.2

Summary of Parameter Uncertainty
for Calculation of
Vacuum Specific Impulse with 0.25% Uncertainty

$$I_{sp_{vac}} = \frac{F_{SITE} + P_a \ A_e}{\dot{m}_T}$$

Parameter	Maximum Allowable Uncertainty	Presently - Quoted Instrument Specification	Present Test * Uncertainty
Measured Thrust (F_{SITE})	0.18%	0.10 to 0.25%	0.15 to 0.50%
Mass flow rate ($\dot{m}_T$)	0.18%	0.05 to 0.50%	0.40 to 1.0 %
Ambient Pressure (P_a)	0.25%	0.10%	0.10 to 0.50%
Nozzle Exit Area (A_e)	0.25%		

* Note: The SSME (NSTL) data are not included since this is a unique situation where a test stand is designed for a specific engine. Here the same parameters are calibrated and measured over the same ranges with the same setups over and over which is not representative of the conditions for most rocket engine research testing. It definitely does not represent the conditions for rocket engine performance code verification.

References

1. "JANNAF Rocket Engine Performance Test Data Acquisition and Interpretation Manual," CPIA Publication 245, April 1975.

2. Reardon, J.E. and Engel, C.D., "IBFF Combustion Design and Data Analysis," REMTECH Technical Report RTR 008-3, Huntsville, Alabama, May 1974.

3. Back, L.H., Cuffel, R.F. and Massier, P.F., "Laminarization of a Turbulent Boundary Layer in Nozzle Flow - Boundary Layer and Heat Transfer Measurements with Wall Cooling," Transactions of ASME Ser. C, 92, pp 333-344, August 1969.

4. Praharaj, S.C. et al, "Boundary Layer Simulation Improvement," REMTECH Technical Report RTR 115-01, Huntsville, Alabama, December 1984.

5. Levinsky, E.S. et al (General Dynamics Corp.) and Palko, R.L. etal (ARO, Inc.), "Semispan Wind Tunnel Test Evaluation of a Computer-Controlled Variable Geometry Wing (Self-optimizing Flexible Technology Wing Program)," AEDC-TR-78-51 (AD-B033600L), January 1979.

6. Levinsky, E.S. et al (General Dynamics Corp.) and Palko, R.L. et al (ARO, Inc.), "Wind Tunnel Test of a Improved Computer-Controlled Variable-Geometry Wing (Self-optimizing Flexible Technology Wing Program)," AEDC-TR-80-42, January 1981.

7. McCay, T.D. and Roux, J.A., Editors, Combustion Diagnostics by Nonintrusive Methods, Progress in Astronautics and Aeronautics, Volume 92, 1983.

8. Goldstein, Richard J., Editor, Fluid Mechanics Measurements, Hemisphere Publishing Corporation, 1983.

9. "Handbook of Recommended Practices for Measurement of Liquid-Propellant Rocket Engine Parameters," prepared by The Experimental Measurements Committee of the ICRPG Performance Standardization Work Group, CPIA No. 179, January 1969.

C-2

APPENDIX A

MEASUREMENT ACCURACY

MEASUREMENT ACCURACY

1. All measurements have error.

2. Uncertainty is an estimate of the maximum error.

3. Uncertainty is process-dependent.

   - instrumentation process
   - measurement-recording-reduction process
   - derived parameter methodology
   - test process

4. Uncertainty has 2 components:

   - Bias
   - Precision

5. Bias - Those factors which cause a constant error in a given data set from a given installation in a given test cell.

6. Precision - Those factors which cause scatter in a given data set:

   - zero shift
   - calibration
   - curve fits
   - installation repeatability
   - balance uncertainties
   - system dynamics
   - unsteady flow
   - dropped/or added bits
   - instrument drift
   - system noise
   - system resolution

7. Bias Limit (B) - The bias components are fixed or systematic errors. The magnitude of the bias cannot be determined unless the measurements can be compared with the true value, which is not feasible. Therefore, bias limits ($\pm$B) are estimated using applicable test information and engineering judgement.

8. Precision Index (S) - Random errors are encountered in repeated measurements and are the differences between the observed values and the average value of a very large sample. These variations tend to spread about an average value in the fashion of a normal distribution curve.   The curve is characterized by the standard deviation, σ .

   The precision index (S) is the computed estimate of the standard deviation, σ , and is calculated as:

$$S = \sqrt{\frac{\sum\limits_{K=1}^{n}(X_k - \overline{X})^2}{n-1}}$$

Where: n = number of measurements
X_k = individual measurments
$\overline{X}$ = average value of X_k

$$\overline{X} = \frac{\sum\limits_{K=1}^{n} X_k}{n}$$

9. Elemental Error - Each measurement system has many potential sources of error. The errors for each source are referred to as elemental errors. It is commonly accepted to divide the elemental error sources for any measurement into three categories indicated by the subscript j:

j	Category
1.	Calibration Errors
2.	Data Aquisition Errors
3.	Data Reduction Errors

10. Calibration Errors (Category j = 1) - The measurement uncertainty analysis assumes a well controlled measurement process in which there are no gross mistakes or errors. It also assumes the reasonable calibration corrections have been applied. Calibrations are performed to improve the test accuracy and to provide test measurement traceability to the National Standards Laboratory. By applying the calibration corrections, some biases are reduced but in the process some other errors may be introduced. Traceability is established and maintained through a calibration hierarchy. Each calibration in the hierarchy constitutes an elemental error source, i.

Example:

i	Source
1.	National Standard Laboratory (SL)
2.	Inter-Laboratory Standard (ILS)
3.	Transfer Standard (TS)
4.	Working Standard (WS)
5.	Measurement Instrument (MI)

Each comparison in the calibration hierarchy has elemental errors associated with it. Estimates of the elemental errors provide precision indices and bias limits in each level of the hierarchy.

Example: Calibration (j = 1)

i	Error Source	Bias Limit	Precision Index
1.	SL → ILS	B_{11}	S_{11}
2.	ILS → TS	B_{21}	S_{21}
3.	TS → WS	B_{31}	S_{31}
4.	WS → MI	B_{41}	S_{41}

REMTECH INC.

11. Data Acquisition Errors (Catergory j = 2) - Error sources, i, are associated with the various elements of the data acquisition system. Data are usually obtained by measuring the electrical output resulting from a pressure, temperature, or force applied to an appropriate measuring instrument. Other elemental error sources such as electrical simulation, probe errors, and environmental effects may also be present.

Example: Data Acquisition (j = 2)

i	Error Source	Bias Limit	Precision Index
1.	Excitation Voltage	B_{12}	S_{12}
2.	Electrical Simulation	B_{22}	S_{22}
3.	Signal Conditioning	B_{32}	S_{32}
4.	Recording Device	B_{42}	S_{42}
5.	Pressure Transducer	B_{52}	S_{52}
6.	Probe Errors	B_{62}	S_{62}
7.	Environmental Effects	B_{72}	S_{72}

12. Data Reduction Errors (Category j = 3) - Computers operate on raw data to produce output in engineering units. Typical errors in this process stem from curve fits and computer resolution.

Example: Data Reduction (j = 3)

i	Error Source	Bias Limit	Precision Index
1	Curve Fit	B_{13}	S_{13}
2	Computer Resolution	B_{23}	S_{23}

13. Combining Measurement Errors - After the elemental error sources are identified, they must be combined into the basic measurement error components, precision and bias. Combining the elemental errors into separate components is essential for modelling the basic measurement uncertainty, for propagating measurement uncertainties to performance parameters, and for uncertainty reporting and validation.

Typically, only calibration, data acquisition, and data reduction error sources are considered and combined to define the basic measurement error.

14. Combining Precision Indices - The precision index (S) is the root-sum-square of the elemental precision indices from all sources.

$$S = \sqrt{\sum_j \sum_i S_{ij}^2}$$

where j defines error categories:
(1) calibration, (2) data acquisition,
and (3) data reduction
and i defines elemental error sources within a category.

Example: The precision index for calibration category, S_1, is defined by:

$$S_1 = S_{cal} = \sqrt{S_{11}^2 + S_{21}^2 + S_{31}^2 + S_{41}^2}$$

In like manner, the precision index for data acquisition, S_2, and data reduction, S_3, are defined.

The basic measurement precision index for the three catagories combined is:

$$S = \sqrt{S_1^2 + S_2^2 + S_3^2}$$

$$= \sqrt{\sum_i S_{i1}^2 + \sum_i S_{i2}^2 + \sum_i S_{i3}^2}$$

$$= \sqrt{\sum_j \sum_i S_{ij}}$$

Note - Caution should be exercised in assigning values to S_{ij}, since they may have been fossilized into the bias term of the component.

15. Combining Bias Limits - Most measurement processes will contain a large number of bias error sources. The bias limit is the root-sum-square of the elemental bias error limits of all categories.

$$B = \sqrt{\sum_j \sum_i B_{ij}}$$

Where j defines error categories (1) calibration, (2) data acquisition, and (3) data reduction.
and i defines elemental error sources within a category.

Example: The individual error limits; calibration (B_1, data acquisition (B_2), and data reduction (B_3), are defined by the root-sum-square of their individual elemental bias limits.

The bias limit for the basic measurement process is then:

$$B = \sqrt{B_1^2 + B_2^2 + B_3^2}$$

$$= \sqrt{\sum_i B_{i1}^2 + \sum_i B_{i2}^2 + \sum_i B_{i3}^2}$$

$$= \sqrt{\sum_j \sum_i B_{ij}^2}$$

Note: If any of the elemental bias limits are nonsymmetrical separate root-sum-squares are used to obtain B+ and B-.

16. Propagation of Basic Measurement Errors to Calculated Parameters - Calculated parameters are a function of basic measurements, such as temperature and pressure. The basic components of uncertainty (S and B) in the measurements are propagated to the calculated parameters through a math model. The effect of the propagation can be approximated using the Taylor series method.

For propagating errors, the concept of the "influence coefficient (θ)" may be convenient. This is the error propagated to the performance parameter due to a unit error in the basic measurement. The "influence coefficient" of each basic measurement is obtained in one of two ways, analytically or numerically.

Analytically - When there is a known mathematical relationship between the calculated parameter (F) and the measured variables (X_1, X_2 -- X_k) the dimensional influence coefficient (θ_k) for the quantity X_k, is obtained by partial differentiation.

Thus, if $F = f(X_1, X_2 -- X_k)$, then $\theta_k = \dfrac{\partial F}{\partial X_k}$.

Numerically - When no mathematical relationship is available or when differentiation is difficult, finite increments may be used to evaluate θ_k.

Here θ_k is given by $\theta_k = \dfrac{\Delta F}{\Delta X_k}$.

For independent measurements, the basic measurement error components S_{xk} and B_{xk} are propagated to the error components (S_F and B_F) using the influence coefficient (θ_k).

$$S_f = \sqrt{\sum_k (\theta_k S_{xk})^2} \quad \text{and} \quad B_f = \sqrt{\sum_k (\theta_k B_{xk})2}$$

Note: Care should be taken to check that the quantities (X_k) are independent. For complex calculations, the same measurement may be used more than once in the formula. If the Taylor's series relates the most elementary measurements to the calculated parameter, the "linked" relationships will be properly considered.

17. Measurement Uncertainty (U) - A single number (Some combination of bias and precision) is needed to express a reasonable limit for error. This single number is called uncertainty (U).

Two equally accepted options are used (U_{ADD} and U_{RSS}). U_{ADD} is the additive model and U_{rss} is the root-sum-square combination.

$$U_{ADD} = B + \frac{t_{95}S}{\sqrt{n}} \quad \text{and} \quad U_{RSS} = \sqrt{B^2 + \left(\frac{t_{95}S}{\sqrt{n}}\right)^2}$$

Where B is the bias limit
S is the precision index
n is the number of samples
and t_{95} is the 95th percentile point for the two-tailed student's "t" distribution from table.

Student's "t" - The "t" value is a function of the number of degrees of freedom (ν) used in calculating S, therefore, $\nu = n-1$ should be used to select the t_{95} value from the table.

Propagation of Degrees of Freedom - When precision indices of elemental error sources are combined (root sum square), the degrees of freedom of the result must be determined if any of the elemental degrees of freedom are less than 30. The Welch-Satterthwaite formula is used for this purpose. It is a function of the degrees of freedom and the magnitude of the elemental precision indices.

If $S = \sqrt{\sum_i S_i^2}$ with degrees of freedom ν_i
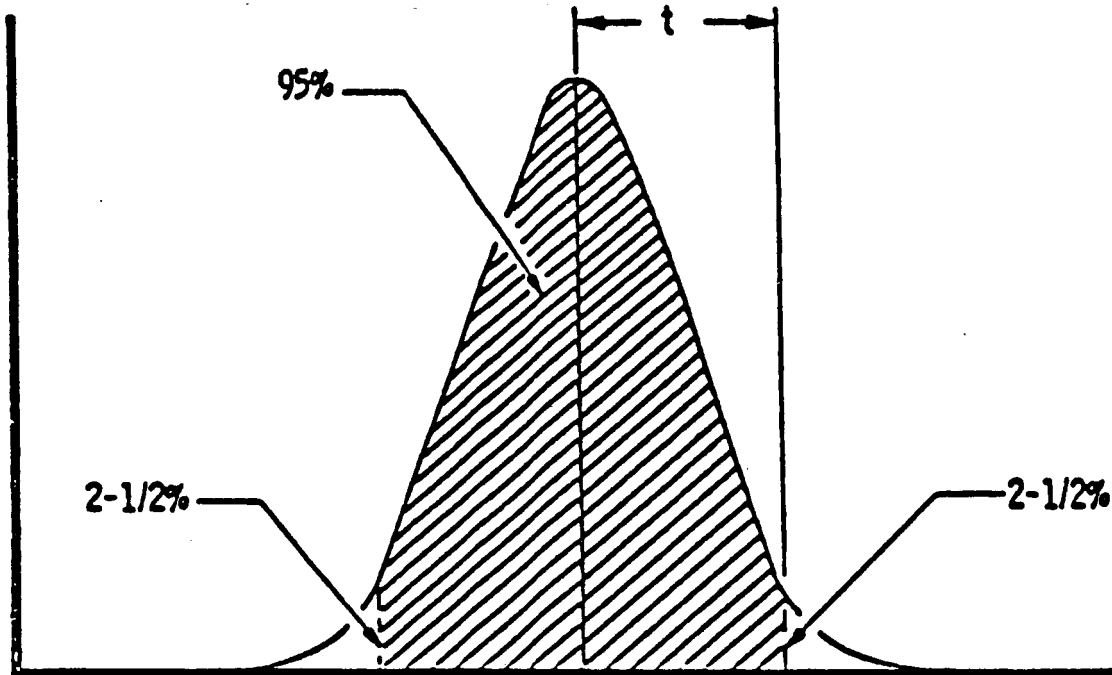
Degrees of Freedom	"t"$_{95}$	Degrees of Freedom	"t"$_{95}$
1	12.706	17	2.110
2	4.303	18	2.101
3	3.182	19	2.093
4	2.776	20	2.086
5	2.571	21	2.080
6	2.447	22	2.074
7	2.365	23	2.069
8	2.306	24	2.064
9	2.262	25	2.060
10	2.228	26	2.056
11	2.201	27	2.052
12	2.179	28	2.048
13	2.160	29	2.045
14	2.145		
15	2.131		
16	2.120	30 or more use 2.0	

Fig. A.1 - Two-tailed Student's "t" Table

REMTECH INC.

then, $\nu = \dfrac{\left[\sum_i s_i^2\right]^2}{\sum_i \left(\dfrac{s_i^4}{\nu_i}\right)}$

or if $S = \sqrt{\sum_j \sum_i s_{ij}^2}$ with degrees of freedom ν_{ij}

then, $\nu = \dfrac{\left[\sum_j \sum_i s_{ij}^2\right]^2}{\sum_j \sum_i \left(\dfrac{s_{ij}^4}{\nu_{ij}}\right)}$

or if $S_F = \sqrt{\sum_k \left(\theta_k S_{xk}\right)^2}$ with degrees of freedom ν_{xk}

then, $\nu_F = \dfrac{\left[\sum_k \left(\theta_k S_{xk}\right)^2\right]^2}{\sum_k \dfrac{\left(\theta_k S_{xk}\right)^4}{\nu_{xk}}}$

18. **Pretest and Posttest Analyses -**

   Pretest Analysis - Although the final uncertainty limits determined from the posttest analysis will be those reported with the test results, the pretest uncertainty analysis could be one of the most important steps in the test preparation. If accuracy requirements have been specified for a test, it is important to know if those requirements can be met. If the pretest analysis shows the uncertainties to be greater than acceptable, and corrective actions can not be taken to reduce the uncertainty to an acceptable level, then the test should be aborted. Therefore, it is important to conduct the pretest uncertainty analysis early in the test planning cycle and update it as better information about test article and/or test facility is made available. The pretest analysis is based on data and information that exist before the test: calibration histories, previous tests with similar instrumentation, prior measurement uncertainty analyses and expert opinions. (Where facts are available, opinions should be secondary.) In complex tests there are often alternatives to evaluate: different thrust models, various instrumentation layouts, and alternate calculation procedures. The pretest analysis should help identify the most preferred test methods and the most critical measurements.

Posttest Analysis - The posttest analysis is required to confirm the pretest estimates and to identify potential problems. Comparison of test results with the pretest analysis is an excellent data validity check. When redundant instrumentation or calculation methods are available, the individual averages should be within the pretest uncertainty range. If there are several ways of obtaining a parameter, the uncertainty ranges should overlap. The final uncertainty limits reported for the test results should be based on the posttest analysis.

19. Uncertainty Reports - The uncertainty components, precision index, bias limit, uncertainty limit (with option used for determination) and influence coefficients should be included in the reports on measurement error along with applicable test conditions. Two separate reports are recommended: The Measurement Uncertainty Summary Report and the Elemental Error Sources Report.

Measurement Uncertainty Summary Report - The error components of precision index (S) and bias limits (B) are necessary to: (1) indicate corrective action if the uncertainty is unacceptably large before the test, (2) to propagate the uncertainty to more complex parameters, and (3) to substantiate the uncertainty limit. The influence coefficients for each measurement are provided to document the calculation of the error components. The test condition must be identified to qualify both the error components and influence coefficients.

Elemental Error Sources Report - The elemental error sources report records all the elemental errors of each basic measurement. The elemental contributions are required to confirm measurement uncertainty estimates and to support any corrective action needed to reduce the uncertainty or to identify data validity problems. The list should also help to ensure against potential missing error sources.

20. HOW TO DO IT - SUMMARY

a. Make a complete, exhaustive list of every possible elemental error source for each measurement: calibration, data acquisition, data reduction.

b. Classify Errors - If you can calculate the standard deviation, call it precision, otherwise, call it bias.

c. For the defined measurement process, make the final classification of errors into bias and precision. RULE - A precision error increases the scatter in the final test results.

d. Propagate elemental errors to final result separately: precision, bias, degrees of freedom.

e. Calculate uncertainty: U_{ADD} or U_{RSS}

f. Report: precision, bias, degrees of freedom, uncertainty (state model used).

g. Pretest and Posttest analysis.